

Impacts of rainforest transformation into oil-palm plantations on silicon pools in soils

Dissertation

for the award of the degree

„Doctor rerum naturalium“ (Dr. rer. nat.)

of the Georg-August-Universität Göttingen

within the doctoral program Geography

of the Georg-August-University School of Science (GAUSS)

submitted by

Britta Greenshields

from Dieburg

Göttingen, 2022

Thesis Committee

Prof. Dr. Daniela Sauer
(Department of Physical Geography, Georg-August Universität Göttingen)

Dr. Barbara von der Lühe
(Department of Geosciences, Westfälische Wilhelms-Universität Münster)

Dr. Marife Corre
(Department of Soil Science of Tropical and Subtropical Ecosystems, Georg-August Universität Göttingen)

Members of the Examination Board

Reviewer 1:
Prof. Dr. Daniela Sauer
(Department of Physical Geography, Georg-August Universität Göttingen)

Reviewer 2:
Prof. em. Dr. Gerhard Gerold
(Department of Landscape Ecology, Georg-August-Universität Göttingen)

Further members of the Examination Board

Dr. Barbara von der Lühe
(Department of Geosciences, Westfälische Wilhelms-Universität Münster)

Dr. Marife Corre
(Department of Soil Science of Tropical and Subtropical Ecosystems, Georg-August Universität Göttingen)

Prof. Dr. Heiko Faust
(Department of Human Geography, Georg-August Universität Göttingen)

Prof. Dr. Alexander Knohl
(Department of Bioclimatology, Georg-August Universität Göttingen)

Date of oral examination: 13th May 2022

Acknowledgements

I would like to thank Prof. Dr. Daniela Sauer and Dr. Barbara von der Lüche for supervising my doctoral thesis and for trusting me as a geologist, to research in tropical soil science. I really enjoyed the practical teachings in the field and laboratory, learning about soils and interacting environmental processes. Special thanks to Dr. Barbara von der Lüche for her continuous support and open discussions about the research work. My thanks also go to my thesis referees, Prof. Dr. Daniela Sauer and Prof. em. Dr. Gerhard Gerold, as well as my thesis advisory committee, Prof. Dr. Daniela Sauer, Dr. Barbara von der Lüche and Dr. Marife Corre for providing guidance throughout the PhD. My sincere thanks to Prof. Dr. Daniela Sauer, Prof. em. Dr. Gerhard Gerold, Dr. Barbara von der Lüche, Dr. Marife Corre, Prof. Dr. Heiko Faust and Prof. Dr. Alexander Knohl for being on the examination board.

My appreciation to the German Research Foundation (DFG) for funding this project (DFG project no. 391702217) which was associated to the Collaborative Research Centre 990 “Ecological and Socioeconomic Functions of Tropical Lowland Rainforest Transformation Systems” (CRC 990, DFG project no. 192626868). Thanks also to the CRC-990 management, in particular to Dr. Barbara Wick, for supporting collaboration. As an associated graduate researcher, I have always felt welcome while staying in Indonesia or being generally involved in CRC-900 activities. My sincere thanks to Dr. Aiyen Tjoa for her cultural guidance and support during fieldwork and research. My thanks also go to Dr. Suria Tarigan and Dr. Harold Hughes for supporting me in my research. For the financial contribution for a symposium and language course in Indonesia, special thanks to the GeoGender Chancenfond.

The work could not have been done without the help of my fieldwork assistants in Jambi, in particular Nando, Daniel, Toni and Somad, and the Jambi office staff, in particular Yuking, Mega and Rizky. Likewise, I am indebted to Dr. Jürgen Grotheer, Petra Voigt and Anja Södje for supporting me with the laboratory work in Göttingen. Special thanks to Laura, Karin, Kerstin, Felix, Jannik, and Marius for helping me analyse an enormous number of samples in the laboratory. I could not have completed my research without them.

Thanks also to my former colleagues at the Department of Physical Geography and my CRC-colleagues. There are many others, who have helped all the way, in reading and consultation – Isabelle, Alexandra, Stephen, Tati, Nora, Rahmi, Carina, Johanna and my family.

Summary

Silicon (Si) is the second most abundant element in the Earth's crust. In rocks, Si primarily occurs as primary silicates. In soils, Si is present mostly as secondary silicates or amorphous silica of biogenic or pedogenic origin. For plants, Si can be an essential element due to its numerous beneficial functions: in soils, Si can mobilize phosphorous (P) by occupying anion adsorption sites. Si also mitigates plant toxicity by binding toxic cations that become mobile at low soil pH. In plants, Si can increase drought resistance by precipitating in various cell components of leaves which reduces transpiration. In recent years, assessing the Si status in arable soils has received more attention because well-balanced Si levels in soils may increase crop yields (economic interest) and mitigate severe droughts (climate change). In SE Asia, Si research is particularly relevant because three parameters come together in this region: highly weathered tropical soils (i.e., desilicated soils), drought risk due to shorter rainy seasons and crops, which are Si accumulators such as rice (*Oryza sativa*), sugarcane (*Saccharum officinarum*) and oil palm (*Elaeis guineensis*). Si-accumulating plants require well-balanced Si levels in soils in addition to common plant nutrients (e.g., N, P, K, Ca, Mg).

Indonesia is the second largest palm oil producer in the world. In 2022, ~ 16 million ha land was under oil-palm cultivation. Oil palms are still commonly planted as monocultures, whereby four management zones can be distinguished: (1) *palm circles* refer to the immediate circulate area around a palm stem that are fertilized; (2) *oil-palm rows* refer to rows of planted oil palms that contain cover crop (understory vegetation); (3) *interrows* are interim spaces between planted oil-palm rows that are sprayed regularly with herbicides and usually serve as harvesting paths; (4) *frond piles* refer to interrows where pruned palm fronds are stacked in piles to serve as litter decomposition sites. Additionally, cover crop is left in place.

Within Indonesia, Sumatra has been greatly affected by land conversion, i.e., from lowland rainforests and agroforestry systems into oil-palm monocultures. Palm oil is a tropical cash crop with high demand on the global market. The monetary value of palm oil continues to encourage smallholder farmers (≤ 2 ha) and private- and state-owned companies (≥ 2 ha) to cultivate oil palms. Currently, research is identifying ways of improving oil-palm management practices with the objective of reusing the same plantation sites. This is of relevance because many oil-palm plantations in Sumatra are on the verge of being replanted. Furthermore, this could also reduce the need to convert more pristine forests.

The aim of this thesis was to investigate the impact of rainforest conversion into oil-palm plantations on stocks of mobile Si and its interacting Si phases in soils and further, to identify measures to sustain plant-soil-Si cycling in this land-use system. The study was conducted in smallholder oil-palm plantations established in two different water regimes (well-drained and riparian areas) in Jambi Province, Indonesia. Four objectives were investigated: i) assessing the current state of soil Si pools under oil-palm plantations, ii) examining, whether oil-palm management practices have caused differing topsoil Si levels within an oil-palm plantation, iii) identifying processes (e.g., erosion or harvest) potentially altering Si cycling under oil-palm cultivation and iv) estimating Si storage, return and losses within oil-palm plantations to present a first Si balance. The objectives were analyzed in three independent studies. The results are as follows:

Si availability and Si fluxes in two water regimes: our data could not provide statistical evidence that Si fluxes differed significantly between well-drained and riparian areas. In fact, soil Si pools and plant Si contents in various oil-palm components were similar or only showed a tendency of higher Si availability in riparian areas. This suggests that an additional influx of dissolved Si by stream water or flooding could be negligible in the soil-plant system under oil-palm cultivation. Alternatively, it could

also imply that Si uptake by oil-palm roots is similar in both water regimes, thereby offsetting a potentially larger Si supply. As Si uptake by oil-palm roots is poorly researched, further analysis would be needed to verify either theory.

Principal drivers of Si cycling under smallholder oil-palm plantations: Si cycling under oil-palm plantations could be mainly driven by biogenic-amorphous silica (i.e., phytoliths alongside silicious microorganisms in topsoils) and mobile Si (i.e., Si in soil solution) at the soil-plant interface. This can be explained by the presence of easily soluble phytoliths occurring in topsoils, litter, and oil-palm biomass. If topsoils were maintained well and a cover crop left in every interrow, Si cycling under oil-palm plantations may potentially be self-sufficient. Nevertheless, Si in soil solution is also replenished by less soluble soil Si pools in minor quantities – in topsoils, mainly by Si bound to organic matter and in subsoils mainly by Si occluded in pedogenic oxides and hydroxides.

Si balance: the data from all three studies enabled us to propose a Si balance for smallholder oil-palm plantations established in well-drained areas: a mature oil palm could store 4 – 5 kg of Si, a smallholder oil-palm plantation in our study area about 570 – 680 kg of Si ha⁻¹. Roughly 0.06 kg of Si could be returned to soil by a pruned dead frond. In one year, pruning and subsequent stacking was estimated to return 110 – 130 kg of Si ha⁻¹ to soil under frond piles. In contrast, a single fruit bunch could store 0.02 – 0.07 kg of Si. In 2015 and 2018, annual fruit bunch harvest (1 ha smallholder plantation) resulted in Si losses of 30 – 70 kg of Si ha⁻¹. Topsoil erosion from vegetation-scarce interrows involved additional Si losses in the range of 5 – 9 kg Si ha⁻¹. A Si-balance was only proposed for well-drained areas as Si concentrations were similar in both water regimes and estimating Si storage, return and losses involved aboveground biomass data based on well-drained sites, as well.

Recommended measures: based on differing topsoil Si concentrations observed in four different management zones (palm circles, oil-palm rows, interrows and frond piles) of an oil-palm plantation, the following measures could maintain or even increase Si levels in soils under smallholder oil-palm plantations in our study area: i) preventing surface sealing (study 1); ii) maintaining a cover crop (e.g., grass and sedges) in vegetation-scarce interrows and returning empty fruit bunches to the palm circle to serve as an organic fertilizer (study 2); iii) suggesting to distribute chipped oil-palm stem parts prior to replanting the same plantation sites (study 3) and iv) ensuring a spatially more even Si return from decomposing palm fronds to soils, e.g., by changing the position of frond-piles every 5 – 10 years (studies 2, 3).

Future research could address Si uptake mechanisms by oil-palm roots, as this could broaden the understanding of Si cycling under oil-palm cultivation.

Zusammenfassung

Silizium (Si) ist nach Sauerstoff (O₂) das zweithäufigste Element in der Erdkruste. Si in Verbindung mit O₂ bildet eine Gruppe gesteinsbildender Minerale – die Silikate. In Gesteinen kommt Si als primäre Silikate (u.a. Quarz, Feldspäte, Glimmer) vor, in Böden, infolge von Verwitterung und Mineralneubildung, hauptsächlich als sekundäre Silikate (u.a. Tonminerale) oder Kieselsäure. Für einige Pflanzen ist Si ein wichtiges Element. In Böden kann Si Phosphor (P) mobilisieren oder Al-Toxizität vorbeugen. In Pflanzen erhöht Si die Resilienz von Pflanzen gegenüber Trockenstress, da es in verschiedenen Zellkomponenten der Blätter abgelagert wird und folglich die Transpiration verringert. Um dem Klimawandel entgegenzuwirken und Ernährungssicherheit zu gewährleisten, wird in der Forschung nach weiteren Möglichkeiten gesucht, die Fruchtbarkeit von Böden vor allem unter Plantagenbewirtschaftung zu erhalten. Ausgewogene Si-Gehalte in Oberböden könnten sowohl Ernteerträge als auch die Resilienz von Pflanzen gegenüber Trockenstress erhöhen. In Südost-Asien hat diese Thematik eine besondere Relevanz, da in dieser Region drei Parameter zusammentreffen: stark verwitterte, (desilifizierte), tropische Böden; ein erhöhtes Risiko von Trockenstress für Nutzpflanzen aufgrund kürzerer Regenzeiten in den Tropen; sowie ein großflächiger Anbau von Reis (*Oryza sativa*), Zuckerrohr (*Saccharum officinarum*) und Ölpalmen (*Elaeis guineensis*), die zur Gruppe der Si-akkumulierenden Pflanzen gehören. Bisher wurde für Reis nachweislich gezeigt, dass neben gewöhnlichen Pflanzennährstoffen (z. B. N, P, K, Ca, Mg), auch nennenswerte Gehalte an Si im Boden verfügbar sein müssten. Es ist anzunehmen, dass dies auch auf die Ölpalme zutrifft.

Indonesien ist der zweitgrößte Palmölproduzent der Welt. Im Jahr 2022 war eine Fläche von ca. 16 Mio. ha mit Ölpalmen bewirtschaftet, meist als Monokultur. Man unterscheidet vier Bewirtschaftungszonen in einer Ölpalmmonokultur: (1) der gedüngte und gejätete Bereich, unmittelbare um den Palmenstamm (*palm circles*), (2) unbehandelte Ölpalmreihen (*oil-palm rows*), (3) Zwischenreihen, die mit Pestiziden aber nicht Düngemitteln behandelt werden und als Zuwege dienen (*interrows*) und (4) Zwischenreihen, in denen abgeschnittene Palmwedel zur Kompostierung gestapelt werden (*frond piles*).

In Indonesien ist Sumatra stark von der Umwandlung von Tieflandregenwäldern und Agroforsten in Ölpalmplantagen betroffen. Palmöl ist eine tropische Nutzpflanze mit weltweit hoher Nachfrage. Daher besteht ein Anreiz für Kleinbauern (≤ 2 ha) und private und staatliche Unternehmen (≥ 2 ha), weiterhin Ölpalmplantagen anzulegen. Die Forschung ist bestrebt, die Bewirtschaftung von Ölpalmplantagen nachhaltiger zu gestalten, sodass Plantagenstandorte wiederverwendet werden können. Für Sumatra ist dies besonders relevant, da im kommenden Jahrzehnt viele Ölpalmplantagen neu angelegt werden müssten. Ferner könnten Primär- und Sekundärwälder durch verbesserte Maßnahmen geschützt werden.

In dieser Arbeit wurden Auswirkungen von Landnutzungsänderungen von Tieflandregenwäldern in Kleinbauern-Ölpalmplantagen auf Si-Vorräte in Böden untersucht. Hierbei wurde der Si-Kreislauf näher betrachtet mit dem Ziel: i) den Ist-Zustand an pflanzenverfügbarem Si in Böden unter Ölpalmplantagen zu quantifizieren, ii) zu bewerten, ob oder inwiefern bisherige Ölpalmbewirtschaftung den Si-Kreislauf verändert hat, iii) Prozesse zu identifizieren, die zu Si-Verlusten oder Si-Zufuhr unter dieser Landnutzung geführt haben und iv) eine Si-Bilanzierung für das System Kleinbauer-Ölpalmplantage zu erstellen. Das Untersuchungsgebiet liegt in der Provinz Jambi in Sumatra. Es wurden Ölpalmplantagen mit terrestrischen (well-drained area) und semi-terrestrischen (riparian area) Böden untersucht. Die Ziele wurden in drei unabhängigen Studien analysiert und ergaben folgende Ergebnisse:

Si-Zufuhr und Si-Verluste in Abhängigkeit von der Hydrologie: es konnten keine signifikanten Unterschiede in der Si-Verfügbarkeit zwischen terrestrischen und semi-terrestrischen Böden erkannt werden. Si-Vorräte in Böden sowie Si-Gehalte in verschiedenen Biomassekomponenten der Ölpalme hatten ähnliche Werte. Lediglich eine Tendenz zu höheren Si-Vorräten im Oberboden konnte bei semi-terrestrischen Böden beobachtet werden. Dies könnte bedeuten, dass die Zufuhr von gelöstem Si durch Grund- oder Stauwasser entweder als vernachlässigbar angesehen werden kann oder dass das überschüssige, gelöste Si nicht von den Wurzeln der Ölpalme aufgenommen werden kann. Die Si-Aufnahme von Ölpalmwurzeln könnte unter beiden hydrologischen Bedingungen ähnlich sein. Da die Si-Aufnahme durch Ölpalmenwurzeln nur unzureichend erforscht ist, wären weitere Studien erforderlich.

Si-Kreislauf: Unter Ölpalmpflanzungen wird biogene Kieselsäure (d.h. Phytolithe und nebensächlich, kieselhaltige Mikroorganismen im Oberboden) vermutlich bevorzugt mobilisiert und liefert der Bodenlösung reichlich Si. Phytolithe sind leicht löslich und kommen im Oberboden, der Streu und der oberirdischen Biomasse von Ölpalmen in nennenswerten Mengen vor. Auch schwer lösliche Si pools in Böden können Si in geringeren Mengen mobilisieren – in Oberböden erfolgt die Nachlieferung hauptsächlich durch organisch gebundenes Si, im Unterboden, durch in pedogenen Oxiden und Hydroxiden gebundenes Si. Ein intakter Oberboden und der Verbleib von Vegetation in Zwischenreihen, könnte ausgewogene Si-Gehalte in Oberböden unter Ölpalmpflanzungen gewährleisten.

Si-Bilanzierung: eine Si-Bilanzierung konnte für Kleinbauer-Ölpalmenpflanzungen (im Untersuchungsgebiet auf terrestrischen Böden) erstellt werden: eine Ölpalme könnte zwischen 4 - 5 kg Si in der Biomasse speichern, eine Pflanzung zwischen 570 - 680 kg Si ha⁻¹. Ein abgeschnittener Palmwedel speichert etwa 0,06 kg Si. In Zwischenreihen, in denen abgeschnittene Palmwedel zur Kompostierung gestapelt werden (frond piles), könnten innerhalb eines Jahres schätzungsweise 110 - 130 kg Si ha⁻¹ dem Boden zurückgeführt werden. Ein einzelner Fruchtstand kann etwa 0,02 - 0,07 kg Si speichern. In den Jahren 2015 und 2018 führte die jährliche Ernte von Fruchtständen (1 ha Kleinbauer-Pflanzung) zu Si-Verlusten von 30 - 70 kg Si ha⁻¹. Zusätzlich führte Oberbodenerosion in kargen Zwischenreihen zu weiterem Si-Verlust von 5 - 9 kg Si ha⁻¹.

Maßnahmen: Um eine ausgewogene Si-Versorgung in Böden in unserem Untersuchungsgebiet zu gewährleisten, wären folgende Maßnahmen förderlich: i) Vermeidung einer Oberbodenversiegelung (Studie 1); ii) Beibehaltung von Vegetation (z. B., verschiedene Gräser) in ungedüngten Zwischenreihen sowie die Verwendung von Fruchtständen als organischer Dünger (Studie 2); iii) Verwendung von Ölpalmbiomasse (vor allem vom Stamm) als organischen Dünger vor einer Neubepflanzung derselben Pflanzungsstandorte; iv) Kompostierung der Palmwedel in Zwischenreihen, die derzeit als ungedüngte Zwischenreihen und Zuwege dienen.

Weitere Studien zur Si-Aufnahme durch Ölpalmwurzeln könnten zu einem besseren Verständnis des Si-Kreislaufes unter Ölpalmpflanzungen beitragen.

List of figures and tables

Chapter 1 General Introduction

- Figure 1.1 Study area in Sumatra, Indonesia
Figure 1.2 Context figure addressing thesis aim

Chapter 2 Effects of turning rainforest into oil-palm plantations on silicon pools in soils within the first 20 years after the transformation

- Figure 2.1 Si concentrations in Acrisols under two land-use/land-cover systems
Figure 2.2 Si concentrations in Stagnosols under two land-use/land-cover systems
Table 2.1 Soil classification of study plots
Table 2.2 Si stocks of six Si fractions in Acrisols and Stagnosols

Chapter 3 Oil-palm management alters the spatial distribution of amorphous silica and mobile silicon in topsoils

- Figure 3.1 Sketch of oil-palm plantations and sediment traps
Figure 3.2 Topsoil Si_M and Si_{Am} concentrations
Figure 3.3 Weekly losses of eroded soil and Si_{Am} in eroded soil
Table 3.1 Topsoil Si_{Am} concentrations in interrows and sediment trap samples
Table 3.2 Annual losses of topsoil and Si_{Am} through erosion

Chapter 4 Estimating oil-palm Si storage, Si return to soils and Si losses through harvest in smallholder oil-palm plantations of Sumatra, Indonesia

- Figure 4.1 Sketch of oil-palm morphology and phyllotaxis
Figure 4.2 Si concentrations in oil-palm parts
Figure 4.3 Correlation of Si concentration with palm-frond age
Figure 4.4 Estimated Si storage, return and losses from smallholder oil-palm plantations
Table 4.1 Sampling scheme and number of sample replicates
Table 4.2 Calculation of Si storage, return and losses from smallholder oil-palm plantations

Chapter 5 General discussion

- Figure 5.1 Synthesis figure: Si balance for well-drained smallholder oil palm plantations

Abbreviations

Silicon and Si fractions

Si	Silicon (element)
SiO ₂	Silica (natural occurrence in terrestrial ecosystems)
SiO ₂ * nH ₂ O	Hydrated silicious bodies (e.g., phytoliths)
Si _M	Mobile Si pool (i.e., Si in soil solution)
Si _{Ad}	Si adsorbed to the surfaces of soil particles
Si _{Org}	Si bound in soil organic matter (SOM)
Si _{Occ}	Si occluded in pedogenic oxides and hydroxides
Si _{Ba}	Biogenic-amorphous silica
Si _{Pa}	Pedogenic-amorphous silica
Si _{Am}	Amorphous silica (refers to both Si _{Ba} and Si _{Pa})

Other abbreviations

LULC	Land-use/land-cover
OP	Oil-palm plantation
LR	Lowland rainforest
FB	Fruit bunch
FFB	Fresh fruit bunch
HO	Well-drained research plots (smallholder oil-palm plantations)
HOr	Riparian research plots (smallholder oil-palm plantations)
HF	Well-drained research plots (lowland rainforest)
HFr	Riparian research plots (lowland rainforest)

Table of contents

Acknowledgements	I
Summary	II
Zusammenfassung	IV
List of figures and tables	VI
Abbreviations	VII
1 General Introduction.....	1
1.1 Context	1
1.1.1 Silicon in terrestrial ecosystems	1
1.1.2 Indonesia and the expansion of oil-palm plantations	2
1.1.3 Impacts of rainforest conversion and resulting research topics	2
1.2 Research aim and objectives	4
1.3 Approach and thesis structure	6
1.4 References	8
2 Effects of turning rainforest into oil-palm plantations on silicon pools in soils within the first 20 years after the transformation.....	11
2.1 Introduction	12
2.2 Materials and methods.....	14
2.2.1 Study area and sampling scheme.....	14
2.2.2 Methods	15
2.3 Results	18
2.3.1 Soil classification and soil characteristics	18
2.3.2 Silicon stocks per hectare in soils under oil-palm plantations and rainforest.....	20
2.3.3 Silicon concentrations in soils under oil-palm plantations and rainforest	20
2.4 Discussion	24
2.4.1 Has 20 years of oil-palm cultivation caused soil Si depletion?	24
2.4.2 Are oil-palm plantations in riparian areas less prone to soil Si depletion?.....	28
2.5 Conclusion.....	29
2.6 Acknowledgements	29
2.7 Author contributions.....	29
2.8 References	30
3 Oil-palm management alters the spatial distribution of amorphous silica and mobile silicon in topsoils	36
3.1 Introduction	37
3.2 Material and methods	39
3.2.1 Study area and sites	39
3.2.2 Study design and sampling	39

3.2.3	Determination of silicon pools in topsoils.....	41
3.2.4	Statistical analyses.....	42
3.3	Results	42
3.3.1	Concentrations of Si_{Am} and Si_M in topsoils.....	42
3.3.2	Topsoil erosion and associated losses of Si_{Am}	45
3.4	Discussion	49
3.4.1	Spatial topsoil Si_{Am} concentration patterns.....	49
3.4.2	Si_{Am} losses through topsoil erosion	50
3.4.3	Spatial topsoil Si_M concentration patterns	51
3.5	Conclusions and recommended measures	52
3.6	Acknowledgements	53
3.7	Author contributions.....	53
3.8	References	54
4	Estimating oil-palm Si storage, Si return to soils and Si losses through harvest in smallholder oil-palm plantations of Sumatra, Indonesia	59
4.1	Introduction	60
4.2	Materials and methods.....	62
4.2.1	Study area	62
4.2.2	Study design and plant sampling.....	63
4.2.3	Extraction methods.....	65
4.2.4	Estimating Si storage in the aboveground biomass of oil palms and 1 hectare of plantation	66
4.2.5	Statistics.....	69
4.3	Results	69
4.3.1	Si and Ca concentrations in oil-palm parts.....	69
4.3.2	Si storage in the aboveground biomass of oil palms, Si return to soils through decomposing pruned palm fronds, and Si losses through harvest on smallholder oil-palm plantations	72
4.4	Discussion	72
4.4.1	Si distribution and accumulation in various oil-palm parts.....	72
4.4.2	Identified Si storage, cycling, and losses on smallholder oil-palm plantations, and favourable management practices	74
4.5	Conclusion.....	76
4.6	Acknowledgements	77
4.7	Author contribution	77
4.8	References	78
5	General discussion.....	83
5.1	Synthesis and key findings	83

5.1.1 Si fluxes and Si uptake mechanisms in differing water regimes	84
5.1.2 Principal drivers of Si cycling under oil-palm cultivation.....	84
5.2 Recommendations and outlook	85
5.3 References	87
Appendices	88

1 General Introduction

1.1 Context

1.1.1 Silicon in terrestrial ecosystems

Silicon (Si) is the second most abundant element in the Earth's crust. In rocks, Si fractions are present in crystalline forms, i.e., Si mainly occurs as primary silicates (e.g., quartz, feldspars, micas). In soils, the variety of Si fractions is much larger (Sauer et al. 2006): Si occurs as hardly weatherable primary silicates (e.g., quartz), secondary silicates (e.g., clay minerals) and amorphous silicious precipitates of biogenic or pedogenic origin (e.g., phytoliths, silicious microorganisms in topsoils or soil-particle coatings and void infillings, respectively). Further, Si can also be adsorbed to soil-particles and pedogenic oxides and hydroxides or be dissolved in soil solution (Sauer et al. 2006). Among all fractions, dissolved Si in soil solution is the only form which can be taken up by plants, i.e., it is readily plant-available Si (mobile Si pool) (Epstein 2009). During soil formation, soil Si pools are formed (Sommer et al. 2006). They can be distinguished into easily soluble (mostly amorphous) or hardly soluble (mostly bound or occluded) pools (Frayse et al. 2009). In terrestrial ecosystems, it is the soil Si pools which are the link between the geosphere and the biosphere because Si released into soil solution from various crystalline or amorphous pools can be taken up by plants (Epstein 2009). In addition, it is the non-crystalline Si fractions, which primarily drive terrestrial Si cycling, in a time-frame relevant to address agricultural research questions.

In agriculture, assessing the Si status in crops and their underlying soils has been receiving more attention: first, for maintaining high crop yields, which is of utmost economic interest. Second, for providing drought resistance, which is a major challenge worldwide due to climate change (Schaller et al. 2020). Due to its beneficial effects, Si is regarded as an “essential element” for plants (Epstein 2009; Liang et al. 2015). In soils, Si can mobilize phosphorous (P) by occupying anion adsorption sites. Si also mitigates plant toxicity by binding toxic cations such as aluminium (Al), cadmium (Cd), and arsenic (As) that become mobile at low soil pH (Street-Perrott and Barker 2008; Schaller et al. 2020). In plants, Si can increase drought resistance by precipitating in cell walls, cell lumen and intercellular spaces of leaves thereby reducing transpiration (Epstein 2009).

Assessing the Si status in soils and plants, or even potential uses of Si as a fertilizer, are particularly of interest in SE Asia because three parameters come together in this region: highly weathered tropical soils (i.e., desilicated soils), drought risk due to shorter rainy seasons and crop plants, which are Si accumulators such as rice (*Oryza sativa*), sugarcane (*Saccharum officinarum*) and oil palm (*Elaeis guineensis*). Si-accumulating plants, characterized by having > 1 % Si by dry weight in leaf tissue, require well-balanced Si levels in soils alongside common plant nutrients (e.g., N, P, K, Ca, Mg) (Ma and Takahashi 2002). While it is already common practice to provide Si fertilization for rice and

sugarcane if planted on Si depleted soils (Matichenkov and Calvert 2002; Haynes 2017), there have hardly been any investigations on the soil and plant Si status for oil palms (Munevar and Romero 2015).

1.1.2 Indonesia and the expansion of oil-palm plantations

Historically, the Indonesian archipelago has always attracted international trade. This is due to Indonesia's richness in old growth forests, natural resources, exotic spices, and tropical crops (Laumonier 1997; Tsujino et al. 2016). Sumatra, the second largest island within the Indonesian archipelago (~1.3x the size of Germany), was under Dutch rule from the late 17th century until Indonesia's independence in 1945 (Laumonier 1997). It was the Dutch colonists, who first planted crops such as rubber (*Hevea brasiliensis*) and oil palm (*Elaeis guineensis*) in plantations in the Eastern lowlands on Sumatra at the beginning of the 20th century (Penot 2004; Corley and Tinker 2016).

In the 1950s, the forest cover in Indonesia was estimated at 85 % (Tsujino et al. 2016). Sumatra's forests were still largely intact (Supriatna et al. 2017). In Sumatra, noticeable deforestation started as of the 1970s when Indonesia granted logging concessions to international businesses (Tsujino et al. 2016) and farmers relocated to Jambi and Lampung Province in Sumatra as a consequence of a governmental transmigration policy, requiring more land for agriculture (McCarthy and Cramb 2009; Gatto et al. 2015; Tsujino et al. 2016). In the late 1980s, the versatile use of palm oil, e.g., vegetable oil, cosmetics, and biofuels, was rapidly increasing demand. As a result, many smallholder farmers transformed previous rubber plantations, degraded forests areas or fallow land into oil-palm plantations (Qaim et al. 2020). The emerging palm oil boom led to clearing of rainforests (Tsujino et al. 2016; Qaim et al. 2020). Palm oil has remained a profitable cash crop (FAO 2020). By the 2010s, about 40 % of the oil-palm plantations were managed by smallholders (≤ 2 ha) in Jambi Province and 60 % by private or state-owned companies (≥ 2 ha) (Euler et al. 2016). Nowadays, the tropical rainforest is limited to national parks and restoration forests (Harrison and Swinfield 2015).

1.1.3 Impacts of rainforest conversion and resulting research topics

Tropical rainforests are among the most diverse ecosystems worldwide. They have many essential ecosystem functions, of which (1) regulating the climate by reducing greenhouse gas emissions and (2) sequestering large quantities of soil organic carbon (SOC) are most well-known (Dislich et al. 2017). Converting tropical lowland rainforests into more profitable cash-crop systems (e.g., oil palm rubber and timber) involves many ecological changes (Drescher et al. 2016; Dislich et al. 2017). Rainforest conversion to oil-palm plantations has decreased biodiversity and ecosystem services (Dislich et al. 2017; Grass et al. 2020), including many essential soil functions (Guillaume et al. 2015; Kurniawan et al. 2018; Hennings et al. 2021). For oil-palm plantations established on sloping terrain., Guillaume et al. (2015) observed decreased stocks of soil organic carbon (SOC) and identified topsoil erosion as a prominent process. In the same study area, Kurniawan et al. (2018) measured higher

nutrient leaching rates from soils under oil-palm plantations. This is crucial as tropical soils as such are highly weathered and nutrient poor soils (Zech et al. 2014) and land-use change might increase the risk of nutrient deficiency.

Under humid-tropical climate conditions, silicate weathering and element leaching from soils occurs, including leaching of plant nutrients and Si, i.e., the soils are naturally desilicified (Haynes 2014). Thus, the soils consist mostly of quartz, low-activity clays such as kaolinite, sesquioxides such as iron (Fe) – aluminium (Al) oxides, and hydroxides (Zech et al. 2014). Plant nutrients and organic matter are predominantly confined to the top few centimetres in topsoils, whereas quartz, kaolinite and sesquioxides are found in the subsoil (Lal 1986). Under humid-tropical climate conditions, litter is also decomposed rapidly by microorganisms, termites, and ants present in the topsoil. This implies that nutrients released from litter into topsoil can be readily taken up again by plants, rather than being stored as larger nutrient stocks in soils (Zech et al. 2014). If the rainforest vegetation is cleared by means of logging or formerly slash-and-burn practices, most nutrients are lost from the ecosystem (Lal 1986) or only partially returned (von der Lühne et al. 2020). To compensate for nutrient deficiency in soils, adequate management practices such as adding fertilizers are required to sustain high crop yields (Maranguit et al. 2017; Darras et al. 2019). Establishing suitable management strategies for smallholder farmers is challenging, as they may vary management practices according to their individual means.

As palm oil remains a current cash crop and consequently a major factor in Indonesia's economy, high palm oil yields are of great importance. This could be achieved by dedicating more pristine land to establish new oil-palm plantations. Alternatively, research is seeking to identify ways of improving oil-palm management with the objective of reusing the same plantation sites (Darras et al. 2019). This would require improving oil-palm management practices or identifying complementary measures (Dislich et al. 2017; Grass et al. 2020). Assessing the Si status in the plant-soil system under oil-palm plantations in Indonesia could result in finding such a complementary measure.

1.2 Research aim and objectives

The aim of this thesis was to investigate the impact of rainforest conversion into oil-palm plantations on stocks of mobile Si and its interacting Si phases in soils and further, to identify measures to sustain plant-soil-Si cycling under smallholder oil-palm plantations in Jambi Province, Indonesia (Fig. 1.1). Therefore, this thesis had the following objectives:

- 1) To assess the current Si status in soils under oil-palm plantations and lowland rainforest and evaluate whether 20 years of oil-palm cultivation has noticeably decreased stocks of different soil Si fractions (**study 1**)
- 2) To determine if current oil-palm management practices have caused a Si concentration pattern in topsoils, i.e., differing topsoil Si concentrations in four oil-palm management zones such as palm circles, oil-palm rows, interrows and frond piles (**study 2**)
- 3) To identify processes such as topsoil erosion, surface runoff, soil compaction (**study 2**) and human impacts such as fruit harvesting (**study 3**) leading to Si losses from oil-palm plantations
- 4) To estimate Si storage, return and losses within oil-palm plantations and evaluate, whether additional management practices have been identified, worth implementing in the future (**study 3**)

All studies were conducted in two different water regimes – well-drained areas versus riparian areas – to assess the parameter *hydrology* in every aforementioned objective. We distinguished water regimes because either corresponded to a prevalent soil type (Acrisol vs. Stagnosols) and topographic position (slope vs. floodplain) and could therefore affect Si fluxes and pools. The study is associated to the CRC-990 investigating long-term effects of rainforest conversion into plantation systems in Indonesia regarding environmental and socioeconomic aspects (Dislich et al. 2017; Grass et al. 2020; Qaim et al. 2020). Analyzing Si cycling under oil-palm plantations will provide a better understanding concerning environmental ecosystem services and potential measures for oil-palm management. This study is of relevance as many oil-palm plantations are soon being replanted for a next generation in Sumatra.

1 General Introduction

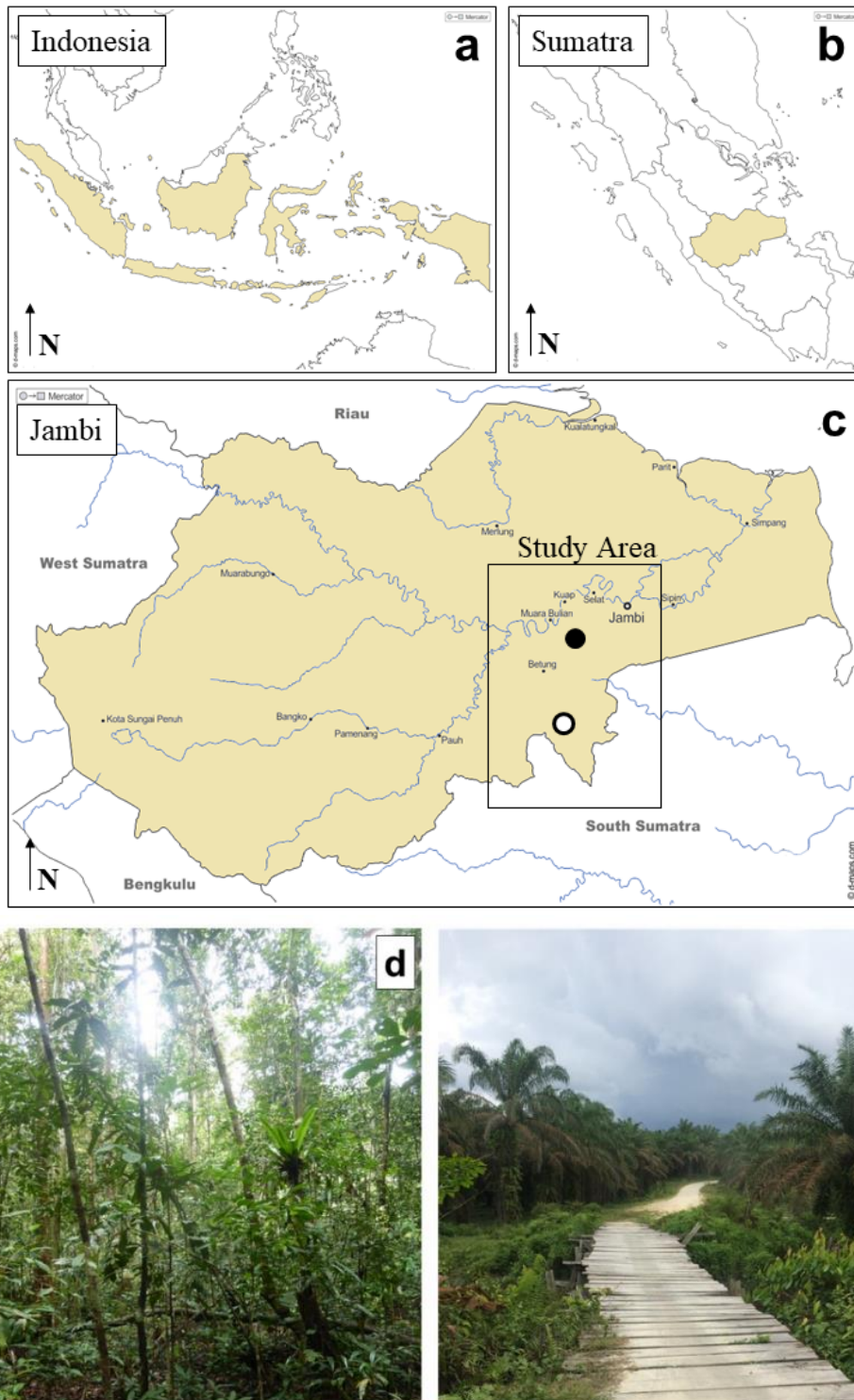


Fig. 1.1 (a-c) Fieldwork was conducted in the Harapan region of Jambi Province, in Sumatra, Indonesia on plots established by the CRC-990 (Collaborative Research Center-990, EForTs) under (d) lowland rainforest and (e) smallholder oil-palm plantations. Oil-palm plots are indicated by the black dot and lowland rainforest plots by the white dot. Maps created with <http://d-maps.com/pays>.

1.3 Approach and thesis structure

To accomplish our aims in this thesis we conducted three independent studies (Fig. 1.2). In the first study, we investigated the effects of land-use/land-cover (LULC) change from lowland rainforests to smallholder oil-palm plantations on Si pools in soils. We compared two soil types in two different water regimes under rainforest and oil-palm plantations. Soil sampling was conducted during a 4-months field campaign. In the laboratory, we quantified stocks of Si in each soil horizon following a sequential Si extraction procedure (Georgiadis et al. 2013; Barão et al. 2014). The results from this study would enable estimating the Si status of soils under both LULC systems and assessing if 20 years of oil-palm cultivations has led to a depletion of soil Si pools.

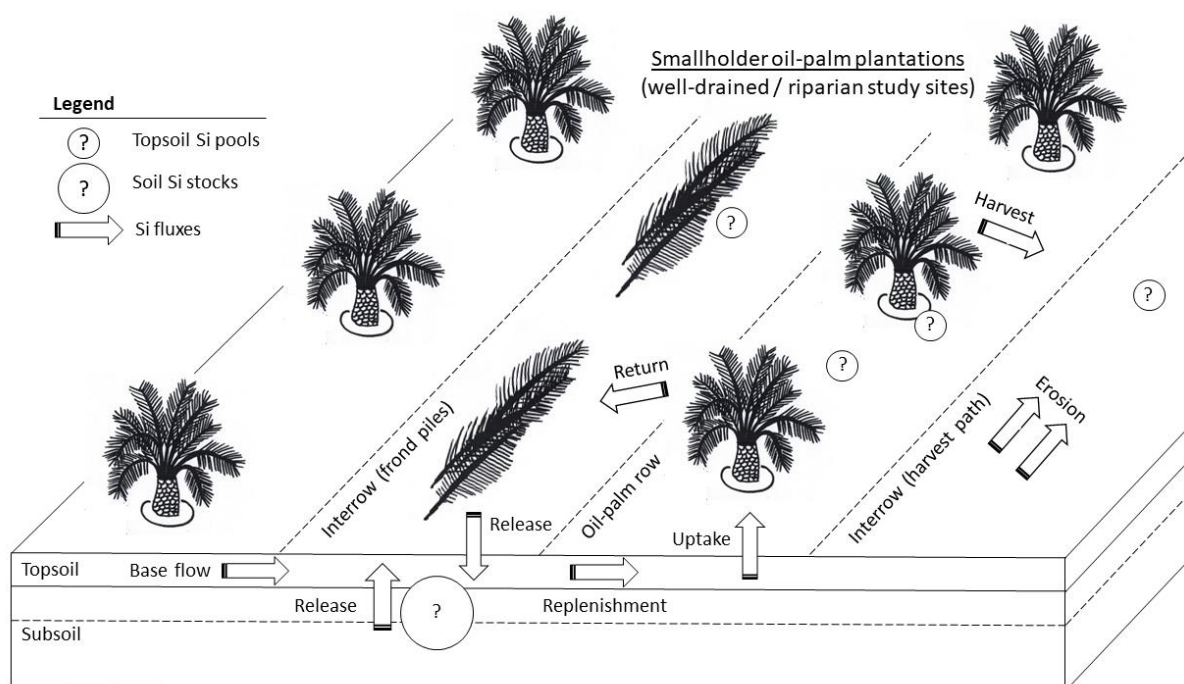


Fig. 1.2 Si cycling in the soil-plan system under smallholder oil-palm plantations with yet poorly studied Si fluxes and Si pools.

In the second study, we investigated whether two essential Si pools, mobile Si and Si in amorphous Si, varied in their concentration within the plantations. During the same 4-months field campaign, we took topsoil samples from four distinct management zones (palm circles, oil-palm rows, interrows and frond piles) within mature oil-palm plantations. In the laboratory, we quantified mobile and amorphous Si by CaCl_2 and NaOH extraction, respectively, (Georgiadis et al. 2013; Meunier et al. 2014). In addition, we conducted a 1-year field experiment to assess the amount of topsoil erosion and its associated losses of amorphous Si in eroded soil material in oil-palm plantations established on sloping terrain. This study would allow us to infer if management practices caused these changes and if erosion was a prominent process on the plantations.

In the third study we wanted to assess whether fruit bunch harvest from oil palms contributed to noticeable Si losses. For this purpose, we conducted a second 3-months field campaign in Jambi Province, Sumatra, to sample various oil-palm components such as palm fronds, fruit bunches and frond bases attached to the oil-palm stem from mature oil-palm plantations. In the laboratory, the Si content in all oil-palm components was determined by the 1 % Na_2CO_3 method after Meunier et al. (2014) and Saccone et al. (2007). We distinguished between harvest and non-harvest components, hence quantifying Si storage, return and losses from oil-palms and oil-palm plantations.

The synthesis attempts to provide a first mechanistic understanding of Si cycling in the soil-plant system under oil-plan plantations, thereby including storage potentials and fluxes (return, recycling, and losses) (Fig 1.2). We aim to understand in which way these various Si fractions interact within the soil-plant Si cycle. This could be taken as a basis to evaluate if the Si cycle has changed under oil-palm cultivation or whether additional management practices have been identified, worth implementing in the future.

This thesis is written as a cumulative thesis. Chapters 2 – 4 include the conducted studies, which are all presented as scientific manuscripts. Chapter 5 will provide a synthesis of the conducted studies, highlighting the key findings and give a conclusive outlook for recommended measures in oil-palm management. Future research topics within this field of research are also addressed. The formatting style of submitted, accepted and published manuscripts was edited to align with the thesis format.

1.4 References

- Barão L, Clymans W, Vandevenne F, et al (2014) Pedogenic and biogenic alkaline-extracted silicon distributions along a temperate land-use gradient. *Eur J Soil Sci* 65:693–705. <https://doi.org/10.1111/ejss.12161>
- Corley RHV, Tinker PBH (2016) *The Oil Palm (World Agricultural Series)* fifth edition, 647 pp., <https://doi.org/10.1017/cbo9781316530122.010,2016>
- Darras KFA, Corre MD, Formaglio G, et al (2019) Reducing Fertilizer and Avoiding Herbicides in Oil Palm Plantations—Ecological and Economic Valuations. *Front For Glob Chang* 2:1–15. <https://doi.org/10.3389/ffgc.2019.00065>
- Dislich C, Keyel AC, Salecker J, et al (2017) A review of the ecosystem functions in oil palm plantations, using forests as a reference system. *Biol Rev* 92:1539–1569. <https://doi.org/10.1111/brv.12295>
- Drescher J, Rembold K, Allen K, et al (2016) Ecological and socio-economic functions across tropical land use systems after rainforest conversion. *Philos Trans R Soc B Biol Sci* 371:20150275. <https://doi.org/10.1098/rstb.2015.0275>
- Epstein E (2009) Silicon: its manifold roles in plants. *Ann Appl Biol* 155:155–160. <https://doi.org/10.1111/j.1744-7348.2009.00343.x>
- Euler M, Schwarze S, Siregar H, Qaim M (2016) Oil Palm Expansion among Smallholder Farmers in Sumatra, Indonesia. *J Agric Econ* 67:658–676. <https://doi.org/10.1111/1477-9552.12163>
- FAO (2020) *Oilseeds, oils & meals*
- Fraysse F, Pokrovsky OS, Schott J, Meunier J-D (2009) Surface chemistry and reactivity of plant phytoliths in aqueous solutions. *Chem Geol* 258:197–206. <https://doi.org/10.1016/j.chemgeo.2008.10.003>
- Gatto M, Wollni M, Qaim M (2015) Oil Palm Boom and Land-Use Dynamics in Indonesia: The role of Policies and Socioeconomic Factors. *Land use policy* 46:292–303. <https://doi.org/10.1016/j.landusepol.2015.03.001>
- Georgiadis A, Sauer D, Herrmann L, et al (2013) Development of a method for sequential Si extraction from soils. *Geoderma* 209:251–261. <https://doi.org/10.1016/j.geoderma.2013.06.023>
- Grass I, Kubitzka C, Krishna V V., et al (2020) Trade-offs between multifunctionality and profit in tropical smallholder landscapes. *Nat Commun* 11:1–13. <https://doi.org/10.1038/s41467-020-15013-5>
- Guillaume T, Damris M, Kuzyakov Y (2015) Losses of soil carbon by converting tropical forest to plantations: erosion and decomposition estimated by $\delta^{13}\text{C}$. *Glob Chang Biol* 21:3548–3560. <https://doi.org/10.1111/gcb.12907>
- Harrison RD, Swinfield T (2015) Restoration of logged humid tropical forests: An experimental programme at Harapan Rainforest, Indonesia. *Trop Conserv Sci* 8:4–16. <https://doi.org/10.1177/194008291500800103>
- Haynes RJ (2017) The nature of biogenic Si and its potential role in Si supply in agricultural soils. *Agric Ecosyst Environ* 245:100–111. <https://doi.org/10.1016/j.agee.2017.04.021>
- Haynes RJ (2014) A contemporary overview of silicon availability in agricultural soils. *J Plant Nutr Soil Sci* 177:831–844. <https://doi.org/10.1002/jpln.201400202>
- Hennings N, Becker JN, Guillaume T, et al (2021) Riparian wetland properties counter the effect of

- land-use change on soil carbon stocks after rainforest conversion to plantations. *Catena* 196:104941. <https://doi.org/10.1016/j.catena.2020.104941>
- Kurniawan S, Corre MD, Matson AL, et al (2018) Conversion of tropical forests to smallholder rubber and oil palm plantations impacts nutrient leaching losses and nutrient retention efficiency in highly weathered soils. *Biogeosciences* 15:5131–5154. <https://doi.org/10.5194/bg-15-5131-2018>
- Lal R (1986) Conversion of tropical rainforest: agronomic potential and ecological consequences. *Adv Agron* 39:173–264. [https://doi.org/10.1016/S0065-2113\(08\)60468-X](https://doi.org/10.1016/S0065-2113(08)60468-X)
- Laumonier Y (1997) The Vegetation and Physiography of Sumatra. In: *Geobotany*. Kluwer Academic Publishers, p 223, <https://doi.org/10.1007/978-94-009-0031-8>
- Liang Y, Nikolic M, Bélanger R, et al (2015) *Silicon in Agriculture*. Dordrecht: Springer
- Ma JF, Takahashi E (2002) Silicon-accumulating plants in the plant kingdom. In: *Soil, fertilizer, and plant silicon research in Japan*. Elsevier Science, Amsterdam, pp 63–71
- Maranguit D, Guillaume T, Kuzyakov Y (2017) Land-use change affects phosphorus fractions in highly weathered tropical soils. *Catena* 149:385–393. <https://doi.org/10.1016/j.catena.2016.10.010>
- Matichenkov V V., Calvert D V. (2002) Silicon as a beneficial element for sugarcane. *J Am Soc Sugarcane Technol* 22:21–29
- McCarthy JF, Cramb RA (2009) Policy narratives, landholder engagement, and oil palm expansion on the Malaysian and Indonesian frontiers. *Geogr J* 175:112–123. <https://doi.org/10.1111/j.1475-4959.2009.00322.x>
- Meunier JD, Keller C, Guntzer F, et al (2014) Assessment of the 1% Na₂CO₃ technique to quantify the phytolith pool. *Geoderma* 216:30–35. <https://doi.org/10.1016/j.geoderma.2013.10.014>
- Munevar F, Romero A (2015) Soil and plant silicon status in oil palm crops in Colombia. *Exp Agric* 51:382. <https://doi.org/10.1017/S0014479714000374>
- Penot E (2004) From shifting agriculture to sustainable rubber agroforestry systems (jungle rubber) in Indonesia: a history of innovations processes. In: *Beyond tropical deforestation*. pp 221–250
- Qaim M, Sibhatu KT, Siregar H, Grass I (2020) Environmental, Economic, and Social Consequences of the Oil Palm Boom. *Annu Rev Resour Econ* 12:1–24. <https://doi.org/10.1146/annurev-resource-110119-024922>
- Sauer D, Saccone L, Conley DJ, et al (2006) Review of methodologies for extracting plant-available and amorphous Si from soils and aquatic sediments. *Biogeochemistry* 80:89–108. <https://doi.org/10.1007/s10533-005-5879-3>
- Schaller J, Frei S, Rohn L, Gilfedder BS (2020) Amorphous silica controls water storage capacity and phosphorus mobility in soils. *Front Environ Sci* 8:94. <https://doi.org/10.3389/fenvs.2020.00094>
- Sommer M, Kaczorek D, Kuzyakov Y, Breuer J (2006) Silicon pools and fluxes in soils and landscapes - a review. *J Plant Nutr Soil Sci* 169:310–329. <https://doi.org/10.1002/jpln.200521981>
- Street-Perrott F. A, Barker PA (2008) Biogenic silica: a neglected component of the coupled global continental biogeochemical cycles of carbon and silicon. *Earth Surf Process Landforms* 33:1436–1457. <https://doi.org/10.1002/esp.1712>
- Supriatna J, Dwiyaheni AA, Winarni N, et al (2017) Deforestation of primate habitat on Sumatra and adjacent Islands, Indonesia. *Primate Conserv* 31:71–82

Tsujino R, Yumoto T, Kitamura S, et al (2016) History of forest loss and degradation in Indonesia. *Land use policy* 57:335–347. <https://doi.org/10.1016/j.landusepol.2016.05.034>

von der Lühe B, Pauli L, Greenshields B, et al (2020) Transformation of Lowland Rainforest into Oil-palm Plantations and use of Fire alter Topsoil and Litter Silicon Pools and Fluxes. *Silicon* 13:4345–4353. <https://doi.org/10.1007/s12633-020-00680-2>

Zech W, Schad P, Hintermaier-Erhard G (2014) *Böden der Welt: ein Bildatlas*, 2. Auflage. Springer-Verla

2 Effects of turning rainforest into oil-palm plantations on silicon pools in soils within the first 20 years after the transformation

Britta Greenshields¹, Barbara von der Lüche¹, Harold J. Hughes¹, Aiyen Tjoa², Nina Hennings³, Daniela Sauer¹

¹Department of Physical Geography, University of Göttingen, Göttingen, Germany

²Faculty of Agriculture, Tadulako University, Palu, Indonesia

³Department of Agroecosystems, University of Göttingen, Göttingen, Germany

Corresponding author: Barbara von der Lüche

Submitted manuscript – Frontiers in Environmental Science

Abstract. Potential effects of land-use/land-cover (LULC) transformation from lowland rainforest into oil-palm plantations on silicon (Si) pools in tropical soils remain poorly understood, although well-balanced levels of plant-available Si in soils may contribute to maintain high crop yields and increase the vitality and drought resistance of oil palms. Therefore, the aim of our study was to identify possible effects of such LULC change on soil Si pools. For this purpose, we compared soil Si pools under lowland rainforest and about 20-year-old oil-palm plantations in Jambi Province, Indonesia. The investigated soils were Acrisols and Stagnosols, in which we quantified six different soil Si pools following a sequential extraction procedure to evaluate, whether 20 years of oil-palm cultivation has led to a depletion of these soil Si pools. The considered pools included mobile Si, adsorbed Si, Si bound in soil organic matter (SOM), Si included in pedogenic oxides and hydroxides, and Si in amorphous silica of biogenic and pedogenic origin. Finally, we also determined total Si. All oil-palm plantations established on sloping terrain and Acrisols only showed decreased Si stocks of mobile Si, adsorbed Si and SOM-bound Si; those established in floodplains and Stagnosols had decreased stocks of SOM-bound Si and biogenic-amorphous silica. Lower Si stocks were mostly attributed to a missing “stable” phytolith pool in the subsoil and less organic matter in topsoils under oil-palm plantations. When comparing well-drained and riparian areas, flooding seemed to increase phytolith dissolution. We conclude that 20 years of oil-palm cultivation has not yet led to a significant depletion of soil Si pools. As topsoils comprise the highest concentrations of SOM-bound Si and Si in amorphous silica of biogenic origin but are susceptible to erosion and surface runoff under managed oil-palm plantations, it would be advisable to instate specific management practices that maintain organic-rich and well-aired topsoils on oil-palm plantations.

Keywords: oil-palm plantation, rainforest, land-use/land-cover change, silicon pools, silicon extraction, tropical soils

2.1 Introduction

Jambi Province in Sumatra, Indonesia, has a long history of crop cultivation, including e.g., rubber, oil palm, sugar cane, coffee, and tea (FAO 2020). Oil-palm (*Eleais guineensis*) cultivation increased noticeably in the 1980s after a governmental transmigration policy had been implemented (McCarthy and Cramb, 2009; Gatto et al., 2015; Tsujino et al., 2016). The economic value of palm oil became increasingly recognized as oil-palm cultivation required less labor, and cash yields per hectare exceeded those of rubber (Euler et al. 2015). Since then, lowland rainforest has been progressively converted to rubber and oil-palm plantations in Jambi Province (Clough et al., 2016; Drescher et al., 2016; Dislich et al., 2017), leading to reduced biodiversity (Kotowska et al., 2015; Nazarrreta et al., 2020) and ecosystem services (Dislich et al., 2017). With respect to soil functioning, this transformation resulted among others in decreased nutrient stocks and increased nutrient leaching (Guillaume et al., 2015; Allen et al., 2016; Kurniawan et al., 2018). Decreasing soil functioning may be mitigated by optimizing oil-palm management, e.g., adapting fertilizer applications, reducing herbicide application, and managing understory vegetation (Darras et al., 2019; Luke et al., 2019; Zemp et al., 2019; Woittiez et al., 2019; Grass et al., 2020).

Such improved oil-palm management practices could also include monitoring the levels of plant-available silicon (Si) in soils as Si is known to increase stress tolerance and crop yield (Epstein, 1994; Najihah et al., 2015; Schaller et al., 2018; Sirisuntornlak et al., 2020). In addition, Si can mitigate toxic effects of various elements in plants (Epstein, 1999). This effect of Si is particularly relevant in the tropics, where crops are often grown on highly weathered, acidic soils, because toxic ions (e.g., Al, Cd, and As) become increasingly soluble in soil solution below a pH of around 4 (Epstein, 1999). However, until present little is known about the status of soil Si pools under oil-palm plantations and how it is affected by land-use/land-cover (LULC) change.

Various practices affect ecosystem Si cycling during LULC change and may involve Si losses from the system. For instance, LULC change through deforestation (logging and/or fire) may enhance the amounts of Si released from soil (Conley et al., 2008; Struyf et al., 2010; von der Lühe et al., 2020), potentially resulting in temporarily increased Si leaching. High Si concentrations measured in topsoils and water seem to originate from the dissolution of plant-derived amorphous silica (Conley et al., 2008), although other Si fractions in soils may also release Si into soil solution (Sauer et al., 2006; Georgiadis et al., 2013a). Struyf et al. (2010) and Clymans et al. (2011b) detected noticeably lower Si concentrations and fluxes after centuries of soil cultivation (250 – 500 years) in watersheds of temperate ecosystems. Conley et al. (2008) already recognized a disruption in the Si cycle within 20 – 40 years after deforestation. Munevar and Romero (2015) suggested that oil-palm cultivation could lead to similar disruptions as described by Conley et al. (2008).

Plants take up Si as monosilicic acid (H_4SiO_4) from soil solution (Liang et al., 2015), whereby several crops such as rice, wheat, sugarcane, maize, and oil palm are referred to as Si accumulators (Ma and Takahashi, 2002; Matichenkov and Calvert, 2002; Liang et al., 2015; Munevar and Romero, 2015). Transpiration causes Si to precipitate in the biomass (Epstein, 1994; Carey and Fulweiler, 2016), partially in the form of cell-shaped amorphous silica bodies called phytoliths, which accumulate with time (Epstein, 1994). In an undisturbed environment, Si returns to soil through litterfall, whereby phytoliths accumulate in the topsoil (Lucas et al., 1993; Alexandre et al., 1997; Schaller et al., 2018). In oil-palm plantations, natural litterfall is disturbed by cutting off and stacking palm fronds in every second oil-palm row, a management practice referred to as frond-pile stacking (Dislich et al., 2017). Thus, the majority of biomass-bound Si returns to soil under frond piles, where phytoliths are released upon litter decomposition (von der Lühe et al., 2022; Greenshields et al., 2023). Additional disturbances of Si cycling may be caused by fruit harvest and topsoil erosion, which can both lead to Si export from the system (Vandevenne et al., 2012; Guntzer et al., 2012; Hughes et al., 2020; Puppe et al., 2021). Fruit bunches are collected immediately after harvesting to be further processed in a mill (Dislich et al., 2017). A lack in understory vegetation, which is often intentionally achieved by herbicide application, permits erosion of phytolith-enriched topsoil (Guillaume et al., 2015). In this way, an important source to replenish plant-available Si in soil solution in highly weathered tropical soils may be lost (Lucas et al., 1993; Derry et al., 2005; Cornelis et al., 2011; de Tombeur et al., 2020).

Based on the above-mentioned potential disturbances of Si cycling under oil-palm cultivation, our study addresses the question, how the transformation of lowland rainforest into oil-palm plantations affects Si pools in soils of two regionally very common Reference Soil Groups, Acrisols and Stagnosols (IUSS Working Group WRB, 2022). We hypothesized that soil Si pools are decreased under oil-palm plantations compared to lowland rainforest for two reasons:

- 1) Oil palms are considered Si-accumulating plants (Munevar and Romero, 2015) that take up substantial amounts of Si from soil solution. Thus, Si losses are to be expected through fruit-bunch harvest and management practices that return litter to soil only in certain areas of the plantation.
- 2) Oil-palm plantations that are kept free of understory vegetation are susceptible to topsoil erosion. As topsoils contain the highest amounts of phytoliths and SOM-bound Si, thus providing major sources of plant-available Si in soils (Conley et al., 2008), considerable Si losses are expected through topsoil erosion.

We further hypothesized that the Stagnosols in our study area, commonly found in riparian areas and lower landscape positions, are less prone to net Si depletion as they may receive dissolved Si through groundwater and slope water from higher landscape positions.

To test the above hypotheses, we quantified various soil Si pools using a sequential extraction method (Georgiadis et al., 2013b). We replaced the originally included extraction of Si from amorphous silica by a modified alkaline extraction technique (Barão et al., 2014a; Unzué-Belmonte et al., 2017).

2.2 Materials and methods

2.2.1 Study area and sampling scheme

2.2.1.1 Study area

The study area is in the Harapan region of Jambi Province, Sumatra, Indonesia (1° 55' 0'' S, 103° 15' 0'' E; 50 m ± 5 m NN). Geologically, the Harapan region is located within the South Sumatra basin, which is comprised of pre-Paleogene metamorphic and igneous bedrock that is covered by lacustrine and fluvial Neogene and Quaternary sediments (de Coster, 2006). The Harapan region has a humid-tropical climate (mean annual temperature ~ 27 °C; mean annual precipitation ~2230 mm) with a rainy season from December to March and a dry period from July to August (Drescher et al., 2016). The region is dominated by loamy Acrisols on hilltops and slopes (well-drained areas) and loamy to clayey Stagnosols in riparian areas (Table 2.1 and Appendix I, Table A1 and A2). The natural vegetation is tropical lowland rainforest (Laumonier, 1997), which, however, has largely disappeared and is almost exclusively found within the Harapan Rainforest - an ecosystem restoration concession in the South of the region (Harrison and Swinfield, 2015). Oil-palm plantations (smallholder-, private company-, and state-owned plantations of Indonesia), rubber monocultures, and rubber agroforestry systems constitute much of the rest of the region (Dislich et al., 2017).

2.2.1.2 Sampling scheme

Our study was conducted on smallholder oil-palm plantations, which typically comprise 2 ha and account for ~ 40 % of oil-palm plantations in the province (Dislich et al., 2017). Oil palms were planted in a triangular planting scheme between 1998 and 2008. Old palm fronds are cut off and stacked in every second row, called “interrow”. The remaining “empty” interrows are used as paths for oil-palm pruning, herbicide application, and fruit-bunch harvesting (Darras et al., 2019; Greenshields et al., 2023). Herbicides (e.g., glyphosate) are commonly sprayed every six months to clear understory vegetation in the interrows and NPK fertilizers are applied within the palm circle (Darras et al., 2019), i.e., the immediate circulate area (~ 2 m radius) surrounding the palm stem (Munevar and Romero, 2015).

Fourteen plots (50 x 50 m) established by the Collaborative Research Centre 990 EForTs (*Ecological and socioeconomic functions of tropical lowland transformation systems*) were selected for soil sampling. Eight plots were located in smallholder oil-palm plantations, whereby four were in well-drained areas (HO1–4) and four in riparian areas (HOR1–4). Another six plots were located in lowland rainforest, whereby again three were in well-drained areas (HF1, 3, 4) and three in riparian areas

(HFr1, 3, 4). Soil profiles (1 m depth) were established either in oil-palm rows (between two palm trees) or in interrows (between two palm rows). The soils were classified according to WRB (IUSS Working Group WRB, 2022). Soil samples were taken of each horizon, whereby horizons exceeding 20-25 cm were subdivided into two sampling depths (top, bottom). Bulk-density samples ($n = 4$ per horizon) were taken in 100 cm² steel cylinders. The samples were air-dried (40 °C, ~ 24 h), sieved (≤ 2 mm) and stored at room temperature until further analysis.

2.2.2 Methods

2.2.2.1 General procedure used to determine six soil Si fractions

We followed the sequential extraction procedure developed by Georgiadis et al. (2013) to extract different soil Si fractions. All extractions were conducted in two lab replicates. After each extraction step, the extract for analysis was obtained by centrifuging (5-15 min, 3000 rpm) and filtering the supernatant through ash-free paper filters (1-2 μ m). Between two subsequent extraction steps, soil samples were rinsed twice with deionized water (18.2 M Ω cm⁻¹) to remove any residues of the previous extractant and dried overnight at 45 °C.

Mobile Si (Si_M) and adsorbed Si (Si_{Ad}) were analyzed by the molybdenum blue method (Grasshoff et al., 2009) using an UV-VIS spectrophotometer (Lamda 40, Perkin Elmer, Ridgau, Germany) at 810 nm. SOM-bound Si (Si_{Org}) and Si occluded in pedogenic Fe-Al oxides and hydroxides (Si_{Occ}) were measured with an inductively coupled plasma atomic emission spectrometer (ICP-AES, iCap 7000, Thermo Fisher Scientific GmbH, Dreieich, Germany).

Mobile Si (Si_M)

Si_M is the Si fraction that is extractable by calcium chloride ($CaCl_2$) solution and is usually present in terrestrial environments as monomeric silicic acid (H_4SiO_4). The soil samples were mixed with 5 ml of 0.01 M $CaCl_2$ and then left shaking for 1 min h⁻¹ for 24 h on an overhead shaker.

Adsorbed Si (Si_{Ad})

Si_{Ad} is the Si fraction that is extractable by acetic acid (Georgiadis et al. 2013a). This extraction aims at determining the amount of silicic acid adsorbed to mineral surfaces (Sauer et al., 2006). The second extraction step was carried out in an analogous manner to the first step, but using 10 ml of 0.01 M acetic acid to extract Si_{Ad} .

Si bound in soil organic matter (Si_{Org})

Si_{Org} refers to Si that is released when soil organic matter (SOM) is oxidized by hydrogen peroxide treatment (Georgiadis et al. 2013a). Si_{Org} was obtained by treating the samples with 20 ml H_2O_2 (17.5 %) and letting the samples react at room temperature until the reaction subsided, typically within half

an hour. Then, an additional 10 ml H₂O₂ (35 %) was added. The samples were placed into a shaking hot water bath at 85 °C and left until the reaction ceased (up to 48 h).

Si occluded in Fe-Al oxides and hydroxides (Si_{occ})

Si_{occ} refers to Si that is released when Fe-Al oxides and hydroxides are dissolved with ammonium-acetate-oxalic acid and UV-light exposure (Georgiadis et al., 2013a). 50 ml of a solution containing 0.2 M ammonium-acetate and 0.14 M oxalic acid were added and samples were placed on an orbital shaker for 8 h, shaking for 1 min h⁻¹. After 8 h, the soil samples were exposed to UV-light while they were left on the orbital shaker for another 16 h, shaking for 1 min h⁻¹.

We used an alkaline extraction that was modified from Barão et al. (2014b) and Unzué-Belmonte et al. (2017) to extract Si from amorphous silica of biogenic and pedogenic origin. In detail, 0.4 l of 0.2 M NaOH solution was poured into a metal beaker, placed into a hot water bath, and heated to 75 °C. Once heated, the same soil sample that had already gone through the previous steps of the sequential Si extraction was added to the alkaline solution. The extraction was run for 45 min, while a stirrer continuously homogenized the solution. During the extraction, subsamples were taken with a fraction collector at 36 times, namely every 45 sec during the first 15 min of the extraction, every 90 sec during the second 15 min, and every 180 sec during the last 15 min. These subsamples were analyzed for Si and Al concentrations photometrically, using the molybdenum blue method and the eriochrome cyanine R method (Shull and Guthan, 1967). In the calibrations, R² = ≥ 0.99 was accepted for Si, and R² ≥ 0.98 was accepted for Al. The method was validated by adding known quantities of oil-palm phytoliths (extracted according to Parr et al. 2001) to soil samples. A precision of 98 % was reached.

Si in amorphous silica of biogenic and pedogenic origin (Si_{Ba} and Si_{Pa})

Si in amorphous silica can be of either biogenic (Si_{Ba}) or pedogenic (Si_{Pa}) origin and is considered the most readily mobilizable Si fraction in soils. Si_{Ba} mainly consists of Si from phytoliths alongside diatoms and other protozoic Si compounds (Sommer et al., 2006, 2013; Haynes, 2017). Si_{Pa} predominantly consists of siliceous Si coatings or void infillings (Sauer et al. 2015); Si_{Pa} can also be occluded within pedogenic Fe-Al oxides and hydroxides (Schaller et al., 2021). Si released from amorphous silica over time during an alkaline extraction can be quantified by solving a first-order mathematical model (Eq. 1) that accounts for the non-linear (first part of the equation) and the linear (second part of the equation) Si release from the residual soil sample material (Unzué-Belmonte et al., 2017).

$$\begin{aligned}
 Si_t (mg g^{-1}) &= \left(\sum_{n=1}^n AlkExSi_i x (1 - e^{-k_i x t}) \right) + b x t \\
 Al_t (mg g^{-1}) &= \left(\sum_{n=1}^n \frac{AlkExSi_i}{Si/Al_i} x (1 - e^{-k_i x t}) \right) + \frac{b x t}{Si/Al_{min}}
 \end{aligned}
 \tag{Eq. 1}$$

$AlkExSi_i$ is the non-linearly released Si from amorphous silica, Si_i and Al_i are the calculated concentrations of Si and Al at a given time, Si/Al_i is the fraction's Si/Al ratio, which is used to determine its origin, k is the fraction's specific Si-release rate constant, t defines the beginning of Si release, b is the non-linear Si intercept and $Si:Al_{min}$ the linear Si intercept. Detailed information on the calculation and computation using an open-access python script (<https://github.com/nschenkels/AlkExSi>, (Unzué-Belmonte et al. 2017)) is given in Unzué-Belmonte (2017). This method requires the analysis of both Si and Al concentrations to calculate AlkExSi (Eq. 1) and to determine Si/Al ratios. Si_{Ba} commonly has Si/Al ratios of ≥ 5 (Koning et al., 2002; Barão et al., 2014a; Unzué-Belmonte et al., 2017), whereas Si_{Pa} has Si/Al ratios of 1 – 4 (Koning et al., 2002). We attributed all amorphous fractions that displayed a dissolution curve typical for phytoliths to Si_{Ba} , even though some of these fractions had Si/Al ratios between 4 and 5.

2.2.2.2 Determination of total Si

We also determined total Si to evaluate, which proportion of total Si was present in those fractions that may serve as sources of readily plant-available Si. Total Si was determined on separately milled (tungsten carbide cups, 10 min, 2000 rpm) soil samples by alkaline fusion using lithium borate (DIN ISO 14869-2, 2003) and analysis by use of inductively coupled plasma atomic emission spectroscopy (ICP-AES).

2.2.2.3 Calculation of Si stocks per hectare

After converting the obtained results to Si concentrations in dry soil samples (105 °C, 24 h), Si stocks were first calculated horizon-wise for every Si pool according to Eq. 2.

$$Si \text{ stock } (Mg \text{ ha}^{-1}) = \frac{[Si] \times BD \times h}{10} \quad \text{Eq. 2}$$

[Si] is the Si concentration in $mg \text{ g}^{-1}$ dry soil, BD the bulk density in $g \text{ cm}^{-3}$, h the soil horizon thickness in cm and 10 is the conversion factor from $mg \text{ cm}^{-2}$ to $Mg \text{ ha}^{-1}$. In this way, we calculated stocks of the six Si fractions stored in each soil horizon within a soil profile. We then summed up the Si stocks of all horizons of a soil profile down to 1 m depth to compare potentially mobilizable Si stocks in soils under oil-palm plantations and lowland rainforest. Riparian areas are often drained before establishing an oil-palm plantation because oil palms cannot be cultivated on water-logged soils (Corley and Tinker, 2016). As we observed fine roots down to 1 m soil depth both in Acrisols and Stagnosols, indicating that the oil-palm can exploit nutrients over this soil depth, we calculated soil Si stocks down to 1 m depth for both WRB Reference Soil Groups.

2.2.2.4 Statistics

Soil profiles were grouped according to WRB Reference Soil Group and LULC type into (1) Acrisols under oil-palm plantations ($n = 5$), (2) Acrisols under lowland rainforest ($n = 4$), (3) Stagnosols under oil-palm plantations ($n = 3$), and (4) Stagnosols under lowland rainforest ($n = 2$). The level of

significance was set at $p \leq 0.05$. Data was tested for normal distribution (Shapiro-Wilk test) and for homogeneity of variances (Levene test). Due to an unbalanced sampling design, skewness and kurtosis in several Si stocks and a limited number of samples, non-parametric tests were used for statistical analysis. The Kruskal-Wallis test was used to detect significant differences between total Si stocks (Table 2.2). We used the open-source software R version 3.6.2 and R CRAN packages ggplot2 (Wickham, 2016), dplyr (Wickham et al., 2023), car (Fox and Weisberg, 2019), psych (Revelle, 2022), pastecs (Grosjean and Ibanez, 2018), and pgrimess (Giraudoux, 2022) to perform these statistical analyses.

2.3 Results

2.3.1 Soil classification and soil characteristics

All soils in the generally well-drained higher areas were classified as Acrisols (IUSS Working Group WRB 2022), both under oil-palm plantations and under lowland rainforest (Table 2.1 and Appendix I Tables A1 and A2). However, even in these higher areas, all soil profiles under lowland rainforest and half of the soil profiles under oil-palm plantations had stagnic properties at ≥ 50 cm soil depth (IUSS Working Group WRB, 2022), indicating that these Acrisols are periodically affected by perched water in their subsoil horizons (Appendix I Tables A1 and A2). Acrisols under both LULC types generally showed the following horizon sequence: Ah – A/E – (EA) – E – EB – Bt – Btg. Soils in riparian areas under both LULC types were mostly classified as Stagnosols. On plots HOr4 and HFr3 the soils were classified as Acrisols (Appendix I Table A1), although both plots were in riparian areas. This was because the CRC plot area designated for destructive research activities such as digging soil pits was located in a well-drained, higher landscape position within the plot. The Acrisol in HFr3 showed stagnic properties starting at a depth of 53 cm. The typical horizon sequence of the Stagnosols was Ah – Eg – Bg – (BEg) – Btg – (Btg1) – (Bgl), both under oil-palm plantations and lowland rainforest. Hydromorphic features of the soil profiles HOr1 – 3 and HFr4 included both iron-oxide mottles inside soil peds, indicating temporarily perched water, as well as iron-oxide precipitates around macropores and on ped surfaces, pointing to groundwater influence (Btg1 and Bgl horizons). Soil-chemical and soil-physical characteristics of the soil profiles are shown in Appendix I Table B1.

Table 2.1 Classification of oil palm and rainforest plots (PT REKI) in the Harapan landscape of Jambi Province in Sumatra, Indonesia.

LULC	Plot	RSG with pre- and suffixes	Soil horizons
Oil palm	HO1	Haplic Acrisol (Loamic, Cutanic, Ochric)	Ah-A/E-E-Bt-Btg1-Btg2-Btg3-Btgc
Oil palm	HO2	Endoferric Endostagnic Petroplinthic Acrisol (Loamic, Cutanic, Ochric)	Ah-A/E-Bt1-Bt2-Btg1-Btg2-Bvm-Bg
Oil palm	HO3	Haplic Acrisol (Loamic, Cutanic, Ochric, Profondic)	Ah-A/E-E-2Bt1-2Bt2
Oil palm	HO4	Endoprotostagnic Acrisol (Loamic, Cutanic, Ochric, Novic)	Ah-A/E-E/A-2AEB-2EB-2BE-2Bt-2Btg
Oil palm	HOr1	Acric Endogleyic Stagnosol (Loamic, Colluvic, Ochric)	Ah-Eg-Bg-2Btg1-2Btg2-2Btg
Oil palm	HOr2	Acric Albic Gleyic Stagnosol (Loamic, Ochric)	Ah-Eg-BEg-Btg1-Btg2
Oil palm	HOr3	Acric Gleyic Stagnosol (Loamic, Ochric, Loaminovic)	Ah-AE-BEg1-BEg2-2Btg1-2Btg2-2Bg11- 2Bg12
Oil palm	HOr4	Protostagnic Acrisol (Loamic, Cutanic, Ochric)	Ah-EA-BE-Bt1-Bt2-Btgc1-Btgc2
Rainforest	HF1	Stagnic Acrisol (Loamic, Cutanic, Ochric)	Ah-EA-B/E-Btg1-Btg2-Btg3
Rainforest	HF3	Stagnic Acrisol (Loamic, Cutanic, Densic, Ochric)	Ah-EA-E-Btg1-Btg2
Rainforest	HF4	Endostagnic Acrisol (Loamic, Cutanic, Ochric)	Ah-EA-E-Bt1-Bt2-Btg1-Btg2
Rainforest	HFr1	Gleyic Stagnosol (Loamic, Ochric)	Ah-EB-BEg-Bg11-Bg12
Rainforest	HFr3	Stagnic Acrisol (Loamic, Cutanic, Ochric)	Ah-E/A-E-Bt-Btg1-Btg2-Btg3
Rainforest	HFr4	Acric Gleyic Stagnosol (Loamic, Ochric)	Ah-Eg-Bg-Btg1-Btg

Table 2.2 Stocks [Mg ha⁻¹, 1 m soil profile] of six Si fractions and total Si in Acrisols and Stagnosols under oil-palm plantations and lowland rainforest.

LULC	RSG		\bar{X} Si _M	\bar{X} Si _{Ad}	\bar{X} Si _{org}	\bar{X} Si _{loc}
Oil palm	Acrisol	5	0.11 ± 0.04	0.16 ± 0.06	1.32 ± 0.51	3.70 ± 1.06
Rainforest	Acrisol	4	0.16 ± 0.03	0.20 ± 0.04	2.72 ± 1.42	2.54 ± 0.53
Oil palm	Stagnosol	3	0.20 ± 0.05	0.23 ± 0.06	2.10 ± 0.30	2.90 ± 0.04
Rainforest	Stagnosol	2	0.11 ± 0.05	0.14 ± 0.07	2.46 ± 1.28	1.63 ± 1.03
			\bar{X} Si _{Ba}	\bar{X} Si _{Pa}	\bar{X} Si _{total}	\bar{X} Sum of six fractions
Oil palm	Acrisol	5	3.50 ± 0.77	64.55 ± 28.93	73'092 ± 7'650	71.24 ± 27.63
Rainforest	Acrisol	4	1.89 ± 1.52	62.57 ± 24.41	101'077 ± 16'278	70.09 ± 24.66
Oil palm	Stagnosol	3	2.08 ± 1.53	54.52 ± 30.73	70'666 ± 18'110	62.04 ± 30.80
Rainforest	Stagnosol	2	7.98 ± 8.45	34.64 ± 1.73	113'727 ± 230	46.96 ± 9.14

Differences between Si stocks (Mg ha⁻¹, mean ± SE) were tested with the non-parameteric Kruskal-Wallice test. Significant differences were neither observed between any individual Si fraction under the two different LULC types, nor between any individual Si fraction in the two different WRB Reference Soil Groups. The sum of all determined Si fractions accounts for ≤ 0.1 % of total Si in these soils.

2.3.2 Silicon stocks per hectare in soils under oil-palm plantations and rainforest

The sum of all extractable Si fractions down to 1 m soil depth amounted to 47.0 – 71.3 Mg ha⁻¹, corresponding to ≤ 0.1 % of the total Si stocks in the soils (Table 2.1 and 2.2). In all soils, Si_{Pa} represented the largest Si stock (34.6 – 64.5 Mg ha⁻¹), followed by Si_{Ba} (1.9 – 8.0 Mg ha⁻¹), Si_{Occ} (1.6 – 3.7 Mg ha⁻¹), Si_{Org} (1.3 – 2.7 Mg ha⁻¹), and finally Si_{Ad} and Si_M (both together ≤ 0.3 Mg ha⁻¹) (Table 2.2).

Acrisols under oil-palm plantations tended to have lower stocks of Si_{Ad}, Si_M, Si_{Org}, and Si_{Ba}, compared to those under rainforest, however these observed differences were not significant ($p \leq 0.05$). Only the stocks of Si_{Org} under oil-palm plantations were significantly lower than those under rainforest (1.3 Mg ha⁻¹ versus 2.7 Mg ha⁻¹) at a level of significance of $p = 0.06$.

In the Stagnosols, only stocks of Si_{Org} and Si_{Ba} tended to be lower under oil-palm plantations compared to lowland rainforest, whereas stocks of all other Si fractions tended to be higher under oil-palm plantations. None of the Si stocks differed significantly ($p \leq 0.05$) between the two LULC types.

Under oil-palm cultivation, stocks of Si_M were twice as high (significant difference at $p = 0.06$) in Stagnosols compared to Acrisols, whereas stocks of Si_{Ad} and Si_{Org} were only slightly higher in Stagnosols than in Acrisols (0.23 Mg ha⁻¹ versus 0.16 Mg ha⁻¹ for Si_{Ad} and 2.1 Mg ha⁻¹ versus 1.3 Mg ha⁻¹ for Si_{Org}). Stocks of all other Si fractions were in a similar range in Stagnosols and Acrisols under oil-palm plantations. Under lowland rainforest, stocks of Si_{Pa} tended to be higher in Acrisols than in Stagnosols (63 Mg ha⁻¹ versus 35 Mg ha⁻¹), while stocks of Si_{Ba} tended to be higher in Stagnosols compared to Acrisols (8.0 Mg ha⁻¹ versus 1.9 Mg ha⁻¹). However, none of the Si stocks differed significantly ($p \leq 0.05$) between Stagnosols and Acrisols under rainforest.

2.3.3 Silicon concentrations in soils under oil-palm plantations and rainforest

2.3.3.1 Silicon concentrations with soil depth in Acrisols under two LULC types

Si_M and Si_{Ad} concentrations in Acrisols ranged from ~ 5 µg g⁻¹ to 15 µg g⁻¹ under both LULC types (Fig. 2.1a, b, g, h). Under lowland rainforest, both Si_M and Si_{Ad} concentrations showed a steady increase in their concentrations with soil depth (Fig. 2.1g, h), whereas the depth distribution of Si_M and Si_{Ad} was much more irregular under oil-palm cultivation (Fig. 2.1a, b).

Si_{Org} concentrations in Acrisols under lowland rainforest were highest (~ 0.4 – 0.6 mg g⁻¹) in the topsoils, i.e., in the Ah and AE horizons (Fig. 2.1i). In contrast, most Acrisols under oil-palm cultivation did not show such a Si_{Org} maximum in the topsoils; instead, Si_{Org} concentrations remained around ~ 0.1 – 0.2 mg g⁻¹ throughout the soil profile, except for the Acrisol in plot HO2 that showed a similar Si_{Org} maximum (~ 0.6 mg g⁻¹) in its Ah horizon (Fig. 2.1c).

2 Effects of turning rainforest into oil-palm plantations on silicon pools in soils

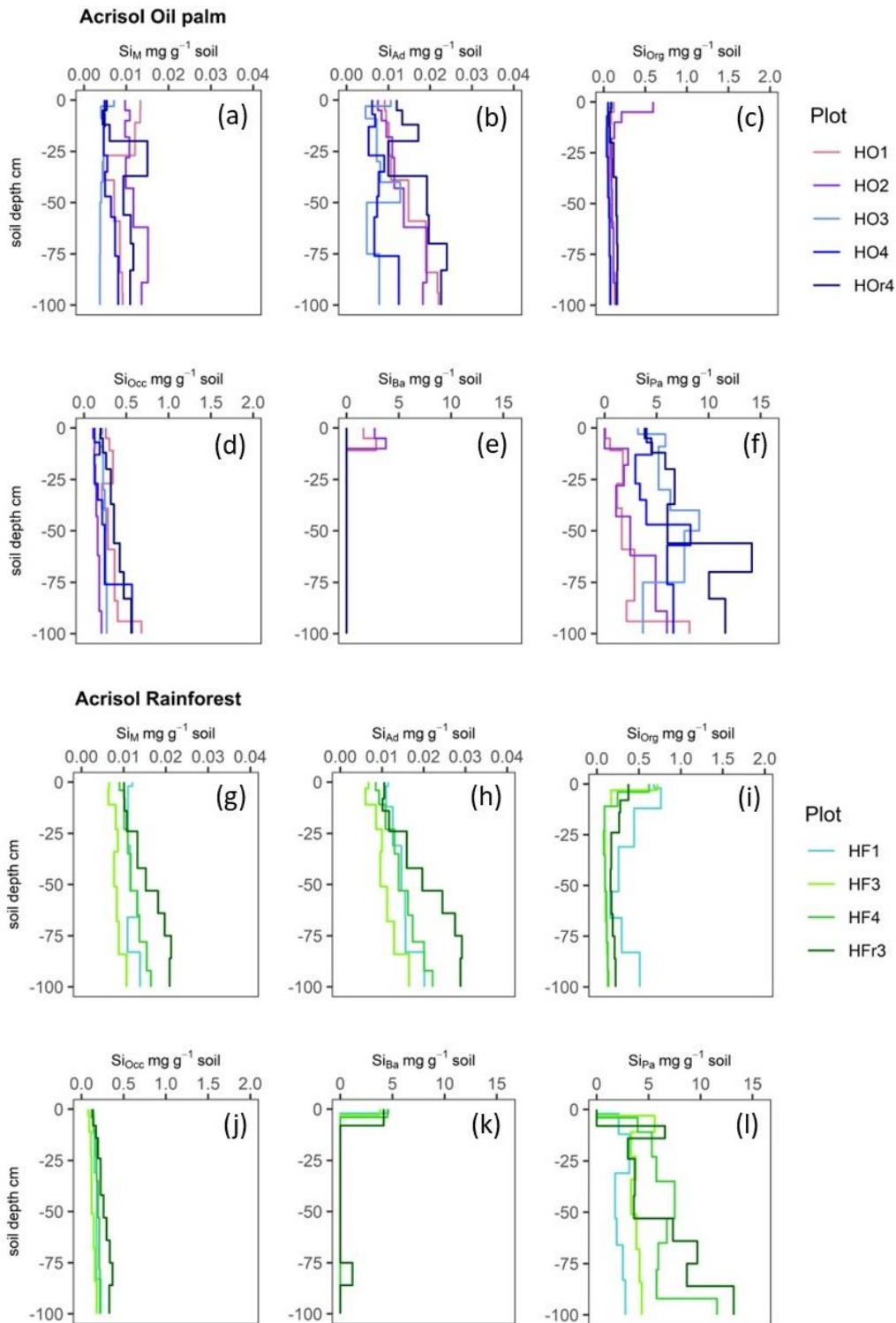


Fig. 2.1 Silicon (Si) concentrations (mg g^{-1} soil) of six Si fractions, including Si_M = mobile Si (**a, g**), Si_{Ad} = adsorbed Si (**b, h**), Si_{Org} = Si bound in soil organic matter (**c, i**), Si_{Occ} = Si occluded in pedogenic oxides and hydroxides (**d, j**), Si_{Ba} = Si in biogenic amorphous silica (**e, k**), Si_{Pa} = Si in pedogenic amorphous silica (**f, l**) in Acrisols under oil-palm plantations (plots: HO1-4, HO4) and rainforest (plots: HF1, HF3, HF4, HF3).

2 Effects of turning rainforest into oil-palm plantations on silicon pools in soils

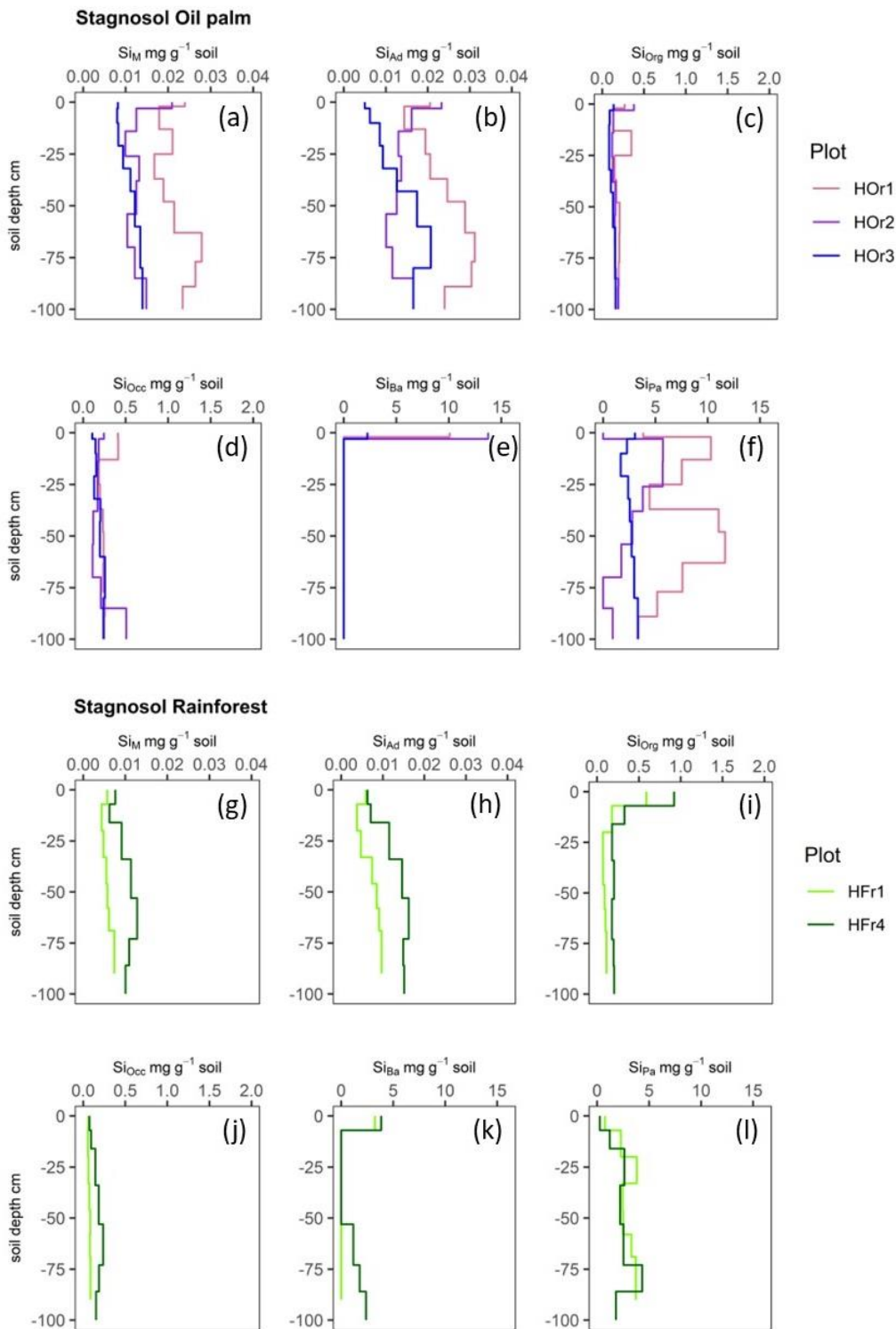


Fig. 2.2 Silicon concentrations (mg g^{-1} soil) of six Si fractions, including Si_M = mobile Si (a, g), Si_{Ad} = adsorbed Si (b, h), Si_{Org} = Si bound in soil organic matter (c, i), Si_{Occ} = Si occluded in pedogenic oxides and hydroxides (d, j), Si_{Ba} = Si in biogenic amorphous silica (e, k), Si_{Pa} = Si in pedogenic amorphous silica (f, l) in Stagnosols under oil-palm plantations (HOR1-3) and rainforest (HFR1, HFR4).

Si_{Occ} concentrations in Acrisols showed a steady increase with soil depth under both LULC types, which was somewhat weaker expressed under rainforest compared to oil-palm plantations (Fig. 2.1d, j). In Acrisols under oil-palm plantations, Si_{Occ} concentrations increased to $\geq 0.4 \text{ mg g}^{-1}$ in the second half meter soil depth in three out of five plots (HO1, HO4, and HOr4), while under lowland rainforest, Si_{Occ} concentrations remained below 0.4 mg g^{-1} in all four plots.

Si_{Ba} concentrations in all four Acrisol profiles under rainforest were highest in topsoils ($\sim 3.8 - 4.6 \text{ mg g}^{-1}$). Under oil-palm plantations, only the two Acrisols in plots HO1 and HO2 showed comparable Si_{Ba} maxima in topsoils ($1.6 - 3.8 \text{ mg g}^{-1}$). Si_{Ba} was not detectable in topsoils of the Acrisols in plots HO3, HO4, and HOr4. Most Acrisols had no Si_{Ba} in any other soil horizons apart from the topsoils. Plot HFr3 was an exception, which showed Si_{Ba} concentrations of $\sim 1.1 \text{ mg g}^{-1}$ in its Btg2 horizon, at 75 – 86 cm depth, as well.

Si_{Pa} stocks in the Acrisols ranged in the same order of magnitude ($0 - 13 \text{ mg g}^{-1}$) under both LULC types and partially tended to increase with soil depth (Fig. 2.1f, l). All four Acrisols under lowland rainforest had no Si_{Pa} in topsoils, while only one out of five Acrisols under oil-palm plantations had no Si_{Pa} in topsoils.

2.3.3.2 Silicon concentrations with soil depth in Stagnosols under two LULC types

Si_M and Si_{Ad} concentrations in Stagnosols under rainforest showed a slight to clear increase with depth, from $\sim 6 \mu\text{g g}^{-1}$ in the topsoils to $\sim 5 - 16 \mu\text{g g}^{-1}$ in the subsoils (Fig. 2.2g, h). Si_M and Si_{Ad} concentrations in Stagnosols under oil-palm plantations showed more irregular depth patterns, ranging between $\sim 5 - 24 \mu\text{g g}^{-1}$ in the topsoils and $\sim 10 - 31 \mu\text{g g}^{-1}$ in the subsoils (Fig. 2.2a, b).

Si_{Org} concentrations in Stagnosols under lowland rainforest showed clear maxima ($\sim 0.6 - 0.9 \text{ mg g}^{-1}$) in the topsoils and ranged around $\sim 0.1 - 0.2 \text{ mg g}^{-1}$ in the subsoils (Fig. 2.2i). Si_{Org} concentrations in Stagnosols under oil-palm plantations showed clear maxima to a lesser extent in the topsoils ($\sim 0.1 - 0.4 \text{ mg g}^{-1}$) and mostly low values ($\sim 0.1 - 0.2 \text{ mg g}^{-1}$) in the subsoils. Plot HOr1 showed a second Si_{Org} maximum ($\sim 0.4 \text{ mg g}^{-1}$) between 13 – 25 cm soil depth (Bg horizon) (Fig. 2.2c).

Si_{Occ} concentrations in Stagnosols under lowland rainforest were low ($\sim 0.06 - 0.24 \text{ mg g}^{-1}$) throughout the soil profile (Fig. 2.2j). Si_{Occ} concentrations in Stagnosols under oil-palm plantations were similarly low. Yet, they showed a somewhat more irregular depth distribution. The Stagnosol in plot HOr1 showed a maximum in the topsoil (0.4 mg g^{-1}); the one in plot HOr2 showed a maximum (0.5 mg g^{-1}) at 80 – 100 cm soil depth in its Btg2 horizon (Fig. 2.2d).

Si_{Ba} concentrations in Stagnosols under lowland rainforest showed clear maxima ($3 - 4 \text{ mg g}^{-1}$) in topsoils. The Stagnosol in plot HFr4 showed increasing Si_{Ba} concentrations up to 2.4 mg g^{-1} again from 53 cm downwards (Fig. 2.2k). Si_{Ba} concentrations in Stagnosols under oil-palm plantations showed a

very pronounced maximum in the topsoils (up to 13 mg g⁻¹), while Si_{Ba} was not at all detectable in any other soil horizons (Fig. 2.2e).

Si_{Pa} concentrations in Stagnosols under lowland rainforest were very low (0 – 0.25 mg g⁻¹) in the topsoils and varied between 1 mg g⁻¹ and 4 mg g⁻¹ in the subsoils (Fig. 2.2l). Si_{Pa} concentrations in Stagnosols under oil-palm plantations were in a range of 0.1 – 10 mg g⁻¹ in the topsoils and showed great variability in the subsoils, varying between 2 mg g⁻¹ and 12 mg g⁻¹ (Fig. 2.2f).

2.4 Discussion

2.4.1 Has 20 years of oil-palm cultivation caused soil Si depletion?

The soil Si pools that are part of biogeochemical Si cycling within oil-palm plantations and rainforests that were investigated in this study altogether made up less than 1 % of the total Si in soils, which is similar to the proportion in a temperate forest ecosystem (Cornu et al., 2022). All oil-palm plantations established on Acrisols in sloping terrain (Table 2.1) only showed a non-significant trend of decreased Si stocks of the soil Si fractions Si_M, Si_{Ad}, Si_{Org} and Si_{Ba} (Table 2.2, Fig. 2.1e, k), but no decrease of the larger pools Si_{Occ} and Si_{Pa}. Thereby, only the decrease in Si_{Org} stocks under oil-palm plantations was significant (p = 0.06). The studied oil-palm plantations established on Stagnosols in floodplains (Table 2.1) tended to have insignificantly decreased stocks of Si_{Org} and Si_{Ba} (Table 2.2, Fig. 2.2c, e). As no statistically significant differences were observed, our hypothesis that rainforest transformation into oil-palm plantations diminishes soil Si pools in Acrisols and Stagnosols was not verified.

2.4.1.1 Acrisols

Soil Si_M, Si_{Ad} and Si_{Org} stocks per hectare and depth distribution

The detected, slightly lower Si_M stocks in Acrisols under oil-palm plantations compared to rainforests were not significant. If they exist, they probably result from low Si_M concentrations in the subsoil horizons of the Acrisols under oil-palm plantations (Fig. 2.1a and g). Both rainforest trees (Lucas et al., 1993; Schaller et al., 2018) and oil palms (Munevar and Romero, 2015; Greenshields et al., 2022) can take up high amounts of Si from soil solution. Yet they differ in their rooting system (Vander Linden and Delvaux, 2019). Roots of rainforest trees either immediately exploit forest litter and the uppermost topsoil for nutrients, or tap into strongly weathered, deep subsoil horizons (up to 7 m soil depth) (Lucas et al., 1993; vander Linden and Delvaux, 2019). In contrast, the rooting system of most crops only reaches ~ 2 m soil depth and is less dense than the rooting system in a rainforest biome (Corley and Tinker, 2016; vander Linden and Delvaux, 2019). White et al. (2012) assumed that Si_M concentrations are similar across a soil profile if Si uptake rates of a plant are in equilibrium with Si leaching and Si discharge in pore water. Low Si_M concentrations throughout the entire soil profile in Acrisols under oil-palm plantations could therefore reflect such an equilibrium state (i.e., similar Si uptake and leaching rates). In contrast rainforest trees predominantly exploit nutrients in upper

horizons, leading to less Si uptake from the lower soil horizons. Furthermore, water percolation through soils, and hence leaching of Si_M , under oil-palm plantations should exceed that under rainforest, which is characterized by a dense, a multi-layered tree canopy.

Lower Si_{Ad} stocks in Acrisols under oil-palm plantations can be attributed to the equally low Si_M stocks in Acrisols under oil-palm plantations (Table 2.2) since Si_M and Si_{Ad} are in a dynamic equilibrium. Consequently, all Acrisols showed a very similar depth distribution in their Si_M and Si_{Ad} concentrations across the 1 m deep soil profiles (Fig. 2.1a, b, g, and h). Like the Si_M concentrations, Si_{Ad} concentrations were lower and much more variable in Acrisols under oil-palm plantations compared to lowland rainforest. Munevar and Romero (2015) made similar observations and showed that in three strongly weathered soil profiles, concentrations of plant-available Si increased with soil depth and were in a range of 73 – 90 mg Si kg⁻¹. This is in the same order of magnitude as our Si_{Ad} concentrations (30 – 197 mg Si kg⁻¹). Georgiadis et al. (2017) found concentrations of Si_M and Si_{Ad} to be strongly influenced by the presence or absence of pedogenic Fe and Al oxides and hydroxides. To a lesser extent, clay minerals may also serve as adsorption sites for Si_{Ad} (Georgiadis et al., 2014, 2017). As most Acrisols under oil-palm plantations (Table 2.1, plots HO2, HO4) and all Acrisols under lowland rainforest (Table 2.1, plots HF1, HF3 and HF4) showed stagnic properties in their subsoil horizons, the pedogenic oxides and hydroxides in these horizons offer abundant adsorption surfaces for Si in the studied Acrisols (Georgiadis et al., 2017). The relevance of this effect is supported by the observation that Si_{Ad} concentrations (Fig. 2.1b, h) show a clearer increase with soil depth than Si_M concentrations (Fig. 2.1a, g).

Earlier studies have shown that a further labile Si pool exists alongside phytoliths, which is activated during litter degradation (Watteau and Villemin, 2001; Schaller and Struyf, 2013). In our study, this additional labile pool is referred to as Si_{Org} , i.e., SOM-bound Si. Lower Si_{Org} stocks under oil-palm plantations compared to lowland rainforest may be attributed to plantation management practices that control the presence or absence of cover crops in oil-palm plantations. Si_{Org} showed diminished Si_{Org} concentrations in four out of five topsoil horizons of Acrisols under oil-palm plantations. In contrast, Si_{Org} concentrations were high in all topsoil horizons of Acrisols under lowland rainforest (Fig. 2.1c and i). This implies that Acrisol topsoils under rainforest have relevant amounts of soil organic matter, while many Acrisol topsoils under oil-palm plantations contain little or no soil organic matter. These observations correspond well to findings from Vander Linden and Delvaux (2019), von der L  he et al. (2022) and Greenshields et al. (2023). Vander Linden and Delvaux (2019) identified soil Si pools associated to topsoils (mainly phytogenic Si) as important soil Si pools in rainforest biomes. In oil-palm plantations, on the other hand, von der L  he et al. (2022) and Greenshields et al. (2023) found litter return and decomposition to be largely restricted to frond piles areas, which may make up as little as 15 % of a plantation (Tarigan et al., 2020). This is a crucial finding because the decomposition of palm fronds provides most plant-available Si to soils under oil-palm plantations. Litter return on oil-

palm plantations is additionally restricted because interrows are commonly kept free of vegetation, which prevents litter production, promotes topsoil erosion and promotes Si leaching from soils (Oliveira et al., 2013; Guillaume et al., 2015; Greenshields et al., 2023).

Increased Si_{Org} concentrations at greater soil depth in one plot under lowland rainforest (Fig. 2.1i, plot HF1) might be related to biological activity or tree uprooting in the past. Soils under tropical rainforest may genuinely be more heterogeneous than soils under plantation systems due to higher biological activity, e.g., by termites (Donovan et al., 2001). The Acrisol in plot HF1 showed a termite borrow at greater soil depth (Appendix I Table A1).

Soil Si_{Occ} , Si_{Ba} and Si_{Pa} stocks per hectare and depth distribution

High Si_{Occ} stocks in Acrisols may be explained by the abundance of pedogenic oxides and hydroxides (Georgiadis et al., 2017) as almost all studied Acrisols had stagnic properties at some depth. Two Acrisols under oil-palm plantations (HO1 and HO4) even contained a layer of Fe concretions at 75 and 90 cm soil depth, respectively, coinciding with higher Si_{Occ} concentrations (Fig. 2.1d) compared to the other Acrisols (HO2, HO3, HF1, 3-4) without such a layer.

Biogenic amorphous silica pools can be depleted after some decades (Barão et al., 2014b; Vandevenne et al., 2015; Unzué-Belmonte et al., 2017) or centuries (Struyf et al., 2010; Clymans et al., 2011) of cultivation. In oil-palm plantations, management practices that result in the presence or absence of cover crops seem to play a crucial role. In our study, the only two Acrisols in oil-palm plantations that had high Si_{Ba} concentrations in their topsoil horizons (HO1–2) were covered by grassy understory vegetation, securing phytolith production and return to the topsoils through the grass litter (Fig. 2.1c). In contrast, no Si_{Ba} was detected in any of the three oil-palm plots that were situated in cleared oil-palm interrows (HO3–4, HO4) (Fig. 1c, Appendix I Table A1). Oil-palm plantations contain up to 25% of other plant species, including grasses and sedges (Rembold et al., 2017). These plants can effectively return phytoliths to soils (Blecker et al., 2006; White et al., 2012; von der Lüche et al., 2022; Greenshields et al., 2023). In addition, protecting the soil surface by cover crops can prevent topsoil erosion. As phytoliths preferentially accumulate in topsoils (Conley et al., 2008), concentrations of Si_{Ba} in cleared oil-palm interrows (HO3, HO4, and HO4) could also have been diminished due to erosion. Guillaume et al. (2015) pointed out that topsoil erosion led to a loss of soil organic carbon (SOC) stocks in oil-palm monocultures (Alexandre et al., 1997; Schaller et al., 2018; Li et al., 2020), where clearing understory vegetation had been part of management practices. Thus, maintaining understory vegetation could not only benefit biodiversity (Luke et al., 2019), but also sustain SOC and stocks of nutrients (Guillaume et al., 2015) and biogenic Si.

Genuinely higher Si_{Ba} concentrations in Acrisols under rainforest (Fig. 2.1e, k) can be explained by the presence of phytoliths in the topsoils of all rainforest plots and in the subsoil of the Acrisol in plot HFr3 (Fig. 2.1k). The latter might be explained by a “stable” phytolith pool that may occur at greater

soil depth (Lucas et al., 1993; Alexandre et al., 1997; Li et al., 2020) if phytolith solubility has been decreased. Li et al. (2020) reported that phytoliths can be preserved in microaggregates. Alexandre et al. (1997) found preserved (“inactive”) phytoliths in the subsoil of a Ferrasol under a tropical rainforest and explained their presence by vertical translocation. Thereby, the preserved phytoliths made up $\leq 10\%$ of the estimated total phytolith pool. Lucas et al. (1993) and Fujii et al. (2018) suggested that microbial activity and ectomycorrhiza fungi can increase the dissolution of secondary silicates (clays) and phytoliths especially in the uppermost meter of a soil, (Fig. 2.1g, k). It is thus possible that a “stable” phytolith pool formed in the subsoil of the Acrisol in plot HFr3 under rainforest, e.g., through tree uprooting, which was then preserved because of the naturally low microbial activity at that depth.

Fairly similar Si_{Pa} stocks in Acrisols under oil-palm plantations and lowland rainforest were also reflected in a similar distribution of Si_{Pa} concentrations with depth under both LULC systems (Fig. 2.1f, l). Apparently, this fraction is more strongly controlled by other factors than land use. An increase of Si_{Pa} concentrations with depth may result from Si release during mineral weathering and dissolution of phytoliths in the topsoils and re-precipitation at some depth, e.g., as siliceous coatings on clay mineral and Fe-oxide surfaces (Lucas et al., 1993; White et al., 2012; Cornelis et al., 2014; Fujii et al., 2018). White et al. (2012) reported that shallow grass roots mainly took up Si from soil solution that had a biogenic Si source, whereas deeper roots predominantly extracted Si from soil solution that originally had a pedogenic Si source. This observation suggests that the Si_{Pa} pool, which in our study tended to increase with soil depth, may be also an important soil Si pool. This is the case especially for deeper-rooting trees that can exploit this deep pool and incorporate it in the Si cycling of the system.

2.4.1.2 Stagnosols

Soil Si_{Org} and Si_{Ba} stocks per hectare and depth distribution

Stagnosols in the riparian areas showed very similar Si_{Org} and Si_{Ba} stocks per hectare and Si_{Org} and Si_{Ba} depth trends compared to the Acrisols of the higher areas. Both Si_{Org} and Si_{Ba} are linked to the presence and decomposition of litter, which explains that both fractions showed clear maxima in the topsoils. Lower Si_{Org} stocks per hectare in Stagnosols under oil-palm plantations compared to Stagnosols under rainforest were directly linked with lower Si_{Org} concentrations in their topsoil horizons (Fig. 2.2c, i). Ah horizons of Stagnosols under oil-palm plantations were not only thinner than under lowland rainforest, but also received less litter. In oil-palm plantations, additional litter is provided by the decay of understory vegetation in oil-palm rows and interrows if management practices allow vegetation cover (Albert et al., 2006; Rembold et al., 2017; von der Lühe et al., 2020; Greenshields et al., 2023).

Lower Si_{Ba} stocks in Stagnosols under oil-palm plantations compared to lowland rainforest likely result from the shallowness of the (partially eroded) topsoils under oil-palm plantations that contain very high Si_{Ba} concentrations, as well as from the absence of any relevant Si_{Ba} concentrations in the subsoils of the Stagnosols under oil-palm plantations (Fig. 2.2e, k). Like Acrisols, Stagnosols under lowland rainforest may have an additional “stable” phytolith pool in the subsoil (Alexandre et al., 1997). High Si_{Ba} concentrations in the topsoils of Stagnosols under both LULC systems, with maximum Si_{Ba} concentrations in the topsoils of Stagnosols under oil-palm plantations, point towards a continuous provision and accumulation of phytoliths in the topsoils (Albert et al., 2006; Greenshields et al., 2023). The high Si_{Ba} concentrations in the shallow topsoils of the Stagnosols under oil-palm plantations can be explained by the fact that palm trees are Si accumulators and may thus produce more phytoliths than lowland rainforest trees (Albert et al., 2015). Besides palm trees (e.g., *Phoenix reclinata*, *Hyphaene petersiana*, *Eleais guineensis* Jacq.), grasses and sedges also produce abundant phytoliths that persist well in soil (Albert et al., 2006), which again points to the importance of a grassy vegetation cover in between the oil-palm rows.

Soil Si_M , Si_{Ad} , Si_{Occ} and Si_{Pa} stocks per hectare and depth distribution

The similarity of the Si_M , Si_{Ad} , Si_{Occ} , and Si_{Pa} stocks per hectare suggests that LULC change has barely affected these Si fractions in Stagnosols. The variability in the depth distributions of Si_M , Si_{Ad} , Si_{Occ} , and Si_{Pa} among the Stagnosols under oil-palm plantations was greater than the difference in the depth trends of these fractions between Stagnosols under the two LULC systems. This observation suggests that factors other than LULC (e.g., the depth distributions of pedogenic oxides and clay minerals) are more important in controlling these fractions than LULC. The only influence of land use on the depth patterns of Si fractions was detected for Si_{Pa} . The absence of this fraction in topsoils of all Stagnosols under rainforest (Fig. 2.2l) suggests that in undisturbed soils, the Si_{Pa} pool exclusively occurs in the subsoils. Si_{Pa} was absent in the topsoil of the Stagnosol in the oil-palm plot HOr2 but present in the topsoils of the Stagnosols in oil-palm plots HOr1 and HOr3 (Fig. 2.2f). This suggests that some anthropogenic mixing of topsoil and subsoil horizons occurred, probably in the course of establishing the oil-palm plantation.

2.4.2 Are oil-palm plantations in riparian areas less prone to soil Si depletion?

The only Si fractions that showed insignificantly larger stocks in Stagnosols in riparian areas compared to Acrisols of the higher landscape positions (both under oil-palm plantations), were the Si_M and Si_{Ad} fractions. These increased Si_M and Si_{Ad} stocks can be attributed to higher Si_M and Si_{Ad} concentrations across the whole soil profile (Fig. 2.1a, b, c and Fig. 2.2a, b, c). This may be due to Si_M influx to riparian areas by regular flooding or due to higher Si dissolution rates in riparian areas compared to well-drained areas. This latter explanation is supported by earlier studies, where

alternating redox conditions in soils explained higher phytolith dissolution rates in riparian areas (Georgiadis et al., 2017; vander Linden and Delvaux, 2019; Greenshields et al., 2023).

2.5 Conclusion

We conclude that 20 years of oil-palm cultivation has not yet caused soil Si depletion, although the oil palm is a Si-accumulating plant. Thus, the assumed depletion effect that we investigated was not proven in this study. All oil-palm plantations established on Acrisols in sloping terrain only showed insignificantly decreased Si stocks of mobile Si, adsorbed Si and SOM-bound Si; those established on Stagnosols in riparian areas had insignificantly decreased stocks of SOM-bound Si and biogenic amorphous silica. All soil Si pools together comprised less than 1 % of the total Si in the soils. Lower Si stocks of biogenic amorphous Si and SOM-bound Si were mostly attributed to a missing “stable” phytolith pool, very shallow, partially eroded Ah horizons and less organic matter in soils under oil-palm plantations, implying that topsoils are particularly vulnerable. When comparing well-drained and riparian areas, flooding seemed to increase Si_M and Si_{Ad} stocks, possibly directly and/or through enhanced phytolith dissolution. As our results lack statistically significant differences, both our hypotheses were not verified. Topsoils are susceptible to erosion under managed oil-palm plantations. It is therefore advisable to protect topsoils on oil-palm plantations by a dense understory vegetation cover.

2.6 Acknowledgements

We thank the Ministry of Forestry, Technology and Higher Education (RISTEKDIKTI), the Indonesian Institute of Sciences (LIPI) and the Ministry of Forestry (PHKA) for granting the research permit 110 / SIP / FRP / E5 / Dit.KI / IV / 2018 to conduct the soil sampling for this project. We thank our Indonesian counterparts, the CRC-990 office members, our fieldwork assistants and the laboratory staff of the Institute of Geography, Dr. Jürgen Grotheer, Ms. Petra Voigt, and Ms. Anja Södje. Without the support of all these colleagues, this work would not have been possible. We thank Dr. Thomas Guillaume for providing complementary soil data of oil-palm plantation sites.

2.7 Author contributions

BvL, DS, HH and AT developed the idea and concept for this project. BG conducted fieldwork and laboratory work with input from all co-authors. NH contributed complementary soil data. BG wrote the first draft of the manuscript. All co-authors contributed to improving earlier manuscript drafts.

2.8 References

- Albert RM, Bamford MK, Cabanes D (2006) Taphonomy of phytoliths and macroplants in different soils from Olduvai Gorge (Tanzania) and the application to Plio-Pleistocene palaeoanthropological samples. *Quat Int* 148:78–94. <https://doi.org/10.1016/j.quaint.2005.11.026>
- Albert RM, Bamford MK, Esteban I (2015) Reconstruction of ancient palm vegetation landscapes using a phytolith approach. *Quat Int* 369:51–66. <https://doi.org/10.1016/j.quaint.2014.06.067>
- Alexandre A, Meunier J-D, Colin F, Koud J-M (1997) Plant impact on the biogeochemical cycle of silicon and related weathering processes. *Geochim Cosmochim Acta* 61:677–682. [https://doi.org/10.1016/S0016-7037\(97\)00001-X](https://doi.org/10.1016/S0016-7037(97)00001-X)
- Allen K, Corre MD, Kurniawan S, et al (2016) Spatial variability surpasses land-use change effects on soil biochemical properties of converted lowland landscapes in Sumatra, Indonesia. *Geoderma* 284:42–50. <https://doi.org/10.1016/j.geoderma.2016.08.010>
- Barão L, Clymans W, Vandevenne F, et al (2014) Pedogenic and biogenic alkaline-extracted silicon distributions along a temperate land-use gradient. *Eur J Soil Sci* 65:693–705. <https://doi.org/10.1111/ejss.12161>
- Blecker SW, McCulley RL, Chadwick OA, Kelly EF (2006) Biologic cycling of silica across a grassland bioclimate sequence. *Global Biogeochem Cycles* 20:1–11. <https://doi.org/10.1029/2006GB002690>
- Carey JC, Fulweiler RW (2016) Human appropriation of biogenic silicon – the increasing role of agriculture. *Funct Ecol* 30:1331–1339. <https://doi.org/10.1111/1365-2435.12544>
- Clough Y, Krishna V V., Corre MD, et al (2016) Land-use choices follow profitability at the expense of ecological functions in Indonesian smallholder landscapes. *Nat Commun* 7:1–12. <https://doi.org/10.1038/ncomms13137>
- Clymans W, Struyf E, Govers G, et al (2011) Anthropogenic impact on amorphous silica pools in temperate soils. *Biogeosciences* 8:2281–2293. <https://doi.org/10.5194/bg-8-2281-2011>
- Conley DJ, Likens GE, Buso DC, et al (2008) Deforestation causes increased dissolved silicate losses in the Hubbard Brook Experimental Forest. *Glob Chang Biol* 14:2548–2554. <https://doi.org/10.1111/j.1365-2486.2008.01667.x>
- Corley RHV, Tinker PBH (2016) *The Oil Palm (World Agricultural Series) fifth edition, 647 pp.*, <https://doi.org/10.1017/cbo9781316530122.010,2016>
- Cornelis JT, Weis D, Lavkulich L, et al (2014) Silicon isotopes record dissolution and re-precipitation of pedogenic clay minerals in a podzolic soil chronosequence. *Geoderma* 235–236:19–29. <https://doi.org/10.1016/j.geoderma.2014.06.023>
- Cornelis J-T, Delvaux B, Georg RB, et al (2011) Tracing the origin of dissolved silicon transferred from various soil-plant systems towards rivers: a review. *Biogeosciences* 8:89–112. <https://doi.org/10.5194/bg-8-89-2011>
- Cornu S, Meunier JD, Ratie C, et al (2022) Allophanes, a significant soil pool of silicon for plants. *Geoderma* 412:1–12. <https://doi.org/10.1016/j.geoderma.2022.115722>

- Darras KFA, Corre MD, Formaglio G, et al (2019) Reducing Fertilizer and Avoiding Herbicides in Oil Palm Plantations—Ecological and Economic Valuations. *Front For Glob Chang* 2:1–15. <https://doi.org/10.3389/ffgc.2019.00065>
- De Coster GL (2006) *The Geology of the central and south sumatra basins, 1974*. pp 77-110
- de Tombeur F, Turner BL, Laliberté E, et al (2020) Plants sustain the terrestrial silicon cycle during ecosystem retrogression. *Science* 369:1245–1248. <https://doi.org/10.1126/science.abc0393>
- Derry LA, Kurtz AC, Ziegler K, Chadwick OA (2005) Biological control of terrestrial silica cycling and export fluxes to watersheds. *Nature* 433:728–731
- DIN ISO 14869-2 (2003) *Soil Quality — Dissolution for the Determination of Total Element Content — Part 2: Dissolution by Alkaline Fusion*. 1–7
- Dislich C, Keyel AC, Salecker J, et al (2017) A review of the ecosystem functions in oil palm plantations, using forests as a reference system. *Biol Rev* 92:1539–1569. <https://doi.org/10.1111/brv.12295>
- Donovan SE, Eggleton P, Dubbin WE, et al (2001) The effect of a soil-feeding termite, *Cubitermes fungifaber* (Isoptera: Termitidae) on soil properties: termites may be an important source of soil microhabitat heterogeneity in tropical forests. *Pedobiologia (Jena)* 45:1–11
- Drescher J, Rembold K, Allen K, et al (2016) Ecological and socio-economic functions across tropical land use systems after rainforest conversion. *Philos Trans R Soc B Biol Sci* 371:20150275. <https://doi.org/10.1098/rstb.2015.0275>
- Epstein E (2009) Silicon: its manifold roles in plants. *Annals of Applied Biology* 155:155–160. <https://doi.org/10.1111/j.1744-7348.2009.00343.x>
- Epstein E (1994) The anomaly of silicon in plant biology. *Proc Natl Acad Sci* 91:11–17. <https://doi.org/10.1073/pnas.91.1.11>
- Fox J, Weisberg S (2019) *An {R} Companion to Applied Regression*. <https://socialsciences.mcmaster.ca/jfox/Books/Companion/> [Accessed February 10, 2023]
- Fujii K, Shibata M, Kitajima K, et al (2018) Plant–soil interactions maintain biodiversity and functions of tropical forest ecosystems. *Ecol Res* 33:149–160. <https://doi.org/10.1007/s11284-017-1511-y>
- Gatto M, Wollni M, Qaim M (2015) Oil Palm Boom and Land-Use Dynamics in Indonesia: The role of Policies and Socioeconomic Factors. *Land use policy* 46:292–303. <https://doi.org/10.1016/j.landusepol.2015.03.001>
- Georgiadis A, Rinklebe J, Straubinger M, Rennert T (2017) Silicon fractionation in Mollic Fluvisols along the Central Elbe River, Germany. *Catena* 153:100–105. <https://doi.org/10.1016/j.catena.2017.01.027>
- Georgiadis A, Sauer D, Herrmann L, et al (2013) Development of a method for sequential Si extraction from soils. *Geoderma* 209:251–261. <https://doi.org/10.1016/j.geoderma.2013.06.023>
- Georgiadis A, Sauer D, Herrmann L, et al (2014) Testing a new method for sequential silicon extraction on soils of a temperate-humid climate. *Soil Res* 52:645–657.

<https://doi.org/10.1071/SR14016>

- Giraoudoux P (2022) *pgirmess: Spatial Analysis and Data Mining for Field Ecologists*, <https://CRAN.R-project.org/package=pgirmess> [Accessed February 10, 2023]
- Grass I, Kubitzka C, Krishna V V., et al (2020) Trade-offs between multifunctionality and profit in tropical smallholder landscapes. *Nat Commun* 11:1–13. <https://doi.org/10.1038/s41467-020-15013-5>
- Grasshoff K, Kremling K, Ehrhardt M (2009) *Methods of sea water analysis, third*. John Wiley & Sons
- Greenshields B, von der Lühe B, Hughes HJ, et al (2023) Oil-palm management alters the spatial distribution of amorphous silica and mobile silicon in topsoils. *SOIL* 9:169–188. <https://doi.org/10.5194/soil-9-169-2023>
- Greenshields B, von der Lühe B, Schwarz F, et al (2022) Estimating oil-palm Si storage, Si return to soils and Si losses through harvest in smallholder oil-palm plantations of Sumatra, Indonesia. *Egusphere* [preprint] 1–22. <https://doi.org/10.5194/egusphere-2022-905>
- Grosjean P, Ibanez F (2018) *pastecs: Package for Analysis of Space-Time Ecological Series*, <https://CRAN.R-project.org/package=pastecs> [Accessed February 5, 2023]
- Guillaume T, Damris M, Kuzyakov Y (2015) Losses of soil carbon by converting tropical forest to plantations: erosion and decomposition estimated by $\delta^{13}\text{C}$. *Glob Chang Biol* 21:3548–3560. <https://doi.org/10.1111/gcb.12907>
- Guillaume T, Kotowska MM, Hertel D, et al (2018) Carbon costs and benefits of Indonesian rainforest conversion to plantations. *Nat Commun* 9:1–11. <https://doi.org/10.1038/s41467-018-04755-y>
- Guntzer F, Keller C, Poulton PR, et al (2012) Long-term removal of wheat straw decreases soil amorphous silica at Broadbalk, Rothamsted. *Plant Soil* 352:173–184. <https://doi.org/10.1007/s11104-011-0987-4>
- Harrison RD, Swinfield T (2015) Restoration of logged humid tropical forests: An experimental programme at Harapan Rainforest, Indonesia. *Trop Conserv Sci* 8:4–16. <https://doi.org/10.1177/194008291500800103>
- Haynes RJ (2017) The nature of biogenic Si and its potential role in Si supply in agricultural soils. *Agric Ecosyst Environ* 245:100–111. <https://doi.org/10.1016/j.agee.2017.04.021>
- Hughes HJ, Hung DT, Sauer D (2020) Silicon recycling through rice residue management does not prevent silicon depletion in paddy rice cultivation. *Nutr Cycl Agroecosyst* 118:75–89. <https://doi.org/10.1007/s10705-020-10084-8>
- IUSS Working Group WRB (2022) *World Reference Base or Soil Resources 2014, update 2015 International soil classification system for naming soils and creating legends for soil maps*. FAO, Rome
- Koning E, Epping E, Van Raaphorst W (2002) Determining biogenic silica in marine samples by tracking silicate and aluminium concentrations in alkaline leaching solutions. *Aquat Geochemistry* 8:37–67. <https://doi.org/10.1023/A:1020318610178>

- Kotowska MM, Leuschner C, Triadiati T, et al (2015) Quantifying above- and belowground biomass carbon loss with forest conversion in tropical lowlands of Sumatra (Indonesia). *Glob Chang Biol* 21:3620–3634. <https://doi.org/10.1111/gcb.12979>
- Kurniawan S, Corre MD, Matson AL, et al (2018) Conversion of tropical forests to smallholder rubber and oil palm plantations impacts nutrient leaching losses and nutrient retention efficiency in highly weathered soils. *Biogeosciences* 15:5131–5154. <https://doi.org/10.5194/bg-15-5131-2018>
- Laumonier Y (1997) *The Vegetation and Physiography of Sumatra*. In: *Geobotany*. Kluwer Academic Publishers, p 223. <https://doi.org/10.1007/978-94-009-0031-8>
- Li Z, de Tombeur F, Vander Linden C, et al (2020) Soil microaggregates store phytoliths in a sandy loam. *Geoderma* 360:114037. <https://doi.org/10.1016/j.geoderma.2019.114037>
- Liang Y, Nikolic M, Bélanger R, et al (2015) *Silicon in Agriculture*. Dordrecht: Springer
- Lucas Y, Luizão FJ, Chauvel A, et al (1993) The relation between biological activity of the rain forest and mineral composition of soils. *Science* 260:521–523
- Luke SH, Purnomo D, Advento AD, et al (2019) Effects of understory vegetation management on plant communities in oil palm plantations in Sumatra, Indonesia. *Front For Glob Chang* 2:1–13. <https://doi.org/10.3389/ffgc.2019.00033>
- Ma JF, Takahashi E (2002) Silicon-accumulating plants in the plant kingdom. In: *Soil, fertilizer, and plant silicon research in Japan*. Elsevier Science, Amsterdam, pp 63–71
- Matichenkov VV, Calvert DV (2002) Silicon as a beneficial element for sugarcane. *J Am Soc Sugarcane Technol* 22:21–29
- McCarthy JF, Cramb RA (2009) Policy narratives, landholder engagement, and oil palm expansion on the Malaysian and Indonesian frontiers. *Geogr J* 175:112–123. <https://doi.org/10.1111/j.1475-4959.2009.00322.x>
- Munevar F, Romero A (2015) Soil and plant silicon status in oil palm crops in Colombia. *Exp Agric* 51:382. <https://doi.org/10.1017/S0014479714000374>
- Najihah NI, Hanafi MM, Idris AS, Hakim MA (2015) Silicon treatment in oil palms confers resistance to basal stem rot disease caused by *Ganoderma boninense*. *Crop Prot* 67:151–159. <https://doi.org/10.1016/j.cropro.2014.10.004>
- Nazarreta R, Hartke TR, Hidayat P, et al (2020) Rainforest conversion to smallholder plantations of rubber or oil palm leads to species loss and community shifts in canopy ants (Hymenoptera: Formicidae). *Myrmecological news* 30:175–186. <https://doi.org/10.25849/myrmecol.news>
- Oliveira PTS, Wendland E, Nearing MA (2013) Rainfall erosivity in Brazil: a review. *Catena* (Amst) 100:139–147. <https://doi.org/10.1016/j.catena.2012.08.006>
- Puppe D, Kaczorek D, Schaller J, et al (2021) Crop straw recycling prevents anthropogenic desilication of agricultural soil–plant systems in the temperate zone – Results from a long-term field experiment in NE Germany. *Geoderma* 403:1–13. <https://doi.org/10.1016/j.geoderma.2021.115187>
- Rembold K, Mangopo H, Tjitrosoedirdjo SS, Kreft H (2017) Plant diversity, forest dependency, and

- alien plant invasions in tropical agricultural landscapes. *Biol Conserv* 213:234–242. <https://doi.org/10.1016/j.biocon.2017.07.020>
- Revelle W (2022) *psych: Procedures for Personality and Psychological Research*, <https://CRAN.R-project.org/package=psychVersion=2.2.9>. [Accessed February 10, 2023]
- Sauer D, Saccone L, Conley DJ, et al (2006) Review of methodologies for extracting plant-available and amorphous Si from soils and aquatic sediments. *Biogeochemistry* 80:89–108. <https://doi.org/10.1007/s10533-005-5879-3>
- Sauer D, Stein C, Glatzel S, et al (2015) Duricrusts in soils of the Alentejo (southern Portugal)- types, distribution, genesis, and time of their formation. *J Soils Sediments* 15:1437–1453. <https://doi.org/10.1007/s11368-015-1066-x>
- Schaller J, Struyf E (2013) Silicon controls microbial decay and nutrient release of grass litter during aquatic decomposition. *Hydrobiologia* 709:201–212. <https://doi.org/10.1007/s10750-013-1449-1>
- Schaller J, Turner BL, Weissflog A, et al (2018) Silicon in tropical forests: large variation across soils and leaves suggests ecological significance. *Biogeochemistry* 140:161–174. <https://doi.org/10.1007/s10533-018-0483-5>
- Schaller J, Puppe D, Kaczorek D, et al (2021) Silicon cycling in soils revisited. *Plants* 10:1–36. <https://doi.org/10.3390/plants10020295>
- Shull KE, Guthan GR (1967) Rapid modified eriochrome cyanine R Method for determination of aluminum in Water. *Journal-American Water Work Assoc* 59:1456–1468. <https://doi.org/10.1002/j.1551-8833.1967.tb03476.x>
- Sirisuntornlak N, Ullah H, Sonjaroon W, et al (2021) Interactive effects of silicon and soil pH on growth, yield and nutrient uptake of maize. *Silicon* 13:289–299. <https://doi.org/10.1007/s12633-020-00427-z>
- Sommer M, Jochheim H, Höhn A, et al (2013) Si cycling in a forest biogeosystem – the importance of transient state biogenic Si pools. *Biogeosciences* 10:4991–5007
- Sommer M, Kaczorek D, Kuzyakov Y, Breuer J (2006) Silicon pools and fluxes in soils and landscapes - a review. *J Plant Nutr Soil Sci* 169:310–329
- Struyf E, Smis A, Van Damme S, et al (2010) Historical land use change has lowered terrestrial silica mobilization. *Nat Commun* 1:1–7. <https://doi.org/10.1038/ncomms1128>
- Tarigan S, Stiegler C, Wiegand K, et al (2020) Relative contribution of evapotranspiration and soil compaction to the fluctuation of catchment discharge: case study from a plantation landscape. *Hydrological Sciences Journal* 65:1239–1248. <https://doi.org/10.1080/02626667.2020.1739287>
- Tsujino R, Yumoto T, Kitamura S, et al (2016) History of forest loss and degradation in Indonesia. *Land use policy* 57:335–347. <https://doi.org/10.1016/j.landusepol.2016.05.034>
- Unzué-Belmonte D, Ameijeiras-Mariño Y, Opfergelt S, et al (2017) Land use change affects biogenic silica pool distribution in a subtropical soil toposequence. *Solid Earth* 8:737–750. <https://doi.org/10.5194/se-8-737-2017>
- Vander Linden C, Delvaux B (2019) The weathering stage of tropical soils affects the soil-plant cycle

- of silicon, but depending on land use. *Geoderma* 351:209–220.
<https://doi.org/10.1016/j.geoderma.2019.05.033>
- Vandevenne F, Barão L, Ronchi B, et al (2015) Silicon pools in human impacted soils of temperate zones. *Global Biogeochem Cycles* 29:1439–1450. <https://doi.org/10.1002/2014GB005049>
- Vandevenne F, Struyf E, Clymans W, Meire P (2012) Agricultural silica harvest: have humans created a new loop in the global silica cycle ? *Front Ecol Environ* 10:243–248.
<https://doi.org/10.1890/110046>
- von der Lühe B, Bezler K, Hughes HJ, et al (2022) Oil-palm and Rainforest Phytoliths Dissolve at Different Rates - with Implications for Silicon Cycling After Transformation of Rainforest Into Oil-palm Plantation. *Silicon*. <https://doi.org/10.1007/s12633-022-02066-y>
- von der Lühe B, Pauli L, Greenshields B, et al (2020) Transformation of Lowland Rainforest into Oil-palm Plantations and use of Fire alter Topsoil and Litter Silicon Pools and Fluxes. *Silicon* 13:4345–4353. <https://doi.org/10.1007/s12633-020-00680-2>
- Watteau F, Villemin G (2001) Ultrastructural study of the biogeochemical cycle of silicon in the soil and litter of a temperate forest. *Eur J Soil Sci* 52:385–396. <https://doi.org/10.1046/j.1365-2389.2001.00391.x>
- White AF, Vivit D V., Schulz MS, et al (2012) Biogenic and pedogenic controls on Si distributions and cycling in grasslands of the Santa Cruz soil chronosequence, California. *Geochim Cosmochim Acta* 94:72–94. <https://doi.org/10.1016/j.gca.2012.06.009>
- Wickham H (2016) *ggplot2: Elegant Graphics for Data Analysis*
- Wickham H, François R, Henry L, et al (2023) *dplyr: A Grammar of Data Manipulation*, <https://CRAN.R-project.org/package=dplyr> [Accessed February 10, 2023]
- Woittiez LS, Turhina SRI, Deccy D, et al (2019) Fertiliser application practices and nutrient deficiencies in smallholder oil palm plantations in Indonesia. *Exp Agric* 55:543–559.
<https://doi.org/10.1017/S0014479718000182>
- Zemp DC, Ehbrecht M, Seidel D, et al (2019) Mixed-species tree plantings enhance structural complexity in oil palm plantations. *Agric Ecosyst Environ* 283:106564.
<https://doi.org/10.1016/j.agee.2019.06.003>

3 Oil-palm management alters the spatial distribution of amorphous silica and mobile silicon in topsoils

Britta Greenshields¹, Barbara von der Lühe¹, Harold J. Hughes¹, Christian Stiegler², Suria Tarigan³, Aiyen Tjoa⁴, Daniela Sauer¹

¹Department of Physical Geography, University of Göttingen, Göttingen, Germany

²Bioclimatology, Büsgen Institute, University of Göttingen, Göttingen, Germany

³Department of Soil and Natural Resources Management, IPB University, Bogor, Indonesia

⁴Department Agrotechnology, Tadulako University, Palu, Indonesia

Corresponding author: Britta Greenshields

Published manuscript – SOIL
<https://doi.org/10.5194/soil-9-169-2023>

Abstract. Effects of oil-palm (*Elaeis guineensis* Jacq.) management on silicon (Si) cycling under smallholder oil-palm plantations have hardly been investigated. As oil palms are Si accumulators, we hypothesized that management practices and topsoil erosion may cause Si losses and changes in spatial Si concentration patterns in topsoils under oil-palm cultivation. To test this hypothesis, we took topsoil samples under mature oil-palm plantations in well-drained and riparian areas of Jambi Province, Indonesia. The samples were taken from four different management zones within each oil-palm plot: palm circles, oil-palm rows, interrows and below frond piles. We quantified mobile Si (Si_M) and Si in amorphous silica (Si_{Am}) by the extraction of $CaCl_2$ and $NaCO_3$, respectively. Both fractions are important Si pools in soils and are essential for plant-soil Si cycling. We further installed sediment traps on sloping, well-drained oil-palm plantations to estimate the annual loss of soil and Si_{Am} caused by erosion. In well-drained areas, mean topsoil Si_{Am} concentrations were significantly higher below frond piles ($3.97 \pm 1.54 \text{ mg g}^{-1}$) compared to palm circles ($1.71 \pm 0.35 \text{ mg g}^{-1}$), oil-palm rows ($1.87 \pm 0.51 \text{ mg g}^{-1}$), and interrows ($1.88 \pm 0.39 \text{ mg g}^{-1}$). In riparian areas, the highest mean topsoil Si_{Am} concentrations were also found below frond piles ($2.96 \pm 0.36 \text{ mg g}^{-1}$) and in grass-covered interrows ($2.71 \pm 0.13 \text{ mg g}^{-1}$), whereas topsoil Si_{Am} concentrations of palm circles were much lower ($1.44 \pm 0.55 \text{ mg g}^{-1}$). We attributed the high Si_{Am} concentrations in topsoils under frond piles and in grass-covered interrows to phytolith release from decaying oil-palm fronds, grasses, and sedges. The significantly lower Si_{Am} concentrations in palm circles (in both well-drained and riparian areas), oil-palm rows, and unvegetated interrows (only in well-drained areas) were explained by a lack of litter return to these management zones. Mean topsoil Si_M concentrations were in the range of $\sim 10 - 20 \text{ } \mu\text{g g}^{-1}$. They tended to be higher in riparian areas, but the differences between well-drained and riparian sites were not statistically significant. Soil-loss calculations based on erosion traps confirmed that topsoil erosion was considerable in oil-palm interrows on slopes. Erosion estimates were in a range of $4 - 6 \text{ Mg ha}^{-1} \text{ yr}^{-1}$, involving Si_{Am} losses in the range of $5 - 9 \text{ kg}^{-1} \text{ ha}^{-1} \text{ yr}^{-1}$. Based on the observed spatial Si patterns, we concluded that smallholders could efficiently reduce erosion and support Si cycling within the system by (1) maintaining a grass cover in oil-palm rows and interrows, (2) incorporating oil-palm litter into plantation management and (3) preventing soil compaction and surface-crust formation.

Keywords: oil-palm plantations, oil-palm management, silicon pools, phytoliths, topsoil erosion, silicon extraction

3.1 Introduction

The transformation of lowland rainforests into cash-crop plantation systems (e.g., timber, rubber, and oil palm) involves vast expansion of oil-palm monocultures in Jambi Province, Indonesia (Drescher et al., 2016; Tsujino et al., 2016). By now, smallholder farmers manage 40 % of oil-palm plantations in Jambi Province (Euler et al., 2016), whereby palm oil remains a tropical cash crop with high demand on the global market (FAO 2020). Oil-palm cultivation has improved the livelihoods of many smallholder farmers, yet at the expense of the natural environment (Clough et al., 2016; Grass et al., 2020; Qaim et al., 2020), leading to a decrease in biodiversity (Drescher et al., 2016; Meijaard et al., 2020) and ecosystem services (Dislich et al., 2017). Due to these “trade-offs” (Grass et al., 2020) and a global interest to reduce deforestation (Tsujino et al., 2016), much research focuses on identifying ways to increase land-use sustainability while keeping current oil-palm plantations profitable (Darras et al., 2019; Luke et al., 2019).

Under humid tropical climate conditions, intense silicate weathering and element leaching from soils take place, including leaching of silicon (Si), *i.e.*, desilication (Haynes, 2014). Farmers commonly apply nitrogen-phosphorous-potassium (NPK) fertilizers and lime to maintain an adequate plant nutrition and soil pH (Darras et al., 2019). However, Si also plays an important role in terrestrial biogeochemical cycling (Struyf and Conley, 2012) and enhances crop production in several ways (Epstein, 2009; Guntzer et al., 2012). In soils, silicic acid can mobilize phosphate by occupying anion adsorption sites. Si also mitigates plant toxicity by binding toxic cations such as aluminium (Al), cadmium (Cd), and arsenic (As) that become mobile at low soil pH (Street-Perrott and Barker, 2008; Schaller et al., 2020). Furthermore, Si can increase drought resistance of plants (Schaller et al., 2020). Silica precipitates in cell walls, cell lumen, and intercellular spaces of leaves and can reduce transpiration (Epstein, 2009). In Si-depleted soils, some crops, including oil palms, can thus benefit from Si fertilization (Klotzbücher et al., 2018).

In terrestrial ecosystems, Si cycling is mostly driven by two Si pools: mobile Si in soil solution (Si_M) and Si present in amorphous silica (Si_{Am}) (Struyf et al., 2010; de Tombeur et al., 2020). Si_M is the Si fraction that is readily available to plants and usually present as monomeric silicic acid (H_4SiO_4) in terrestrial environments (Georgiadis et al., 2013). Si_{Am} is the largest non-mineral Si pool in soils (Barão et al., 2014; Unzué-Belmonte et al., 2017). Its solubility exceeds that of silicate minerals by several orders of magnitude (Iler, 1979; Fraysse et al., 2009). Si_{Am} in soils can be subdivided into Si_{Am} of biogenic origin and of pedogenic origin. The first mainly includes Si in phytoliths, *i.e.*, small biogenic bodies precipitated in plant tissues that are released during plant-litter decomposition (Barão et al., 2014; Clymans et al., 2015; Schaller et al., 2021). Soil microorganisms (testate amoebae, sponges, diatoms) contribute to a lesser extent (Schaller et al., 2021). Si_{Am} of pedogenic origin, *i.e.*, silica precipitated from soil solution, mainly occurs as soil-particle coatings and void infillings (Schaller et

al., 2021). Si_{Am} in topsoils is predominantly of biogenic origin (Clymans et al., 2015; Schaller et al., 2021), whereas Si_{Am} in subsoils is mostly of pedogenic origin (Schaller et al., 2021).

Ecosystem Si cycling can be altered by human impact such as deforestation (Conley et al., 2008), land-use and land-cover (LULC) change (Struyf et al., 2010; Barão et al., 2020), and fire (von der Lühe et al., 2020; Schaller and Puppe, 2021). After LULC transformation from forest to arable land, Si can be lost from the system through harvest, topsoil erosion, and increased Si leaching in soil. Si leaching in soil is triggered by reduced interception, which results in increased percolation (Keller et al., 2012; Vandevenne et al., 2012; Kraushaar et al., 2021). Si-accumulating plants such as rice, wheat, barley, maize, and oil palm (Ma and Takahashi, 2002; Munevar and Romero, 2015), are characterized by Si accumulation of > 1 wt. % in dry leaf tissue and a Si/Ca ratio > 1 (Ma and Takahashi, 2002). Such Si accumulators may accelerate Si turnover at the soil-plant interface by taking up high amounts of Si from soil solution and returning Si-rich litter to soils (Struyf and Conley, 2009, 2012). In oil-palm plantations, we therefore expected Si losses by harvest and topsoil erosion (Vandevenne et al., 2012; Munevar and Romero, 2015). In addition, we expected that the spatial arrangement of oil-palm rows and interrows – with frond piles (frond pile) or without (“empty” interrow) – results in a corresponding spatial Si concentration pattern in topsoils.

Oil palms are planted in rows (Kotowska et al., 2015) (Fig. 3.1a). A distance is kept between the rows to ensure sufficient light exposure (Corley and Tinker, 2016). The space between two oil-palm rows is referred to as an interrow. They serve either as harvesting paths or as deposition sites for cut-off palm fronds that are stacked up in long, flat piles (Corley and Tinker, 2016). Fertilizers are only applied within a circle of $\sim 1.5 - 2$ m around the palm stem (palm circle) (Munevar and Romero, 2015; Formaglio et al., 2020). In addition, nutrients are released from decaying plant litter. Thus, we hypothesized that Si is mainly released and returned to soils in the form of biogenic Si_{Am} under frond piles, leading to higher topsoil Si_{Am} concentrations, while other management zones (including palm circles, oil-palm rows, and empty interrows) might be at risk of Si depletion.

Furthermore, we hypothesized that in oil-palm plantations established on sloping terrain, Si is removed by topsoil erosion in scarcely vegetated interrows. We assumed that phytoliths might be even more prone to erosion than mineral soil particles because of their lower density, leading to a disproportionately high Si_{Am} loss through topsoil erosion. Such additional Si_{Am} loss from interrows would be unfavourable, as interrows may serve as new planting sites in a subsequent plantation cycle after ~ 25 years (Corley and Tinker, 2016). Thus, our study aimed at assessing the impact of management practices in smallholder oil-palm plantations on Si cycling. In addition, we considered it important to account for potential differences in the intensity of natural desilication in different landscape positions. Therefore, we carried out the same study in two different landscape positions, associated with differing water regimes: (i) in well-drained areas with presumably high desilication

rates and (ii) in riparian areas, where we assumed that regular flooding might involve an input of Si dissolved in stream water into the system, partially compensating for desilication.

3.2 Material and methods

3.2.1 Study area and sites

The study was associated with the DFG-funded interdisciplinary Collaborative Research Centre (CRC) 990, addressing environmental and socioeconomic impacts of rainforest conversion into plantation systems in Sumatra, Indonesia (Drescher et al., 2016; Dislich et al., 2017). Thus, it was conducted on CRC 990 plots in smallholder oil-palm plantations in the Harapan landscape of Jambi Province, Sumatra, Indonesia (1° 55' 0'' S, 103° 15' 0'' E; 50 m ± 5 m NN). Geologically, this lowland landscape is characterized by pre-Paleogene metamorphic and igneous bedrock that is overlain by lacustrine and fluvial sediments (de Coster, 2006), in which predominantly loamy mineral soils have formed (Allen et al., 2016). Preliminary results showed that quartz, kaolinite, and Fe-Al-oxides are the most abundant minerals in these highly weathered soils. In our study area, Acrisols are present in well-drained areas, found at higher elevation and on sloping terrain. Stagnosols and Stagnic Acrisols dominated in seasonally flooded riparian plots, *i.e.*, in floodplains (Hennings et al., 2021). The Harapan region is characterized by a humid tropical climate (Af in the Köppen-Geiger classification) with a mean annual temperature of 26.7 °C and a mean annual precipitation of 2230 mm (Drescher et al., 2016). The rainy season has two precipitation maxima: one in December and another one in March. A dry period lasts from July to August (Drescher et al., 2016). The natural vegetation is a mixed dipterocarp lowland rainforest (Laumonier, 1997) which is nearly only preserved in the Harapan rainforest, an ecosystem restoration area in the south of Jambi Province (Harrison and Swinfield, 2015), and in the Barisan mountains in the west of Jambi Province (Drescher et al., 2016). In addition to oil-palm plantations, other important land-use systems in Jambi Province include rubber plantations and agroforestry systems (Dislich et al., 2017).

3.2.2 Study design and sampling

3.2.2.1 Topsoil samples

From April to August 2018, topsoil sampling was conducted in four well-drained (HO1 – HO4) and four riparian plots (HOr1 – HOr4). Oil palms were planted between 1997 and 2001 in well-drained plots, and between 1998 and 2008 in riparian areas (Hennings et al., 2021), following a triangular planting scheme with ~ 9 m distance between the stems (Fig. 3.1a). Interrows were used either as harvesting paths or to stack cut-off palm fronds (frond pile) (Kotowska et al., 2015). In plot HO1, every interrow contained frond piles. Thus, topsoil samples of interrows were obtained only from three well-drained plots. The understorey vegetation of all well-drained plots was occasionally weeded. Two riparian plots (HOr1 and HOr2) had a well-maintained grass cover between the oil palms.

In each of the eight plots, topsoil samples were taken with steel cylinders (height = 4 cm, volume = 100 cm³) at five locations along the slope. At each location, topsoils were sampled from four different management zones, *i.e.*, (1) palm circle, (2) oil-palm row, (3) interrow, and (4) frond pile, to assess spatial patterns of Si_{Am} and Si_M concentrations in topsoils within the oil-palm plantations (Appendix II Table A1 and A2). Interrow topsoil samples were taken at a maximum distance between oil palms. The samples were dried (40 °C, 24 h) and sieved (≤ 2 mm) prior to Si analyses. An aliquot of each sample was dried at 105 °C to determine the water content of the samples dried at 40 °C.

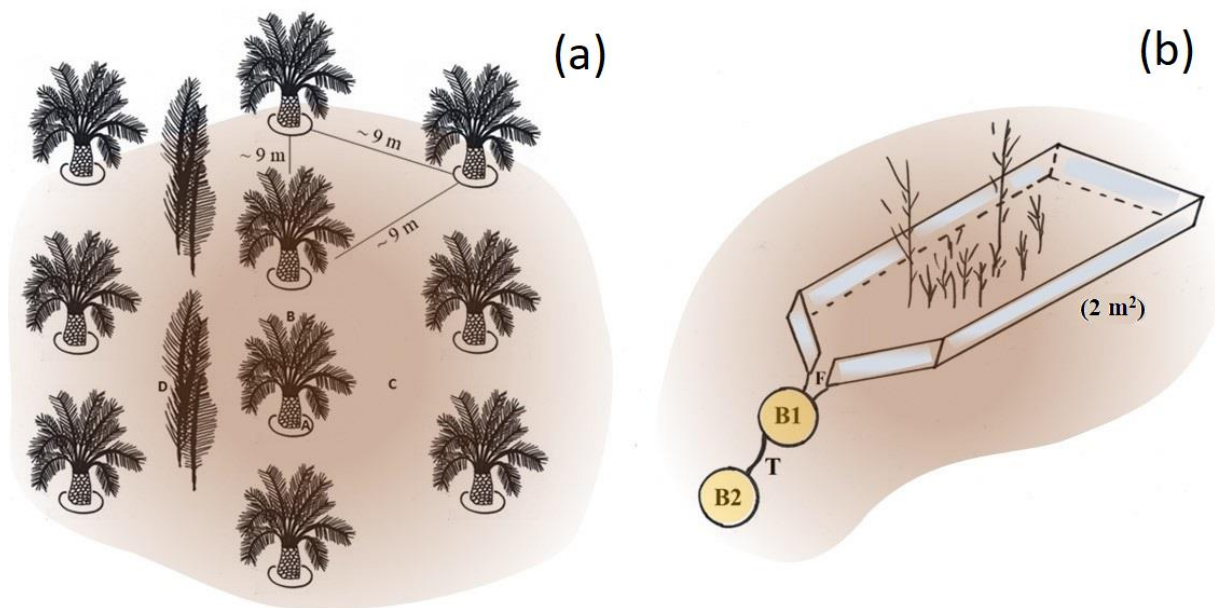


Fig. 3.1 (a) Triangular planting arrangement on smallholder oil-palm plantations in the study area (sketch by B. Greenshields). Topsoil samples were taken in four distinct management zones: (A) palm circles, (B) oil-palm rows, (C) interrows, and (D) below frond piles. (b) This is a 2 m² sediment trap with scarce understorey vegetation installed in pairs in four well-drained plots (sketch by B. Greenshields following Sinukaban et al. 2000). The downslope funnel-shaped part of the aluminium frame (F) directs surface runoff, together with eroded soil material, into a bucket (B1) that is connected to a second bucket (B2) by a 2 cm wide tube (T). Photos of the sediment traps are shown in Appendix II Table A3.

3.2.2.2 Sediment traps

Sediment traps were installed in sets of two in interrows of the well-drained plots HO1 – HO4, on 8 – 12° sloping land (Sinukaban et al., 2000). Each trap consisted of a rectangular aluminium frame (2 x 1 m, 2 m²). Its downslope-facing short side was funnel-shaped, directing surface runoff and eroded soil material into a bucket (Fig. 3.1b and Appendix II Table A3). A second bucket was connected to the first bucket by a 2 cm thick tube to catch potential overflow. The traps were checked and maintained weekly from the beginning of September 2018 to the end of August 2019. The understorey vegetation in the sediment traps was kept in place to ensure that the understorey vegetation was representative of

the oil-palm plantations. Both sediment traps in HO1 were manually weeded after 6 months because inside the traps, vegetation covered nearly 100 % of the soil surface, impeding topsoil erosion. Eroded soil material was collected whenever present, dried (40 °C, 48 h), sieved (≤ 2 mm) and weighed prior to Si analyses. Samples of eroded soil material from plot HO2 were excluded from further analysis because both traps were contaminated by crude oil. Losses of Si_{Am} were calculated for each sediment trap by multiplying the concentration of Si_{Am} of each sediment sample by the amount of eroded soil material collected by each trap (Appendix II Table B3). Erosion estimates were determined for each trap by summing up the amount of eroded soil material for the 12-month period from the beginning of September 2018 until the end of August 2019. Precipitation data of the two closest meteorological stations were used for correlating the observed soil erosion with precipitation. Distances between meteorological stations and plots comprised ~ 2 km for HO1, ~ 3 km for HO2, ~ 8 km for HO3, and ~ 6 km for HO4. At each meteorological station, precipitation was measured by two automated precipitation transmitters (Thies Clima, Göttingen, Germany), at a height of 1.5 m and a horizontal distance of about 6 m.

3.2.3 Determination of silicon pools in topsoils

Silicon in amorphous silica (Si_{Am})

Silicon in amorphous silica (Si_{Am}) was extracted from topsoil samples and eroded soil material by 1 % Na_2CO_3 solution (Meunier et al., 2014). At 85 °C, amorphous silica dissolves within 2 – 3 hours in 1 % Na_2CO_3 solution, thereby rapidly raising the Si concentration in solution. Once amorphous silica is completely dissolved, the release of Si to solution is only sustained by the slower dissolution of silicate minerals which follows a linear trend. Si concentration was measured four times during the linear dissolution phase. A linear equation was fitted to the data. The Si_{Am} concentration was inferred from the y intercept of the linear regression.

In detail, 40 ml of 1 % Na_2CO_3 solution was added to approximately 30 mg of soil material. The samples were then placed into a shaking water bath at 85 °C. To ensure steady Si release from topsoils, the samples were manually shaken at time intervals of 45 min. Aliquots were taken after 3 h, 3.75 h, 4.5 h, and 5.25 h. For this purpose, the samples were taken out of the water bath, cooled in a cold-water basin (10 min) and centrifuged (5 min, 3000 *rpm*). A 0.25 ml aliquot was taken from the supernatant of each sample and neutralized with 2.25 ml 0.021 M HCl. Si concentrations in the aliquots were analysed by the molybdenum blue method (Grasshoff et al., 2009) using a UV-VIS spectrophotometer (Lamda 40, Perkin Elmer, Germany) at 810 nm. We chose 1 % Na_2CO_3 as an extractant and used the extraction method by Meunier et al. (2014) instead of the stronger extractant of 0.1 M NaOH used by Barão et al. (2015) because we assumed that most Si in topsoils is of biogenic origin and dissolved well by Na_2CO_3 (Meunier et al., 2014).

Mobile silicon (Si_M)

Mobile silicon (Si_M) was extracted by a $CaCl_2$ solution, which provides electrolytes resembling natural soil solutions (Sauer et al., 2006; Georgiadis et al., 2013). From each sample, 1 g of soil material was mixed with 5 ml of 0.01 M $CaCl_2$ and left for 24 h, shaking for 1 min h^{-1} on an overhead shaker. Samples were centrifuged (5 min, 3000 rpm) and the supernatant was filtered through ash-free paper filters (1-2 μm). The Si concentrations were analysed in filtrates by the molybdenum blue method. We transformed the measured Si concentration ($\mu g g^{-1}$) into the amount of Si_M per gram 105 °C dried soil.

3.2.4 Statistical analyses

Statistical analyses were conducted on the grand means of topsoil Si concentrations in each water regime and management zone. The two latter were grouped into (i) palm circles in well-drained / riparian areas (each, $n = 4$), (ii) oil-palm rows in well-drained / riparian areas (each, $n = 4$), (iii) interrows in well-drained ($n = 3$) / riparian areas ($n = 4$) and (iv) frond piles in well-drained / riparian areas (each, $n = 4$). The four management zones were tested for significant differences in topsoil Si concentrations, within both the well-drained and within the riparian areas. In addition, we tested the well-drained and riparian areas for significant differences in topsoil Si concentrations by comparing the same management zone under two different water regimes. The data were log transformed to assert normal distribution (Shapiro-Wilk test) and homogeneity of variances (Levene test). Both criteria were met for all groups except for Si_M in topsoils of oil-palm rows in well-drained areas (Appendix II Table B4). We conducted a one-way analysis of variance (ANOVA) to detect if Si_{Am} and Si_M concentrations in topsoils of different management zones differed significantly within well-drained and within riparian areas, as well as between well-drained and riparian areas. Then we used the Tuckey-Kramer post-hoc test to identify, which management zones differed significantly. The level of significance was set at $p \leq 0.05$. We used the open-source software R version 3.6.2 and R CRAN packages ggplot2 (Wickham, 2016), ggpubr (Kassambara, 2022), car (Fox and Weisberg, 2019) and psych (Revelle, 2022) to perform these statistical analyses.

3.3 Results

3.3.1 Concentrations of Si_{Am} and Si_M in topsoils

In well-drained plots, mean topsoil Si_{Am} concentrations were about twice as high under frond piles ($3.97 \pm 0.76 mg g^{-1}$) compared to palm circles ($1.71 \pm 0.36 mg g^{-1}$), oil-palm rows ($1.87 \pm 0.28 mg g^{-1}$), and interrows ($1.88 \pm 0.32 mg g^{-1}$) (Fig. 3.2a, Appendix II Table B1). This difference between frond piles and the other three management zones was significant ($p \leq 0.05$) (Fig. 3.2a). In riparian plots, mean topsoil Si_{Am} concentrations were equally high below frond piles ($2.96 \pm 0.36 mg g^{-1}$) and in interrows ($2.71 \pm 0.13 mg g^{-1}$) (Fig. 3.2b). Compared to these two management zones, mean topsoil Si_{Am} concentrations in palm circles ($1.44 \pm 0.30 mg g^{-1}$) were significantly lower ($p \leq 0.05$) (Fig. 3.2b).

3 Oil-palm management alters the spatial distribution of amorphous silica and mobile silicon in topsoils

Oil-palm rows had intermediate mean topsoil Si_{Am} concentrations ($2.08 \pm 0.63 \text{ mg g}^{-1}$) (Fig. 3.2b), showing no significant difference with respect to any other management zone ($p \leq 0.05$).

In well-drained plots, mean topsoil Si_{M} concentrations were about twice as high under frond piles ($13.68 \pm 6.54 \text{ } \mu\text{g g}^{-1}$) and in palm circles ($11.17 \pm 5.42 \text{ } \mu\text{g g}^{-1}$) compared to oil-palm rows ($6.38 \pm 2.85 \text{ } \mu\text{g g}^{-1}$) and interrows ($5.62 \pm 0.10 \text{ } \mu\text{g g}^{-1}$) (Fig. 3.2c). Only plot HO1 showed exceptionally high topsoil Si_{M} concentrations in oil-palm rows (outlier), which could be attributed to the dense vegetation throughout that smallholder plantation. In riparian plots, mean topsoil Si_{M} concentrations were twice as high under frond piles ($19.56 \pm 6.13 \text{ } \mu\text{g g}^{-1}$) compared to mean topsoil Si_{M} concentrations in palm circles, oil-palm rows, and interrows, which all range around $11 \text{ } \mu\text{g g}^{-1}$ (Fig. 3.2d). Mean topsoil Si_{M} concentrations did not differ significantly ($p \leq 0.05$) between the other management zones within the same water regime (well-drained/riparian), nor did mean topsoil Si_{M} concentrations (in the same management zone) differ between water regimes.

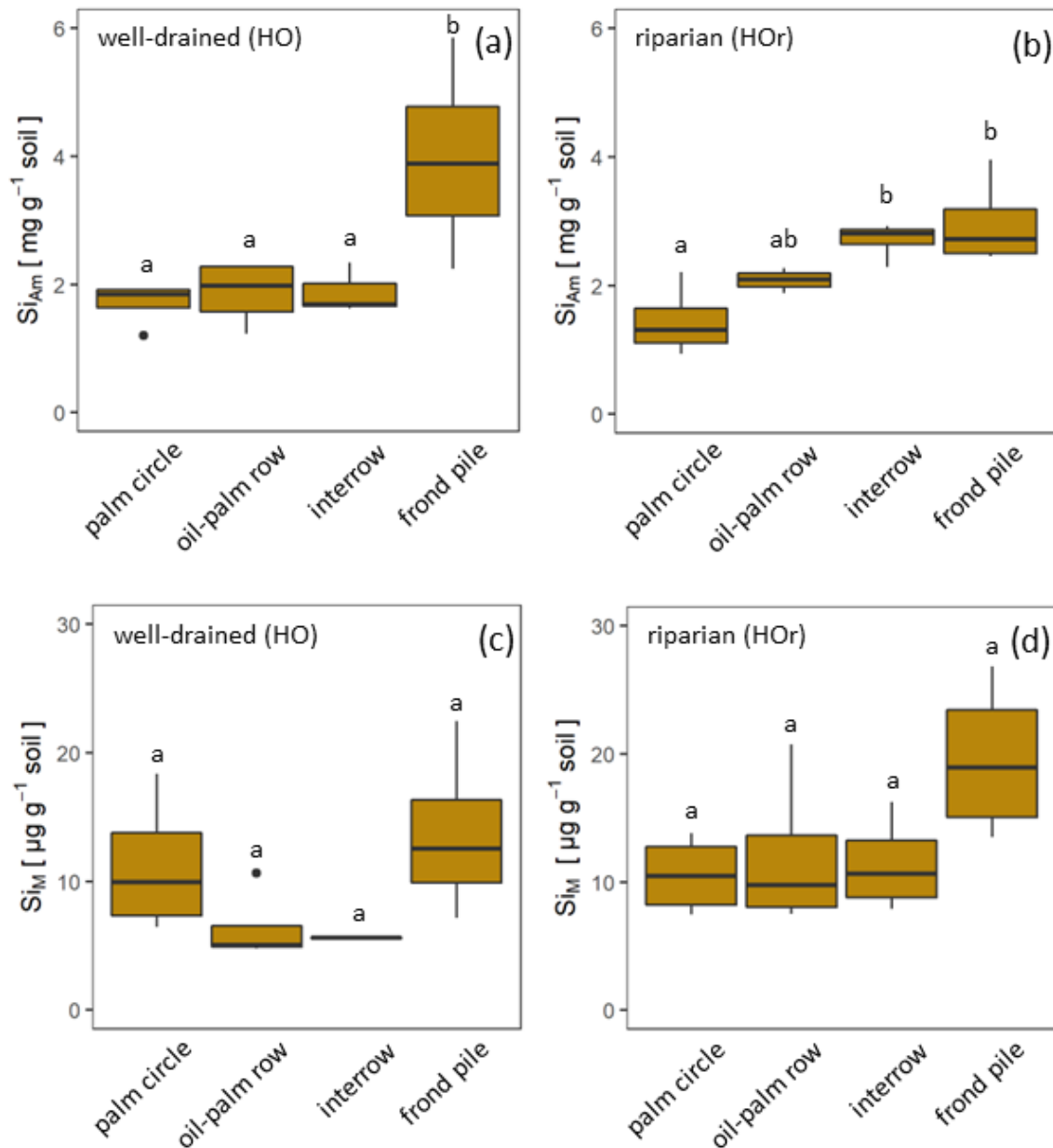


Fig. 3.2 Concentrations of mobile Si (Si_M) and Si in amorphous silica (Si_{Am}) in topsoils of four different management zones: palm circles ($n = 4$), oil-palm rows ($n = 4$), interrows ($n = 3$), and under frond piles ($n = 4$) on smallholder oil-palm plantations in two different landscape positions with differing water regimes (well-drained and riparian). Boxes indicate interquartile ranges and whiskers extend 1.5 times the interquartile range below or above the box. If lower case letters (a, b) differ from one another, this indicates a significant difference between management zones within a water regime ($p \leq 0.05$). Si concentrations were calculated with one-way analysis of variance (ANOVA) and Tukey-Kramer post-hoc test.

3.3.2 Topsoil erosion and associated losses of Si_{Am}

In plots HO3 and HO4, median Si_{Am} concentrations in topsoils of interrows ($1.53 - 1.57 \text{ mg g}^{-1}$) were roughly twice as high as in eroded soil material ($0.66 - 0.88 \text{ mg g}^{-1}$) (Tab. 1). In plot HO1, the median Si_{Am} concentration in eroded soil material (1.61 mg g^{-1}) was twice as high as in eroded soil material of plots HO3 and HO4 ($0.66 - 0.88 \text{ mg g}^{-1}$). Over the entire sampling period of 12 months, the four sediment traps in plots HO1 and HO4 indicated erosion rates of $\sim 4 - 5 \text{ Mg ha}^{-1} \text{ yr}^{-1}$ (Tab. 2). In plot HO3, a similar erosion rate was obtained from trap 1 ($\sim 6 \text{ Mg ha}^{-1} \text{ yr}^{-1}$), whereas the erosion rate observed in trap 2 of plot HO3 was twice as high ($\sim 12 \text{ Mg ha}^{-1} \text{ yr}^{-1}$). Si_{Am} losses through topsoil erosion amounted to $6 - 9 \text{ kg ha}^{-1} \text{ yr}^{-1}$ in the four sediment traps of HO1 and HO3, and $5 - 7 \text{ kg ha}^{-1} \text{ yr}^{-1}$ in both sediment traps of HO4. Figure 3.3 presents weekly losses of topsoil and Si_{Am} in eroded topsoil correlated with daily rainfalls. During the 12-month sampling period, daily rainfalls $\geq 25 \text{ mm d}^{-1}$ were recorded from mid-September 2018 until mid-June 2019 (Fig. 3.3). The rainy season started in November 2018 with daily rainfalls exceeding 60 mm d^{-1} (HO4, weather station near a state-owned plantation) to 70 mm d^{-1} (HO1 and HO3, weather station near the village of Bungku) after a dry spell in October 2018. A second rainy peak lasted from mid-March to mid-April 2019 with daily rainfalls reaching 50 mm d^{-1} (HO1 and HO3) to 70 mm d^{-1} (HO4). The dry season started in mid-June 2019, showing only one intense rainfall event (outlier, HO4) at the end of August 2019.

In plot HO1, a dense cover of mosses, grasses, and 20 – 50 cm high understorey vegetation prevented soil loss from September 2018 until end of January 2019. (Tab. 1, Fig. 3.3a). After manually weeding plot HO1 at the end of January 2019, the vegetation coverage was kept minimal (around 5 %). Noticeable losses of soil and corresponding losses of Si_{Am} occurred between February ($13 - 21 \text{ g m}^{-2}$ of sediment, $16 - 53 \text{ mg m}^{-2}$ of Si_{Am}) and the end of May 2019 ($16 - 100 \text{ g m}^{-2}$ of sediment / $38 - 192 \text{ mg m}^{-2}$ of Si_{Am}) (Fig. 3.3a and 3.3b). In plot HO3, scarce understorey vegetation of herbaceous plants (no grasses and mosses) covered about a third of the sediment traps (Tab. 1). Soil and corresponding Si_{Am} losses were recorded continuously from September 2018 to May 2019 (Fig. 3.3). Each week, losses of topsoil material amounted to $4 - 62 \text{ g m}^{-2}$ (corresponding to $1 - 90 \text{ mg m}^{-2} \text{ Si}_{\text{Am}}$) (Fig. 3.3a, 3.3b). At three sampling dates, one in December 2018 and two in February 2019, peak soil losses $\geq 150 \text{ g m}^{-2}$ occurred. The corresponding Si_{Am} losses of these sampling dates were $\geq 90 \text{ mg m}^{-2}$, hence also representing among the highest Si_{Am} losses throughout the sampling period. In plot HO4, vegetation coverage in the traps increased from 40 % in September 2018 to 60 % in May 2019 (Tab. 1). Soil loss occurred from mid-September 2018 to the end of May 2019 (Fig. 3.3). Losses of eroded soil material barely exceeded 50 g m^{-2} of sediment. However, an event with approximately 20 g m^{-2} of soil loss had corresponding Si_{Am} losses ranging from $5 - 160 \text{ mg m}^{-2}$, thus showing a large variability.

3 Oil-palm management alters the spatial distribution of amorphous silica and mobile silicon in topsoils

Table 3.1 Topsoil Si_{Am} concentrations in interrow and sediment trap samples

Oil-palm plot	Statistics	Interrow	Eroded soil material	Estimated vegetation cover	
	N ^c	Si _{Am} [mg g ⁻¹ _{soil}]	Si _{Am} [mg g ⁻¹ _{soil}]	(Sep / Jan / Apr-May [%])	
HO1 ^a	NA/19	Min.	NA ^d	0.90	100 / 5 / 5
HO1 ^a	NA/19	Median	NA ^d	1.61	
HO1 ^a	NA/19	Mean	NA ^d	1.77	
HO1 ^a	NA/19	Max	NA ^d	3.26	
HO3 ^b	5/38	Min	1.40	0.11	30 / 40 / 30
HO3 ^b	5/38	Median	1.53	0.88	
HO3 ^b	5/38	Mean	1.63	0.82	
HO3 ^b	5/38	Max	1.91	1.97	
HO4 ^b	5/27	Min	1.45	0.03	40 / 50 / 60
HO4 ^b	5/27	Median	1.57	0.66	
HO4 ^b	5/27	Mean	1.69	1.13	
HO4 ^b	5/27	Max	2.21	6.84	

^aSi_{Am} concentrations for plot HO1 as of February 2019 (after manual weeding). ^bSi_{Am} concentrations for plot HO3 and HO4 for the whole sampling duration. ^cReplicates for interrow topsoil samples/replicates for eroded soil samples. ^dEvery interrow on plot HO1 contained stacked frond piles with no sampling possible. NA: not available.

Table 3.2 Annual losses of soil and Si_{Am} through erosion

Plot	Trap	Eroded soil material	Si _{Am}
		[Mg soil ha ⁻¹ yr ⁻¹]	[kg Si _{Am} ha ⁻¹ yr ⁻¹]
HO1	1	5.4	8.7
HO1	2	4.2	7.2
HO3	1	11.7	8.9
HO3	2	6.1	6.0
HO4	1	5.4	6.7
HO4	2	3.6	4.6

3 Oil-palm management alters the spatial distribution of amorphous silica and mobile silicon in topsoils

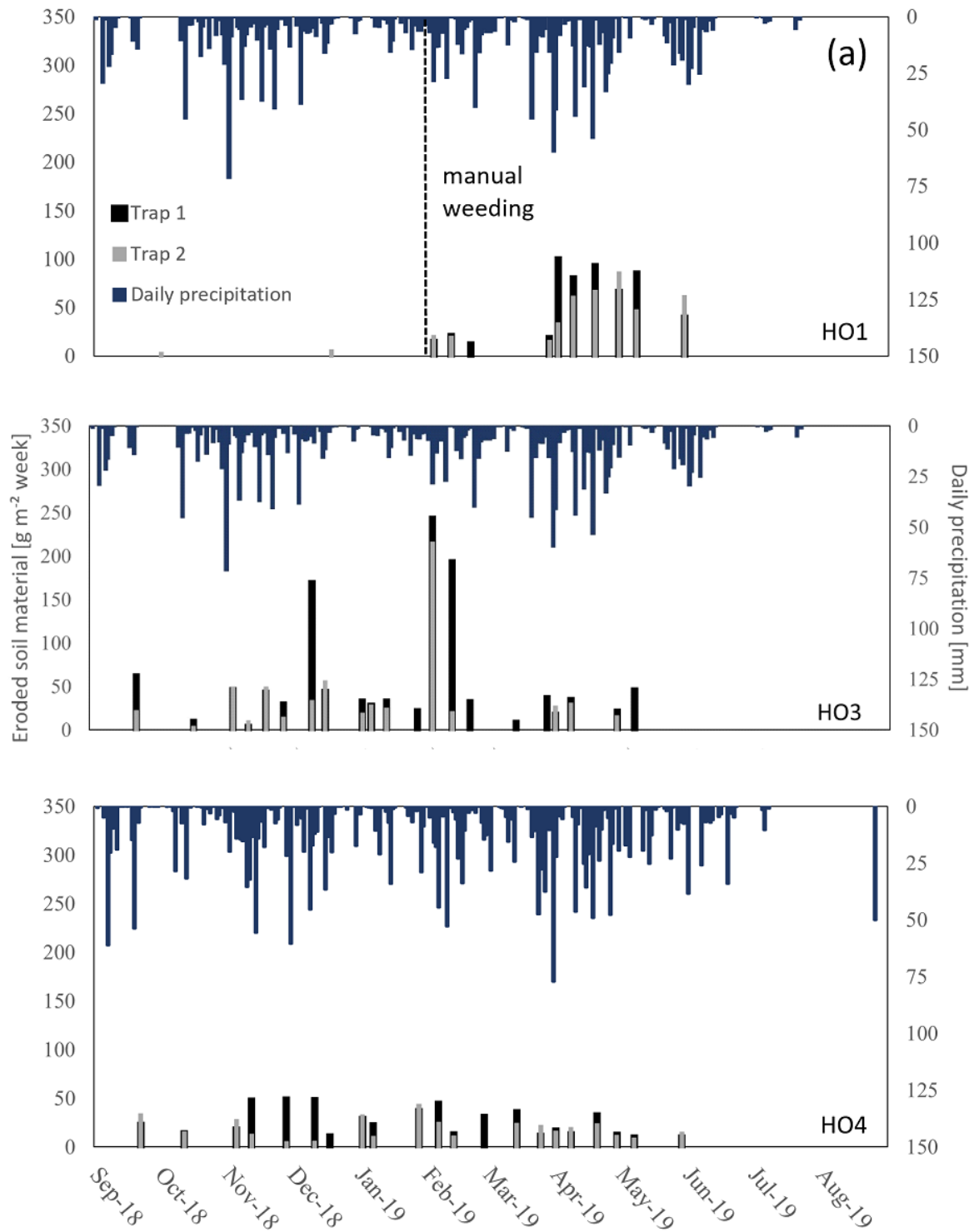
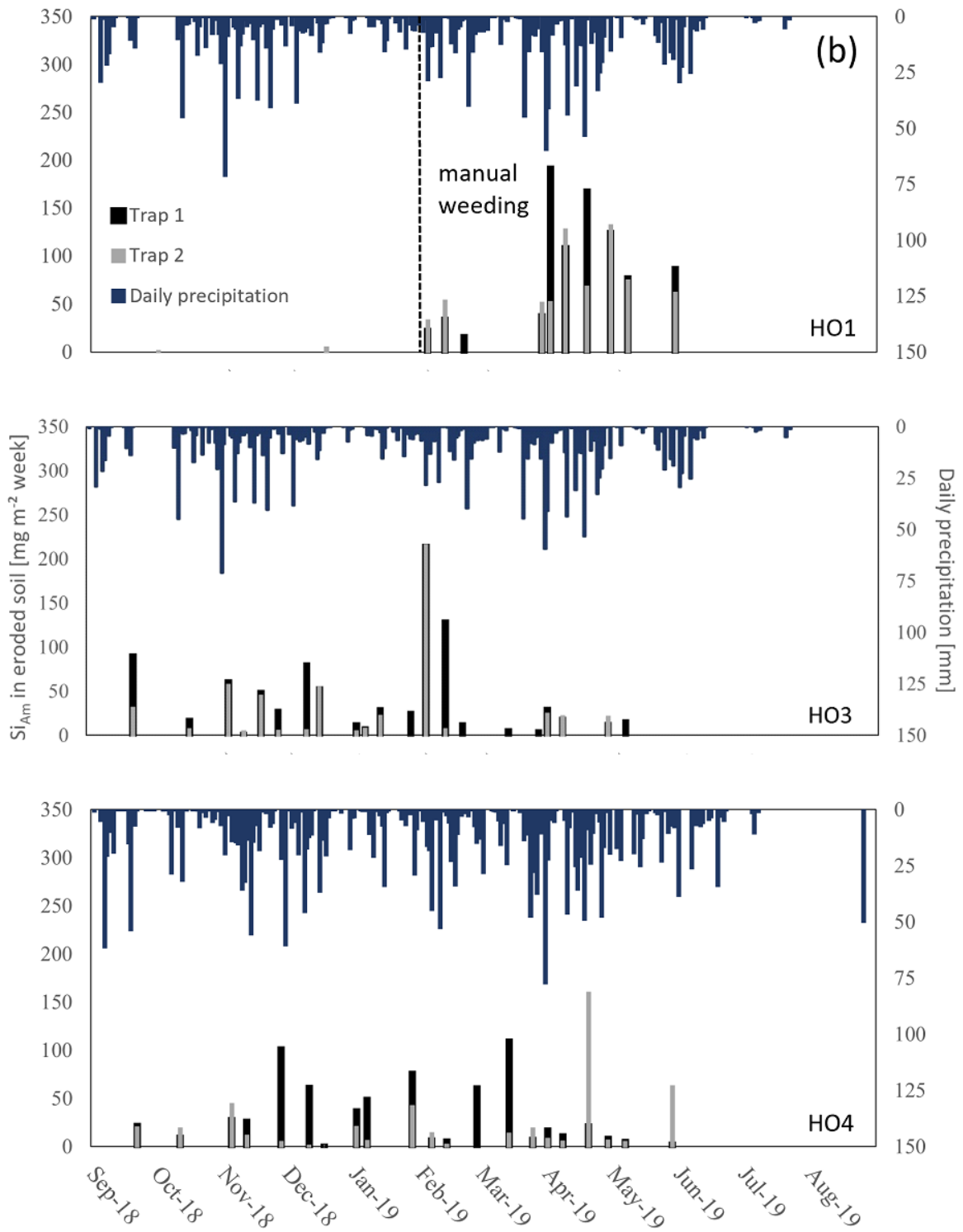


Fig. 3.3 (a) Weekly losses of topsoil and (b) Si in amorphous silica (Si_{Am}) in eroded topsoil, collected from sediment traps ($n = 6$) of oil-palm plantations in well-drained areas.

3 Oil-palm management alters the spatial distribution of amorphous silica and mobile silicon in topsoils



3.4 Discussion

3.4.1 Spatial topsoil Si_{Am} concentration patterns

In oil-palm plantations, cut-off palm fronds stacked in every second interrow represent the main source of phytoliths (Albert et al., 2015; Clymans et al., 2015; Huisman et al., 2018) although these frond pile areas may occupy less than 15 % of the plantation area (Tarigan et al., 2020). Once phytoliths are released into topsoils, they can replenish the topsoil Si_{Am} pool. Therefore, we had hypothesized that Si_{Am} is mainly returned to soils under frond piles (see section 1), leading to a spatial topsoil Si_{Am} pattern with higher Si_{Am} concentrations under frond piles. This hypothesis was corroborated for well-drained plots as topsoil Si_{Am} concentrations were indeed significantly higher (2-fold) under frond piles ($\sim 4 \text{ mg g}^{-1}$) than in all other management zones ($\sim 2 \text{ mg g}^{-1}$) (Fig. 3.2a, Appendix II Table B2.1). Lower Si_{Am} levels in palm circles, oil-palm rows and interrows may reflect the pedogenic Si_{Am} pool with only minor contributions of biogenic Si_{Am} , *e.g.*, from grass phytoliths. A possible reason for this is that decaying palm fronds are not returned to these management zones.

In the riparian plots, topsoil Si_{Am} concentrations were equally high under frond piles and in interrows ($\sim 3 \text{ mg g}^{-1}$). This can only be explained by an additional important source of topsoil Si_{Am} in interrows that was present in the riparian plots. The only potential Si_{Am} source includes litter of grasses (*Poaceae*) and sedges (*Cyperaceae*) which also release considerable amounts of phytoliths upon their decomposition. Grasses and sedges are considered effective Si accumulators, too (Blecker et al., 2006; Quigley et al., 2017). This explanation is further supported by the significantly lower ($p \leq 0.05$) topsoil Si_{Am} concentrations in palm circles ($\sim 1.4 \text{ mg g}^{-1}$) (Fig. 3.2b, Appendix II Table B2.2). Palm circles are weeded and treated with herbicides regularly. Thus, this management zone also lacks litter return and with that a principal source of Si. The significant difference in topsoil Si_{Am} concentrations between interrows and palm circles can only be explained by the presence or absence of grasses as phytolith sources. This observation highlights the importance of grasses and sedges in oil-palm plantations as they can also maintain soil-plant-Si cycling in the system. Thus, our original hypothesis that Si_{Am} is mainly returned to the soils under frond piles, while topsoils in other management zones tend to be depleted in Si_{Am} , is valid only in oil-palm plantations with a negligible grass cover.

The absence of any significant differences in topsoil Si_{Am} concentrations between the two differing water regimes suggests that there was no noticeable Si supply by stream water to topsoils in riparian areas. In fact, release rates of biogenic Si_{Am} from decaying oil-palm and other litter must be similar in both water regimes, likewise, the rate at which oil palms take up Si from soil solution and form phytoliths. This result contrasts with Vander Linden and Delvaux (2019) and Georgiadis et al. (2017), who found that soil type and soil properties affect Si cycling, when comparing well-drained and floodplain soils: Vander Linden and Delvaux (2019) observed that flooding can temporarily increase the soil pH of acidic soils to $\sim 6.5 - 7.2$. In this pH range, phytoliths dissolve faster (Vander Linden

and Delvaux, 2019). Georgiadis et al. (2017) pointed to the effect of alternating redox conditions in soils as caused *e.g.*, by perched water, a fluctuating groundwater table, and flooding. When pedogenic Fe, Al, or Mn oxides and hydroxides are exposed to reducing conditions during flooding, they dissolve and release occluded Si into soil solution. After flooding, when the soil is exposed to oxidizing conditions again, Si can be occluded in and adsorbed to the surfaces of newly formed pedogenic oxides and hydroxides (Georgiadis et al., 2017). Georgiadis et al. (2017) found that these redox-induced dynamics affected mainly the following Si fractions: Si in soil solution (mobile Si), Si adsorbed to Fe oxides and hydroxides, and Si occluded in Fe oxides and hydroxides. Many other researchers found soil pH, soil texture and soil chemistry to govern biogenic and pedogenic Si pools down to at least 1 m soil depth (Alexandre et al., 1997; Struyf and Conley, 2009; Li et al., 2020). The latter soil characteristics were kept constant in our study as we focused specifically on the effect of flooding. The reason that we did not detect any effect of flooding might be the advanced weathering and desilication status of the soils in our study area, which may have led to overall low Si levels of the investigated soils.

3.4.2 Si_{Am} losses through topsoil erosion

Corley and Tinker (2016) summarized some early works by Kee and Chew (1996) and Maene et al. (1979) estimating soil-erosion rates under oil-palm plantations. They reported losses of $\leq 9 \text{ Mg ha}^{-1} \text{ yr}^{-1}$ from sloping oil-palm plantations on Plinthic Acrisols and Haplic Nitisols in Malaysia (Arshad, 2015; Corley and Tinker, 2016). In our study we obtained soil losses of $\sim 4 - 6 \text{ Mg ha}^{-1} \text{ yr}^{-1}$. This puts our estimates into a comparable range (except for trap 1 in plot HO3 that yielded $\sim 12 \text{ Mg ha}^{-1} \text{ yr}^{-1}$). However, short-term experiments can easily overestimate soil-erosion rates if upscaled to landscape level (Breuning-Madsen et al., 2017). The observations by Breuning-Madsen et al. (2017) would imply that the soil losses we obtained for oil-palm plantations are ~ 2 orders of magnitude higher than in a secondary forest (Breuning-Madsen et al., 2017). Considerable erosion (soil loss of $\sim 35 \text{ cm}$ during a 15-year cultivation period, which corresponds to $\sim 28 \text{ Mg ha}^{-1} \text{ yr}^{-1}$) was noted by Guillaume et al. (2015), who compared $\delta^{13}\text{C}$ values in soil profiles on the same well-drained oil-palm plantations of our study region. High erosion rates are to be expected, as oil-palm plantations have a rather open canopy compared to rainforests, permitting raindrops to directly hit the ground (Oliveira et al., 2013; Corley and Tinker, 2016).

During heavy rainfalls, raindrops release kinetic energy that breaks up soil aggregates, especially when hitting bare soil. Mobilized fine and broken aggregates can fill soil pores thereby reducing infiltration, promoting surface runoff (Oliveira et al., 2013; Tarigan et al., 2020) and hence promoting erosion. Besides, soil compaction may be substantial in oil-palm interrows, which are frequently used as harvesting paths and are therefore kept vegetation-free making them particularly prone to surface runoff and erosion (Comte et al., 2012; Guillaume et al., 2016). This explanation is further supported by our sediment-trap data: traps with a low vegetation cover (*e.g.*, HO3 whole year and HO1 as of

February 2019) exposed to daily rainfalls exceeding 25 mm d⁻¹ showed higher losses of soil (~ 50 – 100 g m⁻², Tab 3.1 and Fig. 3.3a) than traps (*e.g.*, HO4 whole year and HO1 prior to February 2019) that had less than 50 % of bare soil at similar rainfall intensities. This again highlights the importance of cover crop in oil-palm plantations countering soil erosion (Guillaume et al., 2016, 2015; Corley and Tinker, 2016; Luke et al., 2019). Furthermore, stacked palm fronds, especially if aligned perpendicularly to the slope, may reduce soil erosion on oil-palm plantations (Corley and Tinker, 2016).

Some of the questions to be answered in this study included the extent to which soil erosion reduces the topsoil Si_{Am} pool in oil-palm plantations and whether the lower density of phytoliths compared to mineral soil particles caused proportionally greater losses of Si_{Am} through soil erosion. To our knowledge, only a few studies exist in which the effect of soil erosion on the topsoil Si_{Am} pool has been addressed. Almost all of them focused on arable soils (Clymans et al., 2015; Unzué-Belmonte et al., 2017; Kraushaar et al., 2021). Clymans et al. (2015) determined mean topsoil Si_{Am} concentrations of 1.76 mg g⁻¹ in arable fields in sloping terrain and temperate climate. This compares well to topsoil Si_{Am} concentrations in interrows from our study (Tab. 1). In contrast, Si_{Am} concentrations in eroded soil material differed by a factor of 2 between plots HO1 (1.61 mg g⁻¹) towards HO3 (0.88 mg g⁻¹) and HO4 (0.66 mg g⁻¹) (Tab. 1 and Appendix II Table B3). A possible explanation could be the differing maintenance of the cover crop. High median Si_{Am} concentrations in eroded soil material were determined in previously vegetated traps (*e.g.*, HO1 until the end of January 2019), whereas lower median Si_{Am} concentrations in eroded soil material were measured in traps with less vegetation (HO3 and HO4, whole year, Tab. 1). We may infer from this observation that the cover crop in plot HO1 maintained higher Si levels in the topsoil through continuous phytolith release from litter. After weeding and keeping the vegetation cover at around 5 %, this phytolith-enriched topsoil was eroded, leading to higher Si_{Am} concentrations in the eroded soil material. In contrast, plots HO3 and HO4 had lower and more dispersed Si_{Am} concentrations in eroded soil material as they lacked an additional Si source. Further, low Si_{Am} concentrations suggest that topsoil with originally high amounts of biogenic Si_{Am} has already been eroded over time, leaving mainly pedogenic Si_{Am}. A greater variability in Si_{Am} concentrations in eroded soil material in plots HO3 and HO4 was probably caused by a slight increase in vegetation cover during the year and secondarily, by varying daily rainfalls (Fig. 3.3). Thus, these observations could provide a basis to state that phytoliths are preferably eroded from topsoils. This in turn would assert our hypothesis. Nevertheless, further field experiments and observations are required to confirm this statement.

3.4.3 Spatial topsoil Si_M concentration patterns

Topsoil Si_M concentrations in well-drained plots were highest under frond piles (~ 14 µg g⁻¹), followed by palm circles (~ 11 µg g⁻¹), and lowest in oil-palm rows and interrows (~ 6 µg g⁻¹). However, these differences were not statistically significant (Fig. 3.2c, 3.2d). Higher topsoil Si_M concentrations under

frond piles can be explained by the high solubility of Si_{Am} that is released from decaying palm fronds in the form of phytoliths. In addition to Si_{Am} (Barão et al., 2014; Unzué-Belmonte et al., 2017), Si associated with soil organic matter (SOM) also represents a readily soluble Si fraction in topsoils (Alexandre et al., 1997; Georgiadis et al., 2013; von der Lühe et al., 2020). Such readily soluble Si fractions usually contribute most Si to the soil solution (Struyf et al., 2010; de Tombeur et al., 2020).

The plots in the riparian areas showed high topsoil Si_{M} concentrations under the frond piles ($\sim 20 \mu\text{g g}^{-1}$). All other management zones had lower topsoil Si_{M} concentrations in the range of $\sim 11 - 12 \mu\text{g g}^{-1}$ (Fig. 3.2b). However, this difference was also not statistically significant. In riparian plots, flooding may lead to a redistribution of Si_{M} across the oil-palm plantation, hence explaining similar topsoil Si_{M} concentrations in palm circles, oil-palm rows and interrows. In riparian areas that are flooded during the rainy season, dissolved Si in stream water (Cornelis et al., 2011; Dürr et al., 2011) may be another source of topsoil Si_{M} alongside Si_{Am} . Therefore, we had hypothesized that Si input from stream water may lead to higher topsoil Si_{M} levels in riparian areas compared to well-drained areas. Indeed, topsoil Si_{M} concentrations under frond piles in riparian plots ($\sim 20 \mu\text{g g}^{-1}$) tended to be higher compared to well-drained plots ($\sim 14 \mu\text{g g}^{-1}$). Likewise, topsoil Si_{M} concentrations in oil-palm rows and interrows in riparian plots ($\sim 11-12 \mu\text{g g}^{-1}$) also tended to be higher compared to well-drained plots ($\sim 6 \mu\text{g g}^{-1}$). However, these differences were not statistically significant so our hypothesis cannot be fully asserted.

3.5 Conclusions and recommended measures

Based on the differing topsoil Si_{Am} concentrations observed in the different management zones, we conclude that current oil-palm management practices cause a distinct spatial topsoil Si_{Am} concentration pattern. Especially the stacking of cut-off palm fronds in long piles and subsequent decomposition promotes Si_{Am} return to soils. Thus, the highest topsoil Si_{Am} concentrations occur below frond piles. Similarly, high concentrations may be found in interrows if additional sources of biogenic Si_{Am} such as Si-accumulating plants (grasses, sedges) are present. Lower topsoil Si_{Am} concentrations in oil-palm rows and unvegetated interrows reflect a lack of Si_{Am} return to soils through plant litter in these management zones. Moreover, pronounced topsoil erosion in unvegetated interrows involves Si_{Am} losses and may therefore cause additional Si_{Am} depletion in this management zone. A dense cover of grasses and mosses in interrows may efficiently reduce erosion and associated Si_{Am} losses.

Topsoil Si_{M} concentrations in the different management zones showed that biogenic Si_{Am} was an important readily available source of Si_{M} . Thus, analogous to topsoil Si_{Am} concentrations, the highest topsoil Si_{M} concentrations also occurred under frond piles. Our hypothesis that regular flooding involves an input of Si dissolved in stream water into the system in riparian areas, partially replenishing the Si_{M} pool, could not be statistically proven in this study. Although topsoil Si_{M} concentrations tended to be higher in riparian areas, the differences between well-drained and riparian plots were not statistically significant.

In conclusion, our findings suggest that erosion could be reduced efficiently, and Si cycling could be maintained within the system if smallholders followed some suggested measures such as (i) maintaining a grass cover in oil-palm rows and interrows, (ii), incorporating oil-palm litter into plantation management, and (iii) preventing soil compaction and surface-crust formation. It would be advisable to raise awareness on topsoil erosion and its potential causes. Furthermore, any logistical efforts and costs involved for implementing these measures (*e.g.*, for ameliorating soil compaction) would have to be feasible.

3.6 Acknowledgements

We thank the German Research Foundation DFG for funding this project (DFG project no. 391702217). The project was associated to the Collaborative Research Center 990 “Ecological and Socioeconomic Functions of Tropical Lowland Rainforest Transformation Systems” (CRC 990, DFG project no. 192626868). We also thank the Ministry of Education, Technology and Higher Education (RISTEKDIKTI) for granting a research permission in Indonesia and the CRC 990 oil-palm smallholder partners. Soil sampling was conducted using the research permits 110/SIP/FRP/E5/Dit.KI/IV/2018 and 187/ E5/E5.4/SIP/2019. Special thanks go to our Indonesian counterparts, the CRC-990 office members, and our fieldwork assistants Nando, Daniel, Somad, and Firdaus in Jambi. We would also like to thank the laboratory staff from the Institute of Geography, University of Göttingen, Jürgen Grotheer, Anja Södje, and Petra Voigt, for their support.

3.7 Author contributions

BvdL and DS designed the study of the paper with input from HJH, ST, and AT. BG conducted soil sampling with input from BvdL, ST, AT, and DS. CS sampled and provided meteorological data. BG conducted laboratory analysis and evaluated the data with input from BvdL, HJH, CS, and DS. BG wrote the first draft. All authors (BG, BvdL, HJH, CS, ST, AT, and DS) contributed to generating and reviewing the subsequent versions of the paper.

3.8 References

- Albert RM, Bamford MK, Esteban I (2015) Reconstruction of ancient palm vegetation landscapes using a phytolith approach. *Quat Int* 369:51–66. <https://doi.org/10.1016/j.quaint.2014.06.067>
- Alexandre A, Meunier J-D, Colin F, Koud J-M (1997) Plant impact on the biogeochemical cycle of silicon and related weathering processes. *Geochim Cosmochim Acta* 61:677–682. [https://doi.org/10.1016/S0016-7037\(97\)00001-X](https://doi.org/10.1016/S0016-7037(97)00001-X)
- Allen K, Corre MD, Kurniawan S, et al (2016) Spatial variability surpasses land-use change effects on soil biochemical properties of converted lowland landscapes in Sumatra, Indonesia. *Geoderma* 284:42–50. <https://doi.org/10.1016/j.geoderma.2016.08.010>
- Arshad AM (2015) Physical land evaluation for oil palm cultivation in district of Temerloh and Kuantan, Pahang, Peninsular Malaysia. *J Biol Agric Heal* 5:104–112
- Barão L, Clymans W, Vandevenne F, et al (2014) Pedogenic and biogenic alkaline-extracted silicon distributions along a temperate land-use gradient. *Eur J Soil Sci* 65:693–705. <https://doi.org/10.1111/ejss.12161>
- Barão L, Teixeira R, Vandevenne F, et al (2020) Silicon Mobilization in Soils: the Broader Impact of Land Use. *Silicon* 12:1529–1538. <https://doi.org/10.1007/s12633-019-00245-y>
- Blecker SW, McCulley RL, Chadwick OA, Kelly EF (2006) Biologic cycling of silica across a grassland bioclimate sequence. *Global Biogeochem Cycles* 20:. <https://doi.org/10.1029/2006GB002690>
- Breuning-Madsen H, Kristensen JÅ, Awadzi TW, Murray AS (2017) Early cultivation and bioturbation cause high long-term soil erosion rates in tropical forests: OSL based evidence from Ghana. *Catena* 151:130–136. <https://doi.org/10.1016/j.catena.2016.12.002>
- Clough Y, Krishna V V., Corre MD, et al (2016) Land-use choices follow profitability at the expense of ecological functions in Indonesian smallholder landscapes. *Nat Commun* 7:1–12. <https://doi.org/10.1038/ncomms13137>
- Clymans W, Struyf E, Van den Putte A, et al (2015) Amorphous silica mobilization by inter-rill erosion: Insights from rainfall experiments. *Earth Surf Process Landforms* 40:1171–1181. <https://doi.org/10.1002/esp.3707>
- Comte I, Colin F, Whalen JK, et al (2012) Agricultural practices in oil palm plantations and their impact on hydrological changes, nutrient fluxes and water quality in Indonesia: a review.
- Conley DJ, Likens GE, Buso DC, et al (2008) Deforestation causes increased dissolved silicate losses in the Hubbard Brook Experimental Forest. *Glob Chang Biol* 14:2548–2554. <https://doi.org/10.1111/j.1365-2486.2008.01667.x>
- Corley RHV, Tinker PBH (2016) *The Oil Palm (World Agricultural Series) fifth edition*, 647 pp., <https://doi.org/10.1017/cbo9781316530122.010,2016>
- Cornelis J, Delvaux B, Georg RB, et al (2011) Tracing the origin of dissolved silicon transferred from various soil-plant systems towards rivers : a review. 89–112. <https://doi.org/10.5194/bg-8-89-2011>

3 Oil-palm management alters the spatial distribution of amorphous silica and mobile silicon in topsoils

- Darras KFA, Corre MD, Formaglio G, et al (2019) Reducing Fertilizer and Avoiding Herbicides in Oil Palm Plantations—Ecological and Economic Valuations. *Front For Glob Chang* 2:1–15. <https://doi.org/10.3389/ffgc.2019.00065>
- De Coster GL (2006) *The Geology of the central and south sumatra basins, 1974*. pp 77-110
- de Tombeur F, Turner BL, Laliberté E, et al (2020) Plants sustain the terrestrial silicon cycle during ecosystem retrogression. *Science* (80-) 369:1245–1248. <https://doi.org/10.1126/science.abc0393>
- Dislich C, Keyel AC, Salecker J, et al (2017) A review of the ecosystem functions in oil palm plantations, using forests as a reference system. *Biol Rev* 92:1539–1569. <https://doi.org/10.1111/brv.12295>
- Drescher J, Rembold K, Allen K, et al (2016) Ecological and socio-economic functions across tropical land use systems after rainforest conversion. *Philos Trans R Soc B Biol Sci* 371:20150275. <https://doi.org/10.1098/rstb.2015.0275>
- Dürr HH, Meybeck M, Hartmann J, et al (2011) Global spatial distribution of natural riverine silica inputs to the coastal zone. *Biogeosciences* 8:597–620. <https://doi.org/10.5194/bg-8-597-2011>
- Epstein E (2009) Silicon: its manifold roles in plants. *Ann Appl Biol* 155:155–160. <https://doi.org/10.1111/j.1744-7348.2009.00343.x>
- Euler M, Schwarze S, Siregar H, Qaim M (2016) Oil Palm Expansion among Smallholder Farmers in Sumatra , Indonesia. *J Agric Econ* 67:658–676. <https://doi.org/10.1111/1477-9552.12163>
- FAO (2020) *Oilseeds, oils & meals*
- Formaglio G, Veldkamp E, Duan X, et al (2020) Herbicide weed control increases nutrient leaching as compared to mechanical weeding in a large-scale oil palm plantation. *Biogeosciences* 17:5243–5262. <https://doi.org/10.5194/bg-2020-153>
- Fox J, Weisberg S (2019) *An {R} Companion to Applied Regression*. <https://socialsciences.mcmaster.ca/jfox/Books/Companion/> [Accessed February 10, 2023]
- Frayse F, Pokrovsky OS, Schott J, Meunier J-D (2009) Surface chemistry and reactivity of plant phytoliths in aqueous solutions. *Chem Geol* 258:197–206. <https://doi.org/10.1016/j.chemgeo.2008.10.003>
- Georgiadis A, Rinklebe J, Straubinger M, Rennert T (2017) Silicon fractionation in Mollic Fluvisols along the Central Elbe River, Germany. *Catena* 153:100–105. <https://doi.org/10.1016/j.catena.2017.01.027>
- Georgiadis A, Sauer D, Herrmann L, et al (2013) Development of a method for sequential Si extraction from soils. *Geoderma* 209:251–261. <https://doi.org/10.1016/j.geoderma.2013.06.023>
- Grass I, Kubitzka C, Krishna V V., et al (2020) Trade-offs between multifunctionality and profit in tropical smallholder landscapes. *Nat Commun* 11:1–13. <https://doi.org/10.1038/s41467-020-15013-5>
- Grasshoff K, Kremling K, Ehrhardt M (2009) *Methods of sea water analysis, third*. John Wiley & Sons
- Guillaume T, Damris M, Kuzyakov Y (2015) Losses of soil carbon by converting tropical forest to

- plantations: erosion and decomposition estimated by $\delta^{13}\text{C}$. *Glob Chang Biol* 21:3548–3560. <https://doi.org/10.1111/gcb.12907>
- Guillaume T, Holtkamp AM, Damris M, et al (2016) Soil degradation in oil palm and rubber plantations under land resource scarcity. *Agric Ecosyst Environ* 232:110–118. <https://doi.org/10.1016/j.agee.2016.07.002>
- Guntzer F, Keller C, Meunier JD (2012) Benefits of plant silicon for crops: A review. *Agron Sustain Dev* 32:201–213. <https://doi.org/10.1007/s13593-011-0039-8>
- Harrison RD, Swinfield T (2015) Restoration of logged humid tropical forests: An experimental programme at Harapan Rainforest, Indonesia. *Trop Conserv Sci* 8:4–16. <https://doi.org/10.1177/194008291500800103>
- Haynes RJ (2014) A contemporary overview of silicon availability in agricultural soils. *J Plant Nutr Soil Sci* 177:831–844. <https://doi.org/10.1002/jpln.201400202>
- Hennings N, Becker JN, Guillaume T, et al (2021) Riparian wetland properties counter the effect of land-use change on soil carbon stocks after rainforest conversion to plantations. *Catena* 196:104941. <https://doi.org/10.1016/j.catena.2020.104941>
- Huisman SN, Raczka MF, McMichael CNH (2018) Palm phytoliths of mid-elevation Andean forests. *Front Ecol Evol* 6:1–8. <https://doi.org/10.3389/fevo.2018.00193>
- Iler RK (1979) The chemistry of silica: solubility, polymerization, colloid and surface properties, and biochemistry. Wiley & Sons, Wiley, 896 pp., <https://doi.org/10.1002/ange.19800920433>
- Kassambara A (2022) ggpubr: “ggplot2” Based Publication Ready Plots R package version 0.5.0, <https://CRAN.R-project.org/package=ggpubr> [Accessed February 8, 2023]
- Keller C, Guntzer F, Barboni D, et al (2012) Impact of agriculture on the Si biogeochemical cycle: Input from phytolith studies. *Comptes Rendus Geosci* 344:739–746. <https://doi.org/10.1016/j.crte.2012.10.004>
- Klotzbücher T, Klotzbücher A, Kaiser K, et al (2018) Impact of agricultural practices on plant-available silicon. *Geoderma* 331:15–17. <https://doi.org/10.1016/j.geoderma.2018.06.011>
- Kotowska MM, Leuschner C, Triadiati T, et al (2015) Quantifying above- and belowground biomass carbon loss with forest conversion in tropical lowlands of Sumatra (Indonesia). *Glob Chang Biol* 21:3620–3634. <https://doi.org/10.1111/gcb.12979>
- Kraushaar S, Konzett M, Kiep J, et al (2021) Suitability of phytoliths as a quantitative process tracer for soil erosion studies. *Earth Surf Process Landf* 46:1797–1808. <https://doi.org/10.1002/esp.5121>
- Laumonier Y (1997) The Vegetation and Physiography of Sumatra. In: *Geobotany*. Kluwer Academic Publishers, p 223, <https://doi.org/10.1007/978-94-009-0031-8>
- Li Z, de Tombeur F, Vander Linden C, et al (2020) Soil microaggregates store phytoliths in a sandy loam. *Geoderma* 360:114037. <https://doi.org/10.1016/j.geoderma.2019.114037>
- Luke SH, Purnomo D, Advento AD, et al (2019) Effects of understory vegetation management on plant communities in oil palm plantations in Sumatra, Indonesia. *Front For Glob Chang* 2:1–13.

<https://doi.org/10.3389/ffgc.2019.00033>

- Ma JF, Takahashi E (2002) Silicon-accumulating plants in the plant kingdom. In: Soil, fertilizer, and plant silicon research in Japan. Elsevier Science, Amsterdam, pp 63–71
- Meijaard E, Brooks T, Carlson KM, et al (2020) The environmental impacts of palm oil in context. *Nat Plants* 6:1418–1426. <https://doi.org/10.1038/s41477-020-00813-w>
- Meunier JD, Keller C, Guntzer F, et al (2014) Assessment of the 1% Na₂CO₃ technique to quantify the phytolith pool. *Geoderma* 216:30–35. <https://doi.org/10.1016/j.geoderma.2013.10.014>
- Munevar F, Romero A (2015) Soil and plant silicon status in oil palm crops in Colombia. *Exp Agric* 51:382. <https://doi.org/10.1017/S0014479714000374>
- Oliveira PTS, Wendland E, Nearing MA (2013) Rainfall erosivity in Brazil: a review. *Catena* 100:139–147. <https://doi.org/10.1016/j.catena.2012.08.006>
- Qaim M, Sibhatu KT, Siregar H, Grass I (2020) Environmental, Economic, and Social Consequences of the Oil Palm Boom. *Annu Rev Resour Economics* 12:1–24. <https://doi.org/10.1146/annurev-resource-110119-024922>
- Quigley KM, Donati GL, Anderson TM (2017) Variation in the soil ‘silicon landscape’ explains plant silica accumulation across environmental gradients in Serengeti. *Plant Soil* 410:217–229. <https://doi.org/10.1007/s11104-016-3000-4>
- Revelle W (2022) psych: Procedures for Personality and Psychological Research, <https://CRAN.R-project.org/package=psychVersion=2.2.9>. [Accessed February 10, 2023]
- Sauer D, Saccone L, Conley DJ, et al (2006) Review of methodologies for extracting plant-available and amorphous Si from soils and aquatic sediments. *Biogeochemistry* 80:89–108. <https://doi.org/10.1007/s10533-005-5879-3>
- Schaller J, Puppe D (2021) Heat improves silicon availability in mineral soils. *Geoderma* 386:114909. <https://doi.org/10.1016/j.geoderma.2020.114909>
- Schaller J, Frei S, Rohn L, Gilfedder BS (2020) Amorphous silica controls water storage capacity and phosphorus mobility in soils. *Front Environ Sci* 8:94. <https://doi.org/10.3389/fenvs.2020.00094>
- Schaller J, Puppe D, Kaczorek D, et al (2021) Silicon cycling in soils revisited. *Plants* 10:1–36. <https://doi.org/10.3390/plants10020295>
- Sinukaban N, Tarigan SD, Purwakusuma W, et al (2000) Analysis of watershed function sediment transfer across various type of filter strips, Final report to ICRAF, pp72
- Street-Perrott F. A, Barker PA (2008) Biogenic silica: a neglected component of the coupled global continental biogeochemical cycles of carbon and silicon. *Earth Surf Process Landforms* 33:1436–1457. <https://doi.org/10.1002/esp.1712>
- Struyf E, Conley D (2012) Emerging understanding of the ecosystem silica filter. *Biogeochemistry* 107:9–18. <https://doi.org/10.1007/s10533-011-9590-2> SYNTHESIS
- Struyf E, Conley DJ (2009) Silica: an essential nutrient in wetland biogeochemistry. *Front Ecol Environ* 7:88–94. <https://doi.org/10.1890/070126>

3 Oil-palm management alters the spatial distribution of amorphous silica and mobile silicon in topsoils

- Struyf E, Smis A, Van Damme S, et al (2010) Historical land use change has lowered terrestrial silica mobilization. *Nat Commun* 1:1–7. <https://doi.org/10.1038/ncomms1128>
- Tarigan S, Stiegler C, Wiegand K, et al (2020) Relative contribution of evapotranspiration and soil compaction to the fluctuation of catchment discharge: case study from a plantation landscape. *Hydrological Sciences Journal* 65:1239–1248. <https://doi.org/10.1080/02626667.2020.1739287>
- Tsujino R, Yumoto T, Kitamura S, et al (2016) History of forest loss and degradation in Indonesia. *Land use policy* 57:335–347. <https://doi.org/10.1016/j.landusepol.2016.05.034>
- Unzué-Belmonte D, Ameijeiras-Mariño Y, Opfergelt S, et al (2017) Land use change affects biogenic silica pool distribution in a subtropical soil toposequence. *Solid Earth* 8:737–750. <https://doi.org/10.5194/se-8-737-2017>
- Vander Linden C, Delvaux B (2019) The weathering stage of tropical soils affects the soil-plant cycle of silicon, but depending on land use. *Geoderma* 351:209–220. <https://doi.org/10.1016/j.geoderma.2019.05.033>
- Vandevenne F, Struyf E, Clymans W, Meire P (2012) Agricultural silica harvest: have humans created a new loop in the global silica cycle? *Front Ecol Environ* 10:243–248. <https://doi.org/10.1890/110046>
- von der Lühe B, Pauli L, Greenshields B, et al (2020) Transformation of Lowland Rainforest into Oil-palm Plantations and use of Fire alter Topsoil and Litter Silicon Pools and Fluxes. *Silicon* 13:4345–4353. <https://doi.org/10.1007/s12633-020-00680-2>
- Wickham H (2016) *ggplot2: Elegant Graphics for Data Analysis*

4 Estimating oil-palm Si storage, Si return to soils and Si losses through harvest in smallholder oil-palm plantations of Sumatra, Indonesia

Britta Greenshields¹, Barbara von der Lühe¹, Felix Schwarz¹, Harold J. Hughes¹, Aiyen Tjoa², Martyna Kotowska³, Fabian Brambach⁴, Daniela Sauer¹

¹Department of Physical Geography, University of Göttingen, Göttingen, Germany

²Faculty of Agriculture, Tadulako University, Palu, Indonesia

³Department of Plant Ecology and Ecosystems Research, University of Göttingen, Göttingen, Germany

⁴Department of Biodiversity, Macroecology & Biogeography, University of Göttingen, Göttingen, Germany

Corresponding author: Britta Greenshields

Accepted manuscript – Biogeosciences
<https://doi.org/10.5194/egusphere-2022-905>

Abstract. Most plant-available Si in strongly desilicated soils is provided through litter decomposition and subsequent phytolith dissolution. The importance of Si cycling in tropical soil-plant systems raised the question if oil-palm cultivation alters Si cycling. As oil palms are considered Si hyper-accumulators, we hypothesized that much Si is stored in the aboveground biomass of oil palms with time. Furthermore, the system might lose considerable amounts of Si every year through fruit-bunch harvest. To test these hypotheses, we analysed Si concentrations in fruit-bunch stalks, fruit pulp and kernels, as well as in leaflets, rachises, and frond bases of mature oil palms on eight smallholder oil-palm plantations in Sumatra, Indonesia. We estimated Si storage in the total aboveground biomass of oil palms, Si return to soils through decomposing pruned palm fronds, and Si losses from the system through harvest. Leaflets of oil-palm fronds had a mean Si concentration > 1 wt. %. All other analysed plant parts had < 0.5 wt. % Si. According to our estimates, a single palm tree stored about 4 – 5 kg Si in its total aboveground biomass. A smallholder oil-palm plantation stored at least 550 kg Si per hectare in the palm trees' aboveground biomass. Pruned palm fronds returned 111 – 131 kg of Si per hectare to topsoils each year. Fruit-bunch harvest corresponded to an annual Si export of 32 – 72 kg Si per hectare in 2015 and 2018. Greater Si losses (of at least 550 kg Si per hectare) would occur from the system if oil-palm stems were removed from plantations prior to replanting. Therefore, it is advisable to leave oil-palm stems on the plantations e.g., by distributing chipped stem parts across the plantation at the end of a plantation cycle (~25 years).

Keywords: oil-palm management, silicon cycling, silicon balance, silicon export through harvest, tropical soils

4.1 Introduction

Indonesia has become one of the largest global palm-oil producers with currently ~16 million ha under oil-palm cultivation (Gaveau et al., 2022). In the 1980s, the emerging palm-oil boom led to clearing of rainforests (Tsujino et al., 2016; Qaim et al., 2020). Since then, palm oil has remained a tropical cash crop with high demand on the global market (Qaim et al., 2020) due to its versatile use, e.g., as vegetable oil, in cosmetics, and biofuels (FAO 2020). In Jambi Province, Indonesia, oil-palm cultivation has improved the livelihoods of many smallholder farmers, yet at the expense of the natural environment (Clough et al., 2016; Grass et al., 2020; Qaim et al., 2020). This has resulted in a decrease in biodiversity (Drescher et al., 2016; Meijaard et al., 2020) and ecosystem services (Dislich et al., 2017). To balance ecosystem preservation (Tsujino et al., 2016) and economic prosperity (Grass et al., 2020), current research aims to identify ways to increase land-use sustainability while keeping current oil-palm plantations profitable (Darras et al., 2019; Luke et al., 2019).

Oil palms, like many other crops, are commonly grown on highly weathered soils that have been exposed to intense element leaching, including phosphorous (P), potassium (K), calcium (Ca) and silicon (Si) (Haynes, 2014). Yet, well-balanced Si levels in soils are essential for many crops because Si can promote the release of adsorbed macro-nutrients and prevent plant toxicity at low soil pH (Epstein, 2009). Plants store Si in their leaf tissue to mitigate biotic and abiotic stresses and to reduce transpiration. Si is taken up from soil solution as monomeric silicic acid (H_4SiO_4) (Haynes, 2017) and is then transported from the roots to the shoot with the xylem flow (Liang et al., 2015). Transpiration increases the Si concentration in the leaf tissue, where Si finally precipitates as amorphous silica bodies called phytoliths ($\text{SiO}_2 \cdot n\text{H}_2\text{O}$) (Liang et al., 2015; Haynes, 2017). It preferentially precipitates in epidermal cell walls, the cell lumen, and intercellular spaces of any plant part, such as the shoot, leaflets, leaf stalk, and fruit (Liang et al., 2015). Si can also precipitate in certain Si cells associated with the vascular system in the stem or endodermis of roots (Epstein, 1994; Haynes, 2017).

Plants can be grouped into three categories based on the Si concentration and Si/Ca ratio in their dry leaf tissue (Ma and Takahashi, 2002): (I) non-accumulators or excluders (Si concentration < 0.5 wt. %; Si/Ca < 0.5); (II) intermediate accumulators (Si concentration $0.5 - 1$ wt. %; Si/Ca $0.5 - 1$) and (III) accumulators (Si concentration > 1 wt. %; Si/Ca > 1). To better distinguish between plants of groups II and III, we will use the term “hyper-accumulator” for plants of group III throughout this paper. Following this terminology, Si hyper-accumulators include e.g., rice (*Oryza sativa* L.), barley (*Hordeum vulgare* L.), maize (*Zea mays* L.), wheat (*Triticum aestivum* L.), and sugarcane (*Saccharum officinarum* L.) (Haynes, 2017). According to Munevar and Romero (2015) oil palms are Si hyper-accumulators, too. They reported high Si concentrations in oil-palm fronds in Colombia and found that the Si concentration increased with leaf age. However, these observations have not yet been confirmed in any other oil-palm growing region. In addition, Si concentrations of oil-palm parts other than leaves need to be quantified to reliably estimate Si storage in oil palms.

Several studies have shown that land conversion from forests to arable land has caused soil Si depletion on the long term (Struyf et al., 2010; Clymans et al., 2015; Carey and Fulweiler, 2016). Thereby, reduced Si return to soils through litter input and Si export through crop harvest were identified as main drivers (Puppe et al., 2021; Vandevenne et al., 2012; Guntzer et al., 2012). The weathering stage of soils can also affect biological Si cycling (Vander Linden and Delvaux, 2019; Carey, 2020; de Tombeur et al., 2020). In strongly weathered soils, Si cycling is predominantly maintained by the recycling of phytoliths (de Tombeur et al., 2020). For these reasons, some crops already receive Si fertilizers, especially when cultivated on strongly weathered, naturally desilicated soils (Datnoff et al., 1997; Li and Delvaux, 2019; Zellner et al., 2021). Under oil-palm plantations, amorphous Si concentrations in topsoil were decreased (by factor 1.25) compared to rainforest topsoil (von der Lühе et al., 2020). Furthermore, the dissolution rate of phytoliths isolated from oil-palm litter was significantly lower compared to rainforest litter (von der Lühе et al., 2022). These previous observations suggest that rainforest conversion to oil-palm plantations can considerably alter Si cycling. This raised our concern that oil-palm cultivation may lead to soil Si depletion with time, to a degree that could negatively affect future crop yields.

Si cycling differs between oil-palm plantations and undisturbed terrestrial ecosystems: in undisturbed terrestrial ecosystems, Si returns to soil through litterfall. Subsequent litter decomposition leads to an accumulation of phytoliths in the topsoil (Conley et al., 2008; Li et al., 2020) which is a key source of Si that can easily become plant-available (Lucas et al., 1993; Alexandre et al., 1997; Schaller et al., 2018). In oil-palm plantations, Si which has been taken up by oil palms mainly returns to soils through decomposing palm fronds (von der Lühе et al., 2022) which are pruned and then commonly stacked in piles in every second row of a plantation (Dislich et al., 2017). Phytolith accumulation in topsoils is therefore largely restricted to frond pile areas (Greenshields et al., 2023; von der Lühе et al., 2022) which may comprise as little as ~ 12 % of the plantation (Tarigan et al., 2020). In oil-palm plantations, Si cycling is expected to be further disrupted by fruit-bunch harvest. Si losses from the system can be considerable as not only fruit, but entire fruit bunches are removed from the system (Kotowska et al., 2015; Euler et al., 2016a). Lastly, oil palms have a ~25-year cultivation cycle (Corley and Tinker, 2016). Many oil-palm plantations in Indonesia are currently approaching the end of their first cultivation cycle in Sumatra. Yet, there is no clear strategy on how to use the biomass of the first-generation oil palms (Awalludin et al., 2015).

To our knowledge, only Munevar and Romero (2015) have quantified Si concentrations in oil-palm leaves so far. Furthermore, no Si concentrations from oil-palm parts other than leaflets have been reported yet. Therefore, our study in a region dominated by smallholder oil-palm plantations in lowland Sumatra, Indonesia, had two aims: first, to test whether oil palms in Indonesia can be considered Si hyper-accumulators, and second, to estimate Si storage in oil palms, Si losses from the system through harvest, and Si return from plants to soils on oil-palm plantations in two different

landscape positions (well-drained areas – slopes; riparian areas – floodplains) and WRB reference soil groups (Acrisols and Stagnosols). We hypothesized that much Si is stored in the aboveground biomass of oil palms with time. Furthermore, the system might lose considerable amounts of Si every year through fruit-bunch harvest. To account for the landscape position, we further hypothesized that soils in riparian areas might be less affected by Si depletion because they additionally receive dissolved silicic acid through flooding and capillary rise of groundwater as well as through lateral water fluxes (inflow) from higher landscape areas. We expected that greater Si availability in riparian areas would result in greater Si uptake, and consequently in greater Si storage in the aboveground biomass of riparian oil-palm plantations.

4.2 Materials and methods

4.2.1 Study area

The study was conducted in the lowlands of Jambi Province, Sumatra, Indonesia ($1^{\circ} 55' 0''$ S, $103^{\circ} 15' 0''$ E; 50 m \pm 5 m above sea level). The region has a humid tropical climate with a mean annual temperature of 26.7 °C and a mean annual precipitation of 2230 mm yr⁻¹ (Drescher et al., 2016). The climate is characterized by two rainy seasons in December and March and a dry season lasting from July to August (Drescher et al., 2016). The geological basement of the study area consists of pre-Paleogene metamorphic and igneous bedrock alongside lacustrine and fluvial sediments (De Coster, 2006). The soils in well-drained areas at higher landscape positions are predominantly Acrisols, whereas the temporarily flooded riparian areas are dominated by Stagnosols (IUSS Working Group WRB, 2022; Hennings et al., 2021). The natural vegetation is a mixed dipterocarp lowland rainforest (Laumonier, 1997). Alongside oil-palm plantations, large areas in the lowlands of Jambi Province are also covered by rubber, jungle rubber and commercial timber (Dislich et al., 2017). We conducted sampling on smallholder oil-palm plantations (≤ 2 ha) at four well-drained (Acrisols) and at four riparian (Stagnosols) sites (Dislich et al., 2017). On each plantation, study plots (50 x 50 m) were established by the Collaborative Research Centre (CRC) 990 – EFForTs (funded by the German Research Foundation). At the time of sampling, oil palms were 18 – 22 years old at the well-drained sites (HO1 – 4), and 11 – 21 years old at riparian sites (HOr1 – 4) (Hennings et al., 2021). The average planting density was 142 ± 17 oil palms per hectare. Oil palms were planted in a triangular planting array with ~ 9 m distance between individual palm trees. Smallholder farmers followed common management practices. Thereby, interrows (i.e., empty spaces on either side of an oil-palm row) served either as harvesting paths or were used to stack pruned palm fronds (Darras et al., 2019). Herbicides (e.g., glyphosate) were sprayed twice per year to clear understorey vegetation in the interrows. The palm circle, a circular area with a radius of ca. 2 m around an oil-palm stem (Munevar and Romero, 2015), was weeded regularly. Inorganic fertilizers (NPK, KCl and urea) were applied twice per year within the palm circle (Allen et al., 2016; Euler et al., 2016b).

4.2.2 Study design and plant sampling

We aimed to quantify Si concentrations in the different plant parts of an oil palm and to subsequently derive Si storage estimates for the average total aboveground biomass of one hectare of oil-palm plantation. For this purpose, we sampled leaflets, rachises, fruit-bunch stalks, fruit pulp, kernels, and frond bases of oil palms (Appendix III Table A1). Oil-palm sampling was coordinated with the regional harvesting schedule to ensure that all sampled oil-palm parts ($n = 3$ for each part) originated from the same palm tree. At each well-drained (HO1 – 4) and riparian site (HOr1 – 4), three morphologically similar oil palms with at least one ripe fruit bunch were selected for sampling (Appendix III Table B2).

The regular phyllotaxis of the oil palm allows to group palm fronds into (i) young fronds, (ii) mature fronds, and (iii) senescing fronds (Rees, 1964; Albakri et al., 2019) (Fig. 4.1a, c, d). Frond no. 1 is the youngest frond, frond no. 9 is the first mature frond, and the senescing frond (\sim leaf no. 40) is the oldest frond still attached to the oil-palm stem (Corley and Tinker, 2016). Grouping fronds according to age is important because we assume that they have different Si concentrations (Munevar and Romero, 2015). Frond no. 17 is commonly used as a reference frond to determine the nutrient status of a palm tree (Ollivier et al., 2017; Amiruddin et al., 2017). We collected leaflets from frond no. 9, frond no. 17 and from a senescing frond. We also sampled rachises and frond bases (attachment of petiole to the stem). In addition, we sampled a ripe fruit bunch of each selected palm tree. The latter was subdivided into fruit-bunch stalk, fruit pulp and kernel (Fig. 4.1a). We did not have the opportunity to sample oil-palm stems (Fig. 4.1b) and therefore used data of Pratiwi et al. (2018) in our Si storage calculations. They quantified SiO_2 concentrations of oil-palm stems in Malaysia, which we converted into Si concentrations. All Si concentrations are presented as wt. % of the dry biomass of each part. The grand means refer to three oil palms per plot which provided the basis for subsequent Si storage calculations.

In well-drained areas, we additionally assessed how Si accumulated with leaf age. For this purpose, we sampled leaflets from two additional mature palm fronds, i.e., frond no. 22 and frond no. 25 from two oil palms per plot. To exclude any bias in the calculations of Si accumulation in leaf tissue, the grand means of frond no. 9, no. 17, no. 22, no. 25, and the senescing frond were all calculated based on two oil palms per plot (Tab. 4.1). Contrary to Munevar and Romero (2015), we only included mature fronds (\geq leaf no. 9). In the field, oil-palm leaflets were wiped clean of dust and then cut into smaller pieces. Fruit were cut-off from the lower part of the fruit bunch. The oil-palm parts were then dried at 60 °C for 48 h. Prior to analysis, leaflets were finely ground (5 min). The rachises, frond bases, and fruit-bunch stalks were first cut into chunks and then chopped finely. Fruit pulp was separated from the kernel. The kernels were cooled with liquid nitrogen so that they could be crushed and ground despite their high oil content. They were then ground into a fine powder in a stainless-steel mortar.

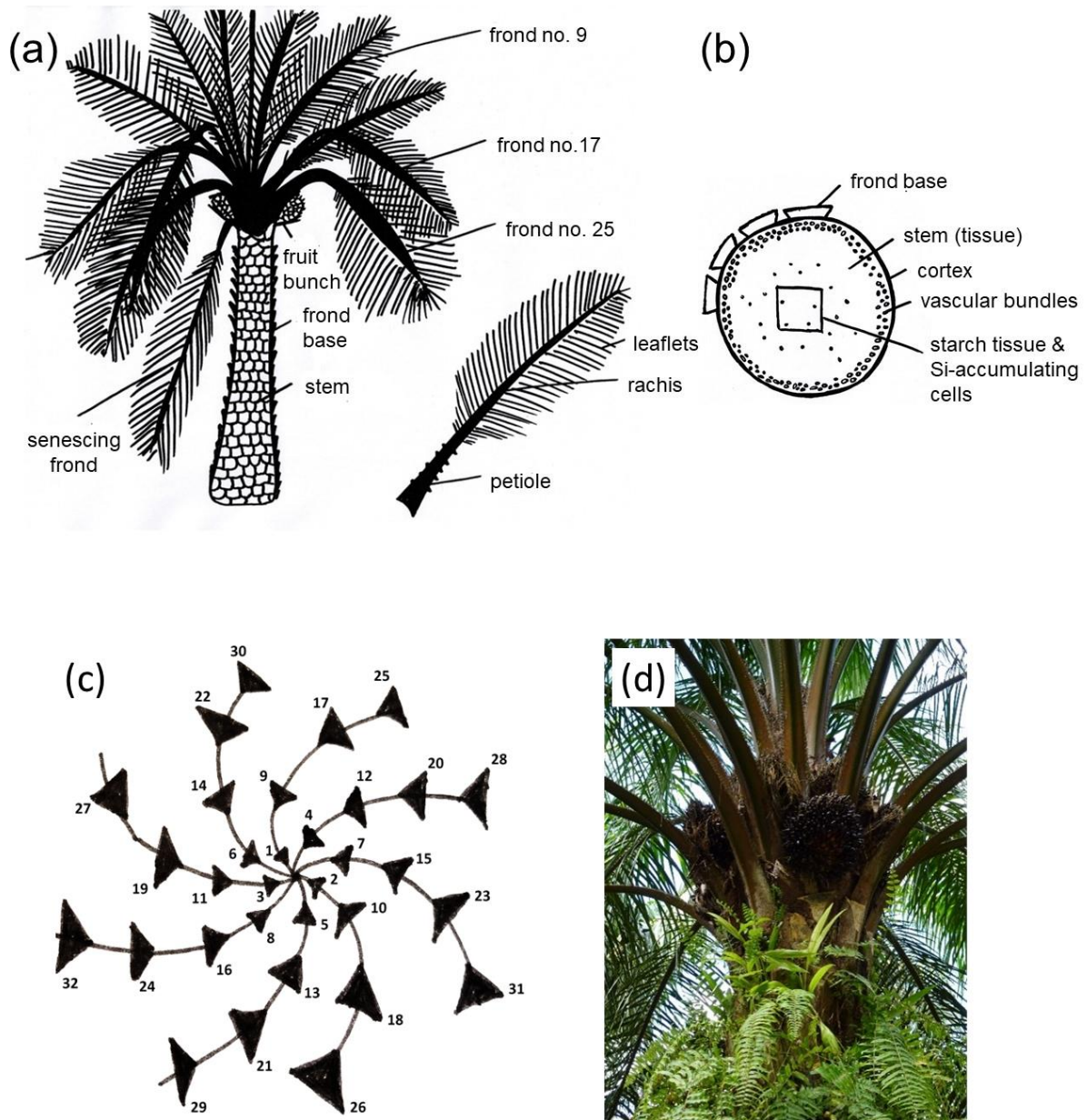


Fig. 4.1 (a) Morphology of the oil palm (*Elaeis guineensis* L.) and plant parts sampled for this study after Lewis et al. (2020). (b) Cross-section through an oil-palm stem, including Si-accumulating cells after Dungani et al. (2013). (c) Phyllotaxis of the oil palm after Albakri et al. (2019). Black triangles represent palm fronds. (d) Oil-palm crown with regular phyllotaxis (photo: B. Greenshields).

Table 4.1 Sampling scheme and numbers of replicates, providing the statistical basis of Figures 2 and 3

Oil-palm part	Water regime ^b	Palm trees (replicates per plot)	Plots (replicates per water regime)	Replicates of palm trees/plots used for Fig. 2	Replicates of palm trees/plots used for Fig. 3
Fronde no. 9	WD	3	4	3/4	2 (<i>excl. palm 3</i>)/4
Fronde no. 17	WD	3	4	3/4	2 (<i>excl. palm 3</i>)/4
Senescing frond	WD	3	4	3/4	2 (<i>excl. palm 3</i>)/4
Rachis	WD	3	4	3/4	***
Fronde base	WD	3	4	3/4	***
Fruit-bunch stalk	WD	3	4	3/4	***
Fruit pulp	WD	3	4	3/4	***
Kernel	WD	3	4	3/4	***
Fronde no. 22	WD	2 (<i>excl. palm 3</i>)	4	***	2 (<i>excl. palm 3</i>)/4
Fronde no. 25	WD	2 (<i>excl. palm 3</i>)	4	***	2 (<i>excl. palm 3</i>)/4
Fronde no. 9	RI	3	4	3/4	***
Fronde no. 17	RI	3	4	3/4	***
Senescing frond ^a	RI	3	3 (<i>excl. HOr2</i>)	3/3	***
Rachis	RI	3	4	3/4	***
Fronde base	RI	3	4	3/4	***
Fruit-bunch stalk	RI	3	4	3/4	***
Fruit pulp	RI	3	4	3/4	***
Kernel	RI	3	4	3/4	***

^a only 3 replicate plots as no senescing fronds were left hanging on palm trees at site HOr2 (differing management practice)

^b WD = well-drained, RI = riparian / ^c Italics = differing from general sampling scheme / *** = not relevant for statistics.

4.2.3 Extraction methods

4.2.3.1 Alkaline extraction for determining Si concentrations of oil-palm parts

Si was extracted from all sampled oil-palm parts by leaching with 1 % Na₂CO₃ after Meunier et al. (2014) and Saccone et al. (2007). As 1 % Na₂CO₃ may not completely dissolve amorphous silica (Saccone et al., 2007; Li and Delvaux, 2019), we conducted a pre-test to compare the efficiency of 1 M NaOH and 1 % Na₂CO₃ to extract Si from various types of plant parts included in this study. NaOH could generally extract Si more efficiently from those plant parts remaining in the system, whereas Na₂CO₃ could extract Si more efficiently from those parts leaving the system through harvest (except for the fruit-bunch stalk, which underestimated Si by 8 %). As the latter are more important for calculating the final Si budget of the system, we decided to use Na₂CO₃. Each plant sample was extracted and analysed in two laboratory replicates. We accepted ≤ 10 % relative error between the two laboratory replicates. In case this threshold was exceeded, a third replicate was done.

40 ml of 1 % Na₂CO₃ solution was added to approximately 50 mg of finely ground plant material in 50 ml centrifugation tubes. The tubes were placed into a shaking hot water bath at 85 °C (continuous shaking, 85 rpm) and were additionally shaken manually after 1 h. The tubes were left to react overnight for 16 hours. On the next day, the samples were cooled off in a cold-water basin for 10 min and were then centrifuged for 5 min at 3000 rpm. An aliquot of 125 µl was transferred into a plastic tube, neutralized with 1125 µl 0.021 M HCl and diluted to 2.5 ml with de-ionised water. Si was

analysed according to the molybdenum blue method (Grasshoff et al., 2009) with a UV-VIS spectrophotometer (Lambda 40, Perkin Elmer, Germany) at 810 nm.

4.2.3.2 HNO₃ digestion for determining calcium (Ca) concentrations of oil-palm parts

Ca concentrations of all sampled oil-palm parts were determined by HNO₃ digestion (Heinrichs and Hermann, 1990; Heinrichs et al., 1986). Prior to analysis, 50 ml teflon beakers were rinsed with de-ionised water (18.3 Ω) and dried (60 °C, 24 h). Approximately 50 – 150 mg of sample was weighed into each teflon beaker. Then 2 ml of concentrated HNO₃ solution was added to each sample. The teflon beakers were closed with a teflon lid and inserted into digestion blocks. These digestion blocks were placed into a drying oven and left to react at 170 °C for 10 hours. Afterwards, the digestion solution was transferred into 50 ml volumetric flasks through ash-free filters and filled up with de-ionised water to 50 ml. Ca concentrations were measured with an inductively coupled plasma atomic emission spectrometer (ICP-AES, iCap 7000, Thermo Fisher Scientific GmbH, Germany) at 317.887 nm.

4.2.4 Estimating Si storage in the aboveground biomass of oil palms and 1 hectare of plantation

For any given oil-palm part, Si storage can be calculated by multiplying the Si concentration by its dry weight biomass. As we quantified Si concentrations of oil-palm subparts, i.e., leaflets, rachises, frond bases, fruit-bunch stalks, fruit pulp and kernels (Section 2.2, Tab. 4.2a), but literature mostly provided dry weights of oil-palm main parts, i.e., the stem with palm-frond bases, palm fronds, palm crown and fruit bunches (Corley et al., 1971; Lewis et al., 2020), estimating Si storage in the aboveground biomass of oil-palms and one hectare oil-palm plantation required some additional calculations as follows: we first estimated the dry biomass of each oil-palm subpart by multiplying the dry biomass of each main part by its percentage contribution of the respective subpart (Tab. 4.2a). We then multiplied the dry biomass of each subpart by its mean Si concentration (Tab. 4.2b) to calculate Si storage of main oil-palm parts. Si storage in the total aboveground biomass of an oil palm was calculated by adding up the amounts of Si stored in an oil-palm stem, in a palm crown composed of 40 mature palm fronds and in 12 – 14 fruit bunches, which is considered an average annual production of a mature oil palm (Corley and Tinker, 2016) (Tab. 4.2c). Si storage in the aboveground oil-palm biomass of one hectare oil-palm plantation was calculated by multiplying the amount of Si stored in one mature oil palm by the average oil-palm-planting density. All calculations were done for well-drained and riparian sites individually. The dry weights of oil-palm main parts obtained from literature only included data from mature oil palms (≥ 6 years) and were further distinguished according to WRB reference soil group. Fruit-bunch biomass varied noticeably among oil palms, whereas the other main parts showed less variability in their dry biomass. Therefore, dry biomass ranges are presented only for fruit bunches.

In addition to the amount of Si stored in oil palms, we also calculated Si return to soils through pruned palm fronds and Si losses through fruit-bunch harvest (Tab. 4.2c). Our estimates of Si return to soils were based on 14 – 16 pruned palm fronds per palm each year, considering the average age of the investigated oil palms (Woittiez et al., 2017, personal communication, A. Tjoa). Our Si-loss estimates through fruit-bunch harvest were based on the harvests of two years in Jambi Province, i.e., the harvests of the years 2015 (well-drained) and 2018 (well-drained and riparian) (Kotowska et al., 2015, this study). We multiplied the average annual fruit-bunch harvest of these two years by the mean Si concentration of a fruit bunch to estimate annual Si losses through fruit-bunch harvest. Again, these calculations were done individually for well-drained and riparian sites.

Table 4.2a Dry biomass estimates of main parts of mature oil palms in SE Asia and relative contributions of oil-palm subparts to the biomass of main parts

Water regime ^a	Main oil-palm part	Average biomass contributions of oil-palm subparts to main part [wt. %]	Dry biomass of main part [kg]	Oil-palm age [yr]	Reference Soil Group (WRB) ^g	Country
WD	Oil-palm stem	Stem (57), frond bases (43)	321 ^d	12	Histosol ^h	Malaysia
WD	Oil-palm stem	Bare stem (100)	182 ^d	12	Histosol ^h	Malaysia
WD	Frond no. 9	Leaflet (25), rachis (75) ^b	5 ^e	6 - 14	Ferrasol	Malaysia
WD	Frond no. 17	Leaflet (25), rachis (75) ^b	5 ^e	6 - 14	Ferrasol	Malaysia
WD	Senescing frond	Leaflet (25), rachis (75) ^b	5 ^e	6 - 14	Ferrasol	Malaysia
WD	Palm crown	Leaflet (25), rachis (75) ^b	200	6 - 14	Ferrasol	Malaysia
WD	Fruit bunch	Stalk (33), pulp (33), kernel (33) ^c	5 - 20 ^f	18 - 22	Acrisol	Indonesia
RI	Fruit bunch	Stalk (33), pulp (33), kernel (33) ^c	6 - 19 ^f	11 - 21	Stagnosol	Indonesia

^aWD = well-drained, RI = riparian

^bthis study, personal communication M. Kotowska

^caverage share estimated

^dLewis et al. (2020) / ^eCorley et al. (1971) / ^fdata from this study

^gWRB = IUSS Working Group WRB (2022): World Reference Base for Soil Resources, fourth edition

^hstem biomass data of mature oil palms in SE Asia were only found for drained Histosols

4 Estimating oil-palm Si storage, Si return to soils and Si losses through harvest

Table 4.2b Calculation of average Si storage in main oil-palm parts of mature oil palms in SE Asia

Water regime ^a	Main oil-palm parts	Mean Si concentrations [wt. %] in the contained subparts ^c	Estimated average Si storage in main oil-palm parts [kg] ^d
WD	Oil-palm stem	Stem (1.13) ^b , frond bases (0.32)	2.51
WD	Oil-palm stem	Bare Stem (1.13) ^b	2.06
WD	Frond no. 9	Leaflet (1.06), rachis (0.29)	0.02
WD	Frond no. 17	Leaflet (1.74), rachis (0.29)	0.03
WD	Senescing frond	Leaflet (3.58), rachis (0.29)	0.06
WD	Palm crown	Leaflet (1.74), rachis (0.29)	1.31
WD	Fruit bunch	Stalk (0.44), pulp (0.37), kernel (0.26)	0.02 – 0.07
RI	Oil-palm stem	Stem (1.13) ^a , frond bases (0.31)	2.50
RI	Oil-palm stem	Bare stem (1.13) ^a	2.06
RI	Frond no. 9	Leaflet (1.08), rachis (0.29)	0.02
RI	Frond no. 17	Leaflet (1.34), rachis (0.29)	0.03
RI	Senescing frond	Leaflet (3.74), rachis (0.29)	0.06
RI	Palm crown	Leaflet (1.34), rachis (0.29)	1.11
RI	Fruit bunch	Stalk (0.48), pulp (0.43), kernel (0.28)	0.02 – 0.07

^aWD = well-drained, RI = riparian

^bPratiwi et al. (2018) determined the SiO₂ concentration in the oil-palm stem, which we converted to Si concentration (2.41 wt. % SiO₂ equaling 1.13 wt. % Si)

^cTotal Si concentrations including error terms and number of replicates are shown in Appendix III Table B1.

^dcalculated by multiplying the mean Si concentration of each oil-palm sub part by the biomass that the subpart contributes to the main oil-palm part; data for fruit bunches mark the range that results from the highly variable fruit-bunch biomass

Table 4.2c Si storage calculation in the aboveground oil-palm biomass in 1 hectare of oil-palm plantation

Water regime ^a	Main parts	Calculation assumptions	Si storage ^d [kg]
WD	One mature oil-palm tree	Stem, crown, 12 - 14 fruit bunches per year	4 - 5
WD	Mature oil-palm plantation (1 ha)	142 oil palms per hectare	572 - 682
WD	Annually pruned palm fronds (1 ha)	14 - 16 pruned fronds per palm, 142 oil palms per hectare ^b	111 - 126
WD	Fruit-bunch harvest in 2015 (1 ha)	15 - 20 Mg ha ⁻¹ fruit-bunch harvest ^c	54 - 72
WD	Fruit bunch harvest in 2018 (1 ha)	9 - 14 Mg ha ⁻¹ fruit-bunch harvest ^b	32 - 50
RI	One mature oil-palm tree	Stem, crown, 12 - 14 fruit bunches per year	4 - 5
RI	Mature oil-palm plantation (1 ha)	142 oil palms per hectare	551 - 660
RI	Annually pruned palm fronds (1 ha)	14 - 16 pruned fronds per palm, 142 oil palms per hectare ^b	115 - 131
RI	Fruit-bunch harvest in 2018 (1 ha)	9 - 11 Mg ha ⁻¹ fruit-bunch harvest ^b	32 - 40

^aWD = well-drained, RI = riparian

^bpersonal communication A. Tjoa

^cKotowska et al. (2015)

^ddata in the fourth column of the table mark the range of Si storage in the oil-palm parts listed in the second column, calculated based on the assumptions shown in the third column.

4.2.5 Statistics

Statistical analyses were conducted on the grand means of three palm trees ($n = 3$) in four replicate plots at well drained and at riparian sites ($n = 4$ each). No senescing frond could be sampled at the riparian site HOr2, as ageing fronds were pruned early to maintain a high crop yield (personal communication, smallholder farmers). Statistical analyses were done on log-transformed data. Normal distribution (Shapiro-Wilk test) and homogeneity of variances (Levene test) were tested for all groups. We conducted a one-way analysis of variances (ANOVA) to test if the Si concentration of each oil-palm part differed significantly between the two water regimes. We conducted a Tukey-Kramer post-hoc test to examine, which oil-palm parts differed significantly in their Si concentrations. Statistical significance was assigned at $p \leq 0.05$ in all analyses. We used the open-source software R version 3.6.2 and R CRAN packages ggplot2 (Wickham, 2016), car (Fox and Weisberg, 2019) and psych (Revelle, 2022) to perform statistical analyses.

For well-drained sites, we fitted a trendline to test if Si accumulated with frond age. The trendline was fitted to the grand means ($n = 4$ plantations, $n = 2$ oil palms per plantation) of four mature frond leaflets (no. 9, no. 17, no. 22, and no. 25). The senescing frond was plotted as frond no. 39 although the exact frond no. was not determined in the field.

4.3 Results

4.3.1 Si and Ca concentrations in oil-palm parts

At well-drained sites, leaflets of all analysed palm fronds had a mean Si concentration of at least 1 wt. % Si, whereas rachises, frond bases, fruit-bunch stalks, fruit pulp and kernels had mean Si concentrations below 0.5 wt. % Si (Fig. 4.2a). Mean Si concentrations in leaflets of frond no. 9 (1.06 ± 0.38 wt. % Si), leaflets of frond no. 17 (1.74 ± 0.47 wt. % Si) and leaflets of the senescing frond (3.58 ± 0.59 wt. % Si) were also significantly higher ($p \leq 0.05$) compared to those of the fruit-bunch stalk (0.44 ± 0.06 wt. % Si), frond base (0.32 ± 0.09 wt. % Si), rachis (0.29 ± 0.03 wt. % Si), fruit pulp (0.37 ± 0.07 wt. % Si), and kernel (0.26 ± 0.07 wt. % Si) (Fig. 4.2a, Appendix III Table B1). Mean Si concentrations in leaflets of the senescing palm frond were significantly higher ($p \leq 0.05$) than Si concentrations in leaflets of frond no. 17 and leaflets of frond no. 9, while mean Si concentrations did not differ significantly between the latter two. All oil-palm parts showed a Si/Ca weight ratio > 1 , except for the rachises, which had a Si/Ca weight ratio of 0.5 (Appendix III Table B1).

At riparian sites, mean Si concentrations followed a similar trend as at the well-drained sites (Fig. 4.2a, 4.2b). Again, leaflets of palm fronds had significantly higher Si concentrations ($p \leq 0.05$) in their tissue than other oil-palm parts (Fig. 4.2b). Mean Si concentrations increased with age from 1.08 ± 0.44 wt. % Si in leaflets of palm frond no. 9 to 3.74 ± 1.13 wt. % Si in leaflets of the senescing palm frond (Fig. 4.2, Appendix III Table B1). Si concentrations in leaflets of the senescing palm fronds

were significantly higher ($p \leq 0.05$) than those in leaflets of palm frond no. 9 and palm frond no. 17 (Fig. 4.2b). In contrast, mean Si concentrations in the rachises, frond bases, fruit bunch stalks, fruit pulp and kernels were in a similar range of around 0.3 to 0.5 wt. % Si (Fig. 4.2b). Rachises had the smallest Si/Ca ratio of 0.7, whereas leaflets of the senescing palm frond had the largest Si/Ca ratio of 4.3 (Appendix III Table B1). When comparing Si concentrations of the same oil-palm part (e.g., rachis) between well-drained and the riparian sites (HO and HOr), Si concentrations were similar. No significant differences were detected (Appendix III Table B1).

At well-drained sites, we additionally assessed how Si accumulated with leaf age in more detail. Mean Si concentrations in leaflets of four mature palm fronds increased linearly ($R^2 = 0.98$) with palm-frond age (Fig. 4.3).

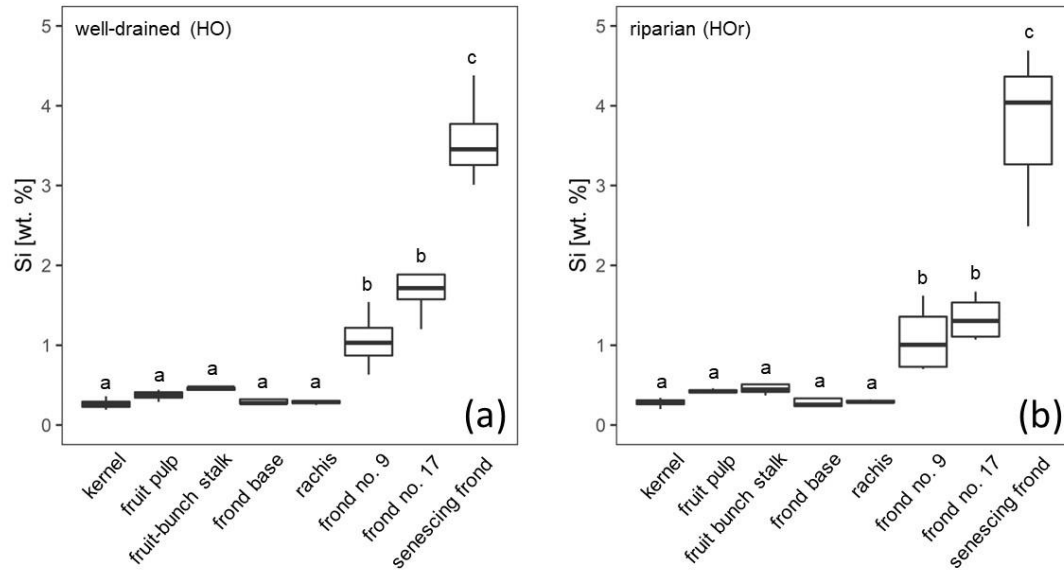


Fig. 4.2 (a) Si concentrations in oil-palm subparts at well-drained and (b) riparian sites. Lower case letters indicate significant differences ($p \leq 0.05$) between oil-palm subparts within the same water regime. $n = 4$ for each plant part, except for the senescing frond which is $n = 3$ at riparian sites.

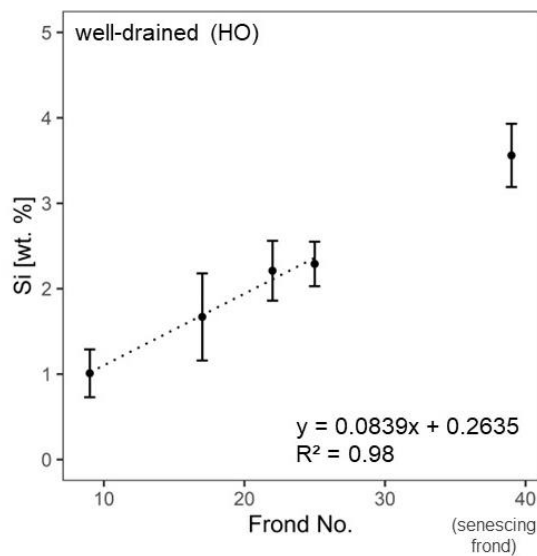


Fig. 4.3 Si concentrations in leaflets of five mature oil-palm fronds (no. 9, 17, 22, 25, senescing palm frond) from well-drained areas.

4.3.2 Si storage in the aboveground biomass of oil palms, Si return to soils through decomposing pruned palm fronds, and Si losses through harvest on smallholder oil-palm plantations

Calculating Si storage in the aboveground biomass of oil palms required biomass data for all plant parts. As it was not permitted to cut-down oil palms to determine the stem and frond-base biomass per palm tree, we used mean biomass estimates of mature oil palms in SE Asia from literature (Tab. 4.2a). Lewis et al. (2020) calculated the average biomass of a bare oil-palm stem (~ 182 kg) and a stem including palm-frond bases (~ 321 kg). This data suggests that palm-frond bases add another ~ 40 wt. % of biomass to an oil-palm stem. Corley et al. (1971) estimated a mature oil-palm frond to weigh ~ 5 kg. Based on these literature data and our own observations, we estimated a palm crown composed of 40 fronds to weigh roughly ~ 200 kg, which is in the same range as a bare oil-palm stem. In comparison, a single fruit bunch weighed between 5 kg and 20 kg (Appendix III Table B2).

Si storage in the analysed oil-palm parts was similar at well-drained and riparian sites (Tab. 4.2b). Among all analysed parts, the oil-palm stem contributed most to the estimated Si storage of one palm tree, amounting to 2.0 – 2.5 kg Si. Thereby, palm-frond bases that are attached to the palm stem up to an age of at least 12 years contributed about 20 wt. % Si (Corley and Tinker, 2016). Compared to the stem, an oil-palm crown composed of 40 palm fronds stored roughly half the amount of Si, about ~ 1.2 kg. The 12 – 14 fruit bunches produced by a palm tree each year stored 0.24 – 0.98 kg Si (0.02 – 0.07 kg Si per fruit bunch). In oil-palm fronds, Si storage increased with palm-frond age from 0.02 kg Si in frond no. 9 to 0.06 kg Si in a senescing frond.

According to our calculations, smallholder plantations at well-drained and riparian sites showed similar Si storage in the total aboveground biomass of oil palms, Si return through decomposing palm fronds, and Si losses through fruit-bunch harvest (Tab. 4.2c). The aboveground biomass of a mature oil palm was estimated to store about 4 – 5 kg Si. Consequently, oil palms in a one-hectare smallholder oil-palm plantation stored at least 550 kg Si in their aboveground biomass. Annual Si return to the topsoil via pruned palm fronds comprised at least 110 kg Si ha⁻¹. About 50 – 70 kg Si ha⁻¹ were lost by annual fruit-bunch harvest in 2015, about 30 – 50 kg Si ha⁻¹ in 2018.

4.4 Discussion

4.4.1 Si distribution and accumulation in various oil-palm parts

Leaflets of all investigated palm frond had mean Si concentrations of > 1 wt. % and a Si/Ca mass ratio > 1. Furthermore, the Si concentration increased with leaf age. Thus, our results reconfirmed the classification of oil palms being Si hyper-accumulators (Ma and Takahashi, 2002). At both well-drained and riparian sites, mean Si concentrations in leaflets of oil-palm fronds (> 1 %) were significantly higher compared to all other aboveground oil-palm parts (≤ 0.8 %) (Fig. 4.2). These observations correspond well to findings of Munevar and Romero (2015), and Carey and Fulweiler

(2016), who reported higher Si concentrations in leaf tissue compared to other plant parts in Si hyper-accumulators, as well.

In plants, Si remains dissolved in the transpiration stream (Carey and Fulweiler, 2012; Epstein, 1994) until it reaches epidermal cell walls, the cell lumen, and intercellular spaces in the leaves (Epstein, 1994). High Si concentrations in leaflets are the results of Si preferentially precipitating at final transpiration sites (Carey and Fulweiler, 2012). In contrast, significantly lower mean Si concentrations in palm-frond bases and rachises could imply that these plant parts are related to the transpiration stream rather than to transpiration and associated Si precipitation. Instead, transpiration and associated Si precipitation in leaflets seem to increase the mean Si concentration in the leaflets with palm-frond age and can be described well by a linear equation (Fig. 4.3). It is assumed that Si first accumulates in lower (abaxial) epidermal cells and with time in upper (adaxial) epidermal cells (Epstein, 1994).

Low mean Si concentrations in the various fruit-bunch parts (stalk, fruit pulp and kernel) suggest that Si is present in fibres, but barely in the hard shell and oily endosperm of the kernel (Omar et al., 2014). In the fruit-bunch stalk, Si is partly embedded within the surface or precipitates directly on the surface of fruit-bunch fibres, but not in cell walls (Omar et al., 2014). Despite low mean Si concentrations in various fruit-bunch parts, a considerable amount of Si is exported through harvest each year. In 2015, the annual fruit-bunch harvest amounted to about 15 – 20 Mg ha⁻¹ dry biomass on well-drained plantations within our study area (Kotowska et al., 2015). This corresponded to an export of 54 – 72 kg ha⁻¹ Si from the system (56 – 74 kg ha⁻¹ Si if 8 % underestimation by Na₂CO₃ extraction from fruit-bunch stalks is considered as reported in chapter 4.2.3.1). In 2018, the yield was lower in plantations of both well-drained and riparian areas, with 9 – 14 Mg ha⁻¹ dry biomass, corresponding to an Si export of 32 – 50 kg ha⁻¹ (33 – 52 kg ha⁻¹ if 8 % underestimation is considered). Thus, Si losses through fruit-bunch harvest were similar for both well-drained and riparian areas.

According to Corley and Tinker (2016), the central part of the oil palm includes some Si-containing tissue, as well (Fig. 4.1b). Si precipitation in the stem may take place along the vascular system or in cell walls. Epstein (1994) assumed that stabilizing the stem through silicifying cells can be a beneficial strategy of plants as it requires less energy than stabilizing the stem by cellulose.

Overall, our results suggest that among all oil-palm parts, palm leaflets accumulate Si most effectively in their tissue. Thus, the management of palm fronds plays a key role in driving and maintaining Si cycling on oil-palm plantations. However, our study also shows that Si precipitates in all aboveground oil-palm subparts. Therefore, specific Si concentrations of all oil-palm parts need to be analysed individually and upscaled to palm tree and plantation level. This allows to evaluate potential impacts of oil-palm cultivation and management practices on Si cycling.

4.4.2 Identified Si storage, cycling, and losses on smallholder oil-palm plantations, and favourable management practices

4.4.2.1 Comparison of plantations in well-drained and riparian areas

At well-drained and riparian sites, smallholder oil-palm plantations showed similar Si storage in the total aboveground biomass of oil palms, Si return to soils through decomposing oil-palm fronds, and Si losses through fruit-bunch harvest (Tab. 4.2c). We assume that this was due to similar Si concentrations in the respective oil-palm parts in both water regimes and because the same biomass data was used to calculate Si storage capacities for all sites (Tab. 4.2a). The number of studies providing oil-palm biomass data is still scarce to have been able to distinguish between riparian and well-drained soils. Therefore, our hypotheses were only partially verified: oil palms store noticeable amounts of Si in their biomass. However, an additional influx of dissolved silicic acid through flooding, capillary rise of groundwater and lateral water fluxes (interflow) from higher-lying areas did not increase Si storage in oil-palm plantations of riparian areas.

4.4.2.2 Favourable management practices using palm fronds and fruit-bunch parts

In our study area, one hectare of smallholder oil-palm plantation stored about 551 – 682 kg Si in the total aboveground biomass. Pruned palm fronds returned ~ 111 – 131 kg Si each year to the topsoils (Fig. 4.4). Annual Si losses through fruit-bunch harvest amounted to 32 – 72 kg ha⁻¹ yr⁻¹ (33 – 74 kg ha⁻¹ yr⁻¹ if 8 % underestimation by Na₂CO₃ is considered) which corresponds to around 6 – 10 % of the amount of Si stored in the total aboveground biomass. Although much Si is recycled in the system by the practice of frond-pile stacking, it could still be optimized, e.g., by changing the positions of frond piles every 5 – 10 years. Such practices would lead to a more evenly distributed Si return to topsoils across plantations.

The relevance of Si losses by harvest has been previously addressed by Puppe et al. (2021), Guntzer et al. (2012) and Vandevenne et al. (2012). In our study, Si storage in fruit bunches was localized mainly in the fruit-bunch stalk and fruit pulp (section 4.4.1). Like oil palms, many Si hyper-accumulators store less Si in their grains than in the harvest residues (Carey and Fulweiler, 2016; Hughes et al., 2020; Vandevenne et al., 2012): in wheat (*Triticum aestivum*), oat (*Avena sativa*), and barley (*Hordeum vulgare*) straw, the mean Si concentration was higher than in the respective cereal grain (Vandevenne et al. (2012). Hughes et al. (2020) found rice grains (*Oryza sativa*) under different rice-residue management practices to accumulate 59 ± 43 kg Si ha⁻¹ yr⁻¹, but rice straw to accumulate 82 ± 25 kg Si ha⁻¹ yr⁻¹. Carey and Fulweiler (2016) as well as Guntzer et al. (2012) made similar observations and concluded that non-edible plant parts (e.g., straw) could serve well as an organic fertilizer. These observations highlight the importance of managing harvest residues.

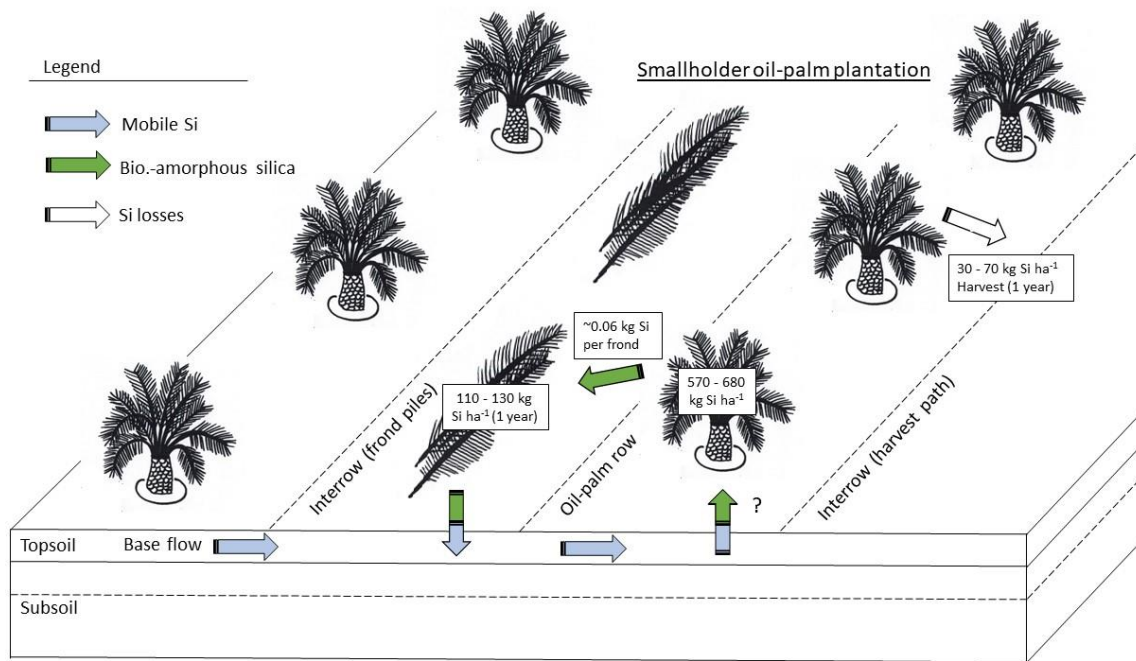


Fig. 4.4 Si storage in the aboveground biomass of oil palms, Si return to soils through decomposing pruned palm fronds, and Si losses through harvest on smallholder oil-palm plantations in Jambi Province, Sumatra.

Indeed, fruit-bunch harvest may alter Si cycling with time, although a significant impact may only be seen on a longer term than covered by this study (Clymans et al., 2011; Guntzer et al., 2012). Therefore, we recommend reducing Si losses through harvest by returning the empty fruit bunches (the residues not used to produce palm oil) to the palm circle on smallholder plantations. In this way, empty fruit bunches may serve as organic fertilizer and may increase amounts of bioavailable Si in the rooting area of the oil palm. This is already common practice on state-owned oil-palm plantations. However, it remains low priority for smallholder farmers because of the logistical effort and costs involved in the transport of empty fruit bunches back to oil-palm plantations (Woittiez et al., 2018; Euler et al., 2016a).

4.4.2.3 Favourable management practices using stem residues

Si concentrations in the stem (Tab. 4.2b) may seem low. Yet, multiplying the Si concentration by the large stem biomass (Aholoukpè et al., 2018) showed that the stem provides the largest Si pool of the oil palm's aboveground biomass. In contrast, palm leaflets showed the highest Si concentrations (Tab. 4.2b) but contributed only 25 wt. % to the biomass of a palm frond. This led to smaller total Si storage in the crown compared to the stem of a palm tree. Both oil-palm parts are highly relevant for Si cycling in the system. We strongly recommend keeping both the stem and the palm-frond residues on the plantation, especially when an oil-palm plantation is cleared for replanting. Oil palms could benefit from Si fertilization like other Si hyper-accumulators (Klotzbücher et al., 2018; Datnoff et al., 1997; Li and Delvaux, 2019).

Oil-palm plantations are usually cultivated for about 25 years (Corley and Tinker, 2016). Thereafter, the oil-palm stem is considered a waste product (Onoja et al., 2019; Awalludin et al., 2015). It used to be common practice to burn the stem as the ash was regarded to sustain soil fertility (Selamat et al., 2019) by releasing Si and other nutrients into topsoil (Selamat et al., 2019; von der Lühé et al., 2020). Yet, these nutrients including Si, are released from the ash in such high amounts and so rapidly that they are highly susceptible to leaching. Many nutrients could be lost from the system before a new generation of oil palms can take them up. Thus, despite the short-term fertilizing effect of the ash, this process may enhance nutrient and Si depletion for the long term (von der Lühé et al., 2020). Nowadays, replanting follows a zero-burning policy (Corley and Tinker, 2016) to reduce greenhouse gas emissions and air pollution. Furthermore, this policy shall prevent fires from getting out of control which could impact natural vegetation. Without burning, most stem biomass remains on the plantations as it has no monetary value for industrial or agricultural applications (Awalludin et al., 2015; Onoja et al., 2019). Currently, oil-palm stems are chipped and then distributed as an organic fertilizer at the end of a 25-year plantation cycle (Corley and Tinker, 2016). It has been suggested to provide governmental support to implement this practice on smallholder plantations, as well (Woittiez et al., 2018). However, this practice has not yet been widely used as many oil-palm plantations in Jambi Province (including those in our study area) are only on the verge of being replanted in the next decade.

In view of the large area (~ 16 million ha) under oil-palm cultivation in Indonesia (Gaveau et al., 2022), governments are interested in finding economically more lucrative applications for oil-palm residues (Awalludin et al., 2015; Chang, 2014; Rubinsin et al., 2020; Santi et al., 2019), including stems (Awalludin et al., 2015) that could boost the economy and benefit smallholder farmers. As a result, most research focusses on economically beneficial applications, e.g., in the renewable energy sector such as for fuel and gas production, but also for production of composites and fertilizers (Onoja et al., 2019). A clear advantage of the current practice, i.e., spreading chipped stem parts across the plantation as an organic fertilizer, is that it supports the system's internal nutrient and Si cycling. This reduces the need to buy industrial fertilizers and avoids any costs and carbon dioxide emissions related to the transport of the stems. Selling the biomass waste for industrial purposes, the production of building materials (e.g., gypsum composites and wood fibre alternatives) (Selamat et al., 2019; Pratiwi et al., 2018; Dungani et al., 2013) or for paper production (Pratiwi et al., 2018) would mean that farmers would have to compensate for the nutrient export from their plantations by buying more industrial fertilizers. In addition, both the transport of the palm stems from the plantations and the transport of fertilizers to the plantations would involve costs and carbon dioxide emissions.

4.5 Conclusion

In this study, we assessed the amounts of Si involved in internal Si cycling in the oil-palm system as well as the amounts of Si leaving the system through fruit-bunch harvest. Our study reconfirmed

previous assumptions in that oil palms can be considered Si hyper-accumulators (mean Si concentration > 1 wt. % in leaflets, Si/Ca mass ratio > 1). Mean Si concentrations increased with leaf age. A senescing frond stored three-times the amount of Si in its leaf tissue compared to a mature palm frond. Total Si storage in the biomass of mature oil palms amounted to 551 – 682 kg ha⁻¹. Oil-palm stems stored the greatest amounts of Si per hectare due to their large biomass. Therefore, keeping oil-palm stems (including frond bases) in the system could be an effective measure of maintaining balanced Si levels on the long-term, i.e., over several oil-palm generations. On the short-term, i.e., within one oil-palm generation, pruning and stacking palm fronds in frond piles turned out to be an effective management practice. This practice returned 111 – 131 kg Si per hectare and year to soils. Nevertheless, we found that fruit-bunch harvest involved a considerable annual Si export of 32 – 72 kg ha⁻¹ from the system. Consequently, fertilization may be needed after several oil-palm generations. We recommend the following management measures that enhance Si cycling in the system: (1) ensuring a spatially more even Si return from decomposing palm fronds to soils, e.g., by changing the position of frond-piles every 5 – 10 years (2) returning empty fruit bunches to the palm circle to serve as organic fertilizer; and (3) leaving all oil-palm residues on the plantation after a plantation cycle of 25 years, especially oil-palm stems (chopped and evenly distributed across the plantation) although the use of these residues for industrial purposes may be financially attractive to plantation owners.

4.6 Acknowledgements

We thank the German Research Foundation (DFG, Deutsche Forschungsgemeinschaft) for funding this project (DFG project no. 391702217). The project was associated to the Collaborative Research Center (CRC) 990 “Ecological and Socioeconomic Functions of Tropical Lowland Rainforest Transformation Systems” (CRC 990, DFG project no. 192626868). We also thank the Ministry of Education, Technology and Higher Education (RISTEKDIKTI) for granting a research permission in Indonesia and the CRC 990 oil-palm smallholder partners. Plant sampling was conducted using the research permit 187/ E5/E5.4/SIP/2019. Special thanks go to our Indonesian counterparts, the CRC-990 office members, our fieldwork assistants Nando and Toni in Jambi and our student assistant Kerstin in Göttingen. We would also like to thank the laboratory staff from the Institute of Geography, University of Göttingen, Jürgen Grotheer, Anja Södje and Petra Voigt for their support.

4.7 Author contribution

BvL and DS designed the study of the manuscript with input from HH and AT. BG conducted plant sampling with input from BvL and FB. MK and FB provided botanical and harvest data. FS conducted laboratory analyses with input from BvL and BG. FS and BG evaluated the data with input from BvL, HH, MK, FB, and DS. BG wrote the first draft. All authors (BG, BvL, FS, HH, AT, MK, FB, and DS) contributed to generating and reviewing the subsequent versions of the paper.

4.8 References

- Aholoukpè HNS, Dubos B, Deleporte P, et al (2018) Allometric equations for estimating oil palm stem biomass in the ecological context of Benin, West Africa. *Trees* 32:1669–1680. <https://doi.org/10.1007/s00468-018-1742-8>
- Albakri ZM, Saufi M, Kassim M, et al (2019) SCIENCE & TECHNOLOGY Analysis of Oil Palm Leaf Phyllotaxis towards Development of Models to Determine the Fresh Fruit Bunch (FFB) Maturity Stages, Yield and Site-Specific Harvesting. *Pertanika J Sci & Technol* 27:659–672
- Alexandre A, Meunier J-D, Colin F, Koud J-M (1997) Plant impact on the biogeochemical cycle of silicon and related weathering processes. *Geochim Cosmochim Acta* 61:677–682. [https://doi.org/10.1016/S0016-7037\(97\)00001-X](https://doi.org/10.1016/S0016-7037(97)00001-X)
- Allen K, Corre MD, Kurniawan S, et al (2016) Spatial variability surpasses land-use change effects on soil biochemical properties of converted lowland landscapes in Sumatra, Indonesia. *Geoderma* 284:42–50. <https://doi.org/10.1016/j.geoderma.2016.08.010>
- Amirruddin AD, Muharam FM, Mazlan N (2017) Assessing leaf scale measurement for nitrogen content of oil palm: Performance of discriminant analysis and support vector machine classifiers. *Int J Remote Sens* 38:7260–7280. <https://doi.org/10.1080/01431161.2017.1372862>
- Awalludin MF, Sulaiman O, Hashim R, Nadhari WNAW (2015) An overview of the oil palm industry in Malaysia and its waste utilization through thermochemical conversion, specifically via liquefaction. *Renew Sustain Energy Rev* 50:1469–1484. <https://doi.org/10.1016/j.rser.2015.05.085>
- Carey J (2020) Soil age alters the global silicon cycle. *Science* (1979) 369:1161–1162. <https://doi.org/10.1126/science.abd9425>
- Carey JC, Fulweiler RW (2016) Human appropriation of biogenic silicon – the increasing role of agriculture. *Funct Ecol* 30:1331–1339. <https://doi.org/10.1111/1365-2435.12544>
- Carey JC, Fulweiler RW (2012) The Terrestrial Silica Pump. *PLoS One* 7:4. <https://doi.org/10.1371/journal.pone.0052932>
- Chang SH (2014) An overview of empty fruit bunch from oil palm as feedstock for bio-oil production. *Biomass and Bioenergy* 62:174–181. <https://doi.org/10.1016/j.biombioe.2014.01.002>
- Clough Y, Krishna V V., Corre MD, et al (2016) Land-use choices follow profitability at the expense of ecological functions in Indonesian smallholder landscapes. *Nat Commun* 7:1–12. <https://doi.org/10.1038/ncomms13137>
- Clymans W, Struyf E, Govers G, et al (2011) Anthropogenic impact on amorphous silica pools in temperate soils. *Biogeosciences* 8:2281–2293. <https://doi.org/10.5194/bg-8-2281-2011>
- Clymans W, Struyf E, Van den Putte A, et al (2015) Amorphous silica mobilization by inter-rill erosion: Insights from rainfall experiments. *Earth Surf Process Landf* 40:1171–1181. <https://doi.org/10.1002/esp.3707>
- Conley DJ, Likens GE, Buso DC, et al (2008) Deforestation causes increased dissolved silicate losses in the Hubbard Brook Experimental Forest. *Glob Chang Biol* 14:2548–2554. <https://doi.org/10.1111/j.1365-2486.2008.01667.x>

- Corley RHV, Hardon JJ, Tan GY (1971) Analysis of growth of the oil palm (*Elaeis guineensis* Jacq.) I. Estimation of growth parameters and application in breeding. *Euphytica* 20:307–315. <https://doi.org/10.1007/BF00056093>
- Corley RHV, Tinker PBH (2016) *The Oil Palm* (World Agricultural Series) fifth edition, 647 pp., <https://doi.org/10.1017/cbo9781316530122.010,2016>
- Darras KFA, Corre MD, Formaglio G, et al (2019) Reducing Fertilizer and Avoiding Herbicides in Oil Palm Plantations—Ecological and Economic Valuations. *Front For Glob Chang* 2:1–15. <https://doi.org/10.3389/ffgc.2019.00065>
- Datnoff LE, Deren CW, Snyder GH (1997) Silicon fertilization for disease management of rice in Florida. *Crop Protection* 16:525–531. [https://doi.org/10.1016/S0261-2194\(97\)00033-1](https://doi.org/10.1016/S0261-2194(97)00033-1)
- De Coster GL (2006) *The Geology of the central and south sumatra basins*, 1974. pp 77-110
- Dislich C, Keyel AC, Salecker J, et al (2017) A review of the ecosystem functions in oil palm plantations, using forests as a reference system. *Biol Rev* 92:1539–1569. <https://doi.org/10.1111/brv.12295>
- Drescher J, Rembold K, Allen K, et al (2016) Ecological and socio-economic functions across tropical land use systems after rainforest conversion. *Philos Trans R Soc B Biol Sci* 371:20150275. <https://doi.org/10.1098/rstb.2015.0275>
- Dungani R, Jawaid M, Khalil HPSA, et al (2013) A review on quality enhancement of oil palm trunk waste by resin impregnation: Future materials. *Bioresources* 8:3136–3156. <https://doi.org/10.15376/biores.8.2.3136-3156>
- Epstein E (2009) Silicon: its manifold roles in plants. *Annals of Applied Biology* 155:155–160. <https://doi.org/10.1111/j.1744-7348.2009.00343.x>
- Epstein E (1994) The anomaly of silicon in plant biology. *Proc Natl Acad Sci* 91:11–17. <https://doi.org/10.1073/pnas.91.1.11>
- Euler M, Hoffmann MP, Fathoni Z, Schwarze S (2016a) Exploring yield gaps in smallholder oil palm production systems in eastern Sumatra, Indonesia. *Agricultural Sciences* 146:111–119. <https://doi.org/10.1016/j.agry.2016.04.007>
- Euler M, Schwarze S, Siregar H, Qaim M (2016b) Oil Palm Expansion among Smallholder Farmers in Sumatra, Indonesia. *J Agric Econ* 67:658–676. <https://doi.org/10.1111/1477-9552.12163>
- Fox J, Weisberg S (2019) *An {R} Companion to Applied Regression*. <https://socialsciences.mcmaster.ca/jfox/Books/Companion/> [Accessed February 10, 2023]
- Gaveau DLA, Locatelli B, Salim MA, et al (2022) Slowing deforestation in Indonesia follows declining oil palm expansion and lower oil prices. *PLoS One* 17:e0266178. <https://doi.org/10.1371/journal.pone.0266178>
- Grass I, Kubitzka C, Krishna V V., et al (2020) Trade-offs between multifunctionality and profit in tropical smallholder landscapes. *Nat Commun* 11:1–13. <https://doi.org/10.1038/s41467-020-15013-5>
- Grasshoff K, Kremling K, Ehrhardt M (2009) *Methods of sea water analysis*, third. John Wiley &

Sons

- Greenshields B, von der Lühe B, Hughes HJ, et al (2023) Oil-palm management alters the spatial distribution of amorphous silica and mobile silicon in topsoils. *SOIL* 9:169–188. <https://doi.org/10.5194/soil-9-169-2023>
- Guntzer F, Keller C, Meunier JD (2012) Benefits of plant silicon for crops: A review. *Agron Sustain Dev* 32:201–213. <https://doi.org/10.1007/s13593-011-0039-8>
- Haynes RJ (2014) A contemporary overview of silicon availability in agricultural soils. *J Plant Nutr Soil Sci* 177:831–844. <https://doi.org/10.1002/jpln.201400202>
- Haynes RJ (2017) The nature of biogenic Si and its potential role in Si supply in agricultural soils. *Agric Ecosyst Environ* 245:100–111. <https://doi.org/10.1016/j.agee.2017.04.021>
- Heinrichs H, Brumsack HJ, Loftfield N, König N (1986) Verbessertes Druckaufschlußsystem für biologische und anorganische Materialien. *Zeitschrift für Pflanzenernährung und Bodenkunde* 149:350–353
- Heinrichs H, Hermann AG (1990) *Praktikum der Analytischen Geochemie*. In: Lehrbuch. Springer-Verlag, Berlin, p 669
- Hennings N, Becker JN, Guillaume T, et al (2021) Riparian wetland properties counter the effect of land-use change on soil carbon stocks after rainforest conversion to plantations. *Catena* 196:104941. <https://doi.org/10.1016/j.catena.2020.104941>
- Hughes HJ, Hung DT, Sauer D (2020) Silicon recycling through rice residue management does not prevent silicon depletion in paddy rice cultivation. *Nutr Cycl Agroecosyst* 118:75–89. <https://doi.org/10.1007/s10705-020-10084-8>
- IUSS Working Group WRB (2022) *World Reference Base or Soil Resources 2014, update 2015 International soil classification system for naming soils and creating legends for soil maps*. FAO, Rome
- Klotzbücher T, Klotzbücher A, Kaiser K, et al (2018) Impact of agricultural practices on plant-available silicon. *Geoderma* 331:15–17. <https://doi.org/10.1016/j.geoderma.2018.06.011>
- Kotowska MM, Leuschner C, Triadiati T, et al (2015) Quantifying above- and belowground biomass carbon loss with forest conversion in tropical lowlands of Sumatra (Indonesia). *Glob Chang Biol* 21:3620–3634. <https://doi.org/10.1111/gcb.12979>
- Laumonier Y (1997) *The Vegetation and Physiography of Sumatra*. In: Geobotany. Kluwer Academic Publishers, p 223. <https://doi.org/10.1007/978-94-009-0031-8>
- Lewis K, Rumpang E, Kho LK, et al (2020) An assessment of oil palm plantation aboveground biomass stocks on tropical peat using destructive and non-destructive methods. *Sci Rep* 10:1–12. <https://doi.org/10.1038/s41598-020-58982-9>
- Li Z, de Tombeur F, Vander Linden C, et al (2020) Soil microaggregates store phytoliths in a sandy loam. *Geoderma* 360:114037. <https://doi.org/10.1016/j.geoderma.2019.114037>
- Li Z, Delvaux B (2019) Phytolith-rich biochar: A potential Si fertilizer in desilicated soils. *GCB Bioenergy* 11:1264–1282. <https://doi.org/10.1111/gcbb.12635>

- Liang Y, Nikolic M, Bélanger R, et al (2015) *Silicon in Agriculture*. Dordrecht: Springer
- Lucas Y, Luizão FJ, Chauvel A, et al (1993) The relation between biological activity of the rain forest and mineral composition of soils. *Science* 260:521–523
- Luke SH, Purnomo D, Advento AD, et al (2019) Effects of understory vegetation management on plant communities in oil palm plantations in Sumatra, Indonesia. *Front For Glob Chang* 2:1–13. <https://doi.org/10.3389/ffgc.2019.00033>
- Ma JF, Takahashi E (2002) Silicon-accumulating plants in the plant kingdom. In: *Soil, fertilizer, and plant silicon research in Japan*. Elsevier Science, Amsterdam, pp 63–71
- Meijaard E, Brooks T, Carlson KM, et al (2020) The environmental impacts of palm oil in context. *Nat Plants* 6:1418–1426. <https://doi.org/10.1038/s41477-020-00813-w>
- Munevar F, Romero A (2015) Soil and plant silicon status in oil palm crops in Colombia. *Exp Agric* 51:382. <https://doi.org/10.1017/S0014479714000374>
- Ollivier J, Flori A, Cochard B, et al (2017) Genetic variation in nutrient uptake and nutrient use efficiency of oil palm. *J Plant Nutr* 40:558–573. <https://doi.org/10.1080/01904167.2016.1262415>
- Omar FN, Mohammed MAP, Baharuddin AS (2014) Effect of silica bodies on the mechanical behaviour of oil palm empty fruit bunch fibres. *Bioresources* 9:7041–7058. <https://doi.org/10.15376/biores.9.4.7041-7058>
- Onoja E, Chandren S, Abdul Razak FI, et al (2019) Oil Palm (*Elaeis guineensis*) Biomass in Malaysia: The Present and Future Prospects. *Waste and Biomass Valorization* 10:2099–2117. <https://doi.org/10.1007/s12649-018-0258-1>
- Pratiwi W, Sugiharto A, Sugesty S (2018) The effect of pulping process variable and elemental chlorine free bleaching on the quality of oil palm trunk pulp. *J Selulosa* 8:85. <https://doi.org/10.25269/jsel.v8i02.218>
- Puppe D, Kaczorek D, Schaller J, et al (2021) Crop straw recycling prevents anthropogenic desilication of agricultural soil–plant systems in the temperate zone – Results from a long-term field experiment in NE Germany. *Geoderma* 403:1–13. <https://doi.org/10.1016/j.geoderma.2021.115187>
- Qaim M, Sibhatu KT, Siregar H, Grass I (2020) Environmental, Economic, and Social Consequences of the Oil Palm Boom. *Annu Rev Resour Economics* 12:1–24. <https://doi.org/10.1146/annurev-resource-110119-024922>
- Rees AR (1964) The apical organization and phyllotaxis of the oil palm. *Ann Bot* 28:57–69. <https://doi.org/10.1093/oxfordjournals.aob.a083895>
- Revelle W (2022) *psych: Procedures for Personality and Psychological Research*, <https://CRAN.R-project.org/package=psych> Version = 2.2.9. [Accessed February 10, 2023]
- Rubinsin N, Daud WRW, Kamarudin SK, et al (2020) Optimization of oil palm empty fruit bunches value chain in peninsular malaysia. *Food and Bioproducts Processing* 119:179–194. <https://doi.org/10.1016/j.fbp.2019.11.006>
- Saccone L, Conley DJ, Koning E, et al (2007) Assessing the extraction and quantification of

- amorphous silica in soils of forest and grassland ecosystems. *Eur J Soil Sci* 58:1446–1459. <https://doi.org/10.1111/j.1365-2389.2007.00949.x>
- Santi LP, Kalbuadi DN, Goenadi DH (2019) Empty fruit bunches as potential source for biosilica fertilizer for oil palm. *J Trop Biodivers Biotechnol* 4:90–96. <https://doi.org/10.22146/jtbb.38749>
- Schaller J, Turner BL, Weissflog A, et al (2018) Silicon in tropical forests: large variation across soils and leaves suggests ecological significance. *Biogeochemistry* 140:161–174. <https://doi.org/10.1007/s10533-018-0483-5>
- Selamat ME, Hashim R, Sulaiman O, et al (2019) Comparative study of oil palm trunk and rice husk as fillers in gypsum composite for building material. *Constr Build Mater* 197:526–532. <https://doi.org/10.1016/j.conbuildmat.2018.11.003>
- Struyf E, Smis A, Van Damme S, et al (2010) Historical land use change has lowered terrestrial silica mobilization. *Nat Commun* 1:1–7. <https://doi.org/10.1038/ncomms1128>
- Tarigan S, Stiegler C, Wiegand K, et al (2020) Relative contribution of evapotranspiration and soil compaction to the fluctuation of catchment discharge: case study from a plantation landscape. *Hydrological Sciences Journal* 65:1239–1248. <https://doi.org/10.1080/02626667.2020.1739287>
- Tsujino R, Yumoto T, Kitamura S, et al (2016) History of forest loss and degradation in Indonesia. *Land use policy* 57:335–347. <https://doi.org/10.1016/j.landusepol.2016.05.034>
- Vander Linden C, Delvaux B (2019) The weathering stage of tropical soils affects the soil-plant cycle of silicon, but depending on land use. *Geoderma* 351:209–220. <https://doi.org/10.1016/j.geoderma.2019.05.033>
- Vandevenne F, Struyf E, Clymans W, Meire P (2012) Agricultural silica harvest: have humans created a new loop in the global silica cycle? *Front Ecol Environ* 10:243–248. <https://doi.org/10.1890/110046>
- von der Lühe B, Bezler K, Hughes HJ, et al (2022) Oil-palm and Rainforest Phytoliths Dissolve at Different Rates - with Implications for Silicon Cycling After Transformation of Rainforest Into Oil-palm Plantation. *Silicon*. <https://doi.org/10.1007/s12633-022-02066-y>
- von der Lühe B, Pauli L, Greenshields B, et al (2020) Transformation of Lowland Rainforest into Oil-palm Plantations and use of Fire alter Topsoil and Litter Silicon Pools and Fluxes. *Silicon* 13:4345–4353. <https://doi.org/10.1007/s12633-020-00680-2>
- Wickham H (2016) *ggplot2: Elegant Graphics for Data Analysis*
- Woittiez LS, Slingerland M, Rafik R, Giller KE (2018) Nutritional imbalance in smallholder oil palm plantations in Indonesia. *Nutr Cycl Agroecosyst* 111:73–86. <https://doi.org/10.1007/s10705-018-9919-5>
- Woittiez LS, Slingerland M, Rafik R, Giller KE (2018) Nutritional imbalance in smallholder oil palm plantations in Indonesia. *Nutr Cycl Agroecosystems* 111:73–86. <https://doi.org/10.1007/s10705-018-9919-5>
- Zellner W, Tubaña B, Rodrigues FA, Datnoff LE (2021) Silicon's Role in Plant Stress Reduction and Why This Element Is Not Used Routinely for Managing Plant Health. *Plant Dis* 105:2033–2049. <https://doi.org/10.1094/PDIS-08-20-1797-FE>

5 General discussion

5.1 Synthesis and key findings

This thesis provides a first understanding of Si cycling in the soil-plant system under smallholder oil-palm plantations in Sumatra, Indonesia. In soils, Si fractions were quantified and distinguished to a detail unavailable thus far (c.f. **Chapter 2**). Within smallholder oil-palm plantations, environmental processes (plant-soil-Si cycling) and anthropogenic impacts (plantation management, Si losses) were investigated to assess if or in which way current oil-palm cultivation has altered Si cycling (c.f. **Chapter 3**). In oil palms, the total Si content was quantified for oil-palm parts other than oil-palm leaflets (c.f. **Chapter 4**). This made it possible to calculate Si storage estimates for oil palms and oil-palm plantations and, furthermore, to present a Si balance at the soil-plant interface. As illustrated in Fig. 5.1 combining the key findings of these studies provides a broader picture of Si cycling, including potential Si recycling and Si losses in this land-use system. Our data enabled us to propose a Si balance for smallholder oil-palm plantations established in well-drained areas as the calculations involved aboveground biomass (AGB) data predominantly originating from well-drained soils, as well.

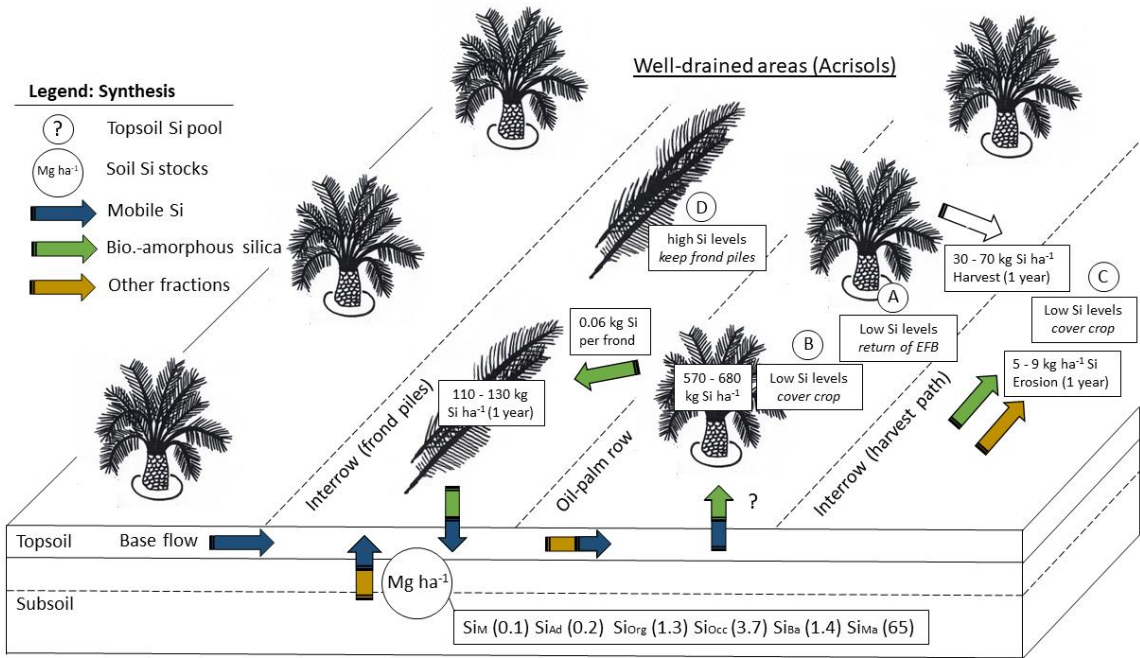


Fig. 5.1 Key findings of all three studies for smallholder oil-palm plantations located in well-drained areas. Sketch, B. Greenshields

5.1.1 Si fluxes and Si uptake mechanisms in differing water regimes

One of the principal objectives was to compare Si cycling in oil-palm plantations in two different water regimes – well-drained versus riparian areas. We distinguished water regimes because either corresponded to a prevalent soil type (Acrisol/Stagnosols) and topographic position (slope/floodplain) and could therefore affect Si fluxes and soil Si pools. We hypothesized that soils in riparian areas were less prone to natural desilication due to an additional influx of dissolved Si (Si_M pool) by stream water from higher landscape positions, or through regular flooding. Thus, we expected riparian areas to have larger soil Si stocks than well-drained areas. Likewise, we presumed oil palms planted in riparian areas to accumulate more Si in their aboveground biomass than those planted in well-drained areas.

When comparing these areas, our data could not provide statistical evidence that Si cycling differed significantly between these water regimes: **Study 1** showed that Si stocks were barely decreased in soils under oil-palm plantations, regardless of soil type and water regime (c.f. **Chapter 2, Tab. 2.2**). Likewise, **study 2** suggested that topsoil Si_M concentrations were similar (c.f. **Chapter 3, Fig. 3.2c, 3.2d**) in four different management zones (palm circles, oil-palm rows, frond piles, interrows serving as harvesting paths) within an oil-palm plantation. Lastly, **study 3** revealed similar total Si content in various oil-palm parts (e.g., in frond, stem and fruit-bunch parts) (c.f. **Chapter 4, Fig. 4.2**).

These observations suggest that an additional Si influx by stream water or flooding could be negligible in the soil-plant system under oil-palm cultivation. Alternatively, our results could also imply that Si uptake by oil-palm roots is similar in both water regimes, thereby offsetting potentially larger Si supply. Si uptake by oil-palm roots remains poorly researched. Most plants take up nutrients via the root hairs of fine roots (Rascio and Navari-Izzo 2011; Haynes 2017). Yet rice, which is one of the most studied Si-accumulating plants, takes Si up by its thicker lateral roots. In fact, root hairs play no essential role (Ma 2001). Alternatively, Si uptake by oil-palm roots could also resemble the uptake mechanism of (metal)-hyperaccumulating plants (Rascio and Navari-Izzo 2011; Balafrej et al. 2020). In this case, Si would be permanently concentrated within the root zone of the oil palm, taken up according to the needs of the plant and accumulated in leaf tissue. In summary, this discussion highlights the question whether Si uptake mechanisms can be projected from one Si-accumulating crop (e.g., rice, sugarcane or wheat) onto another (oil palm), or whether these processes are unique for each crop, in which case, more field observations would be required to support either theory.

5.1.2 Principal drivers of Si cycling under oil-palm cultivation

A further aim was to understand in which way various Si fractions interact within the soil-plant-Si cycle. Additionally, it was intended to identify processes, potentially leading to alterations and Si losses from smallholder oil-palm plantations. We expected soil Si pools to be noticeably depleted under oil-palm plantations compared to lowland rainforest due to high Si uptake by oil-palm roots and Si losses through topsoil erosion and fruit bunch harvest.

Study 1 showed that Si pools mostly present in topsoil (Si_{Org} and Si_{Ba} pool) tended to be lower after converting lowland rainforest into oil-palm plantations. Yet the study lacks the statistical evidence that oil-palm cultivation has significantly decreased soil Si pools (c.f. **Chapter 2, Fig. 2.1, Fig. 2.2, and Tab. 2.2**). In **study 2**, we identified topsoil erosion to be a prominent process on oil-palm plantations established on sloping terrain, involving considerable Si_{Am} losses in unvegetated interrows (c.f. **Chapter 3, Tab. 3.1**). Likewise **study 3** showed that fruit-bunch harvest also resulted in Si losses from the system (c.f. **Chapter 4, Tab. 4.2a-c**). Furthermore, we observed that oil-palm management practices in fact has caused a spatial topsoil Si concentration pattern within an oil-palm plantation: frond piles were zones with high topsoil Si_{Am} levels, whereas the palm circles, oil-palm rows and interrows serving as harvesting paths were zones with low topsoil Si_{Am} levels (**Fig. 5.1 and Chapter 3, Fig. 3.2a, 3.2b**). Lastly, we observed that in oil-palm plantations of our study area, the amount of Si stored and returned to soils by pruned oil-palm fronds was higher than Si losses through fruit bunch harvest (**Fig. 5.1**).

We presume that topsoil Si_{Am} concentrations under oil-palm plantations are governed by litter input especially of Si-accumulating plants, decay and subsequent phytolith release into topsoils. Furthermore, topsoil Si_{M} concentrations in the different management zones reflect the importance of biogenic Si_{Am} (originating mostly from frond piles) as a readily available source of Si_{M} . Therefore, Si cycling under oil-palm cultivation could be mainly driven by biogenic-amorphous silica (i.e., mainly phytoliths, alongside silicious microbes in topsoils) and mobile Si (i.e., Si in soil solution) at the soil-plant interface (**Fig. 5.1**). As we applied different chemical extraction methods in accordance with the research aim of each study, biogenic-amorphous Si is represented as the Si_{Ba} pool in study 1 (c.f. **Chapter 2**), as the major component of the topsoil Si_{Am} pool in study 2 (c.f. **Chapter 3**) and as the principal component of total Si in plants in study 3 (c.f. **Chapter 4**). Nevertheless, other soil Si pools also release Si into soil solution (**Fig. 5.1**). In the highly weathered soils within our study area, higher Si contributions from subsoil Si pools may be attributed to Si occluded in pedogenic oxides and hydroxides (Si_{Occ} pool) (c.f. **Chapter 2, Tab. 2.2, Fig. 2.1, Fig. 2.2**).

The results from all three studies highlight the importance of phytoliths in the soil-plant system under oil-palm cultivation. From **study 1 and 2** we inferred that cover crop seemed to be an effective measure to sustain phytoliths in topsoils, and hence maintain well-balanced Si levels (c.f. **Chapter 2 and Chapter 3**). However, the question remains whether the presence of phytoliths in topsoils, palm fronds and litter from other Si-accumulating plants (e.g., grasses and sedges) already suffices to sustain Si cycling in this land-use system, or whether additional measures are needed.

5.2 Recommendations and outlook

Current oil-palm management already shows a tendency of altering soil Si pools: higher Si_{Am} levels were detected in topsoils under frond piles or in interrows that contained a dense grass or cover crop

(c.f. **Chapter 3, Tab. 3.1, and Fig. 3.2b**). Lower Si_{Am} levels were detected in topsoils of vegetation-scarce interrows, especially on sloping terrain (c.f. **Chapter 3, Tab. 3.1, and Fig. 3.2a**). Furthermore, Si is also exported from the system by fruit-bunch harvest (c.f. **Chapter 4**). These tendencies could become more pronounced with on-going oil-palm cultivation. It is therefore essential to counter this trend.

Although oil-palm management practices already include measures to ensure well-balanced Si levels in soils, these measure as such could still be improved or applied in our study area: frond piles could be stacked in “empty”, vegetation-scarce interrows after a short time-period, e.g., 5 – 10 years as supposed to waiting until the end of a plantation cycle. Smallholder farmers could maintain a grassy, and well-weeded cover crop, especially in current interrows of oil-palm plantations. Likewise, they could return empty fruit bunches to palm circles to serve as an organic fertilizer. The implementation of this is not yet given. Finally, distributing oil-palm residue, especially chipped stem parts prior to replanting the same plantation sites, could additionally supply Si to the system.

Future research could address Si uptake mechanisms by oil-palm roots as this could broaden the understanding of Si cycling in this land-use system.

5.3 References

- Balafrej H, Bogusz D, Abidine Triqui Z-E, et al (2020) Zinc Hyperaccumulation in Plants: A Review. *Plants* 9:. <https://doi.org/10.3390/plants9050562>
- Haynes RJ (2017) The nature of biogenic Si and its potential role in Si supply in agricultural soils. *Agric Ecosyst Environ* 245:100–111. <https://doi.org/10.1016/j.agee.2017.04.021>
- Ma JF (2001) Role of Root Hairs and Lateral Roots in Silicon Uptake by Rice. *Plant Physiol* 127:1773–1780. <https://doi.org/10.1104/pp.127.4.1773>
- Rascio N, Navari-Izzo F (2011) Heavy metal hyperaccumulating plants: How and why do they do it? And what makes them so interesting? *Plant Sci* 180:169–181. <https://doi.org/10.1016/j.plantsci.2010.08.016>

Appendices

Appendix I Supplement – Chapter 2 (study 1)

I – Table A1	Photographs of soil profiles under oil-palm plantations
I – Table A2	Photographs of soil profiles under lowland rainforest
I – Table B1	Soil chemical and physical properties of studied soil profiles
I – Table B2	Si concentrations of various Si fractions
I – Table B3	Contents of Si fractions in soils (per dm ³ of soil)
I – Figure 1	Contents of Si fractions in soils under oil-palm plantations (per dm ³ of soil)
I – Figure 2	Contents of Si fractions in soils under lowland rainforest (per dm ³ of soil)

Appendix II Supplement – Chapter 3 (study 2)

II – Table A1	Elevation transects for topsoil sampling, fieldwork 2018
II – Table A2	Photographs of topsoil sampling
II – Table A3	Photographs of sediment traps
II – Table B1	Mean topsoil Si _{Am} and Si _M concentrations (oil-palm plots)
II – Table B2	Topsoil Si _{Am} and Si _M concentrations (oil-palm plots)
II – Table B3	Weekly losses of eroded soil material and Si _{Am} in eroded soil material (sediment traps)
II – Table B4	Statistical analyses
II – Table B5	Statistical analyses with corresponding ANOVA-analysis

Appendix III Supplement – Chapter 4 (study 3)

III – Table A1	Photographs of oil-palm parts, fieldwork 2019
III – Table B1	Si and Ca concentrations in oil-palm parts, and statistical analyses
III – Table B2	Morphological characteristics of sampled oil palms and Si concentrations in fruit bunches, fieldwork 2019

Table A1 Soils under oil-palm plantations




Soil Profile	Position and main characteristics
	<p>HO1: Haplic Acrisol (Loamic, Cutanic, Ochric)</p> <p>Position: located on an upper slope within an oil-palm row, loamy Acrisol with low soil organic matter content in the topsoil, evidence of fertilizer application, burning and rill erosion.</p> <p>Topsoil (0 – 11 cm): Ah – A/E, olive-brown soil horizons with weak granular soil structure, few fine roots, many coarse roots, and worm casts.</p> <p>E horizon (11 – 27 cm): brownish yellow soil horizon with moderate subangular blocky soil structure, mostly coarse roots, and worm casts.</p> <p>Subsoil (27 – 100 cm): Bt – Btg1 – Btg2 – Btg3 – Btgc, yellowish brown soil horizons with moderate subangular and angular blocky structure, clay coatings, few fine to very fine roots and few Fe concretions, followed by a reddish yellow horizon with a strong subangular and angular blocky soil structure, clay coatings, few very fine roots and abundant Fe concretions.</p>
	<p>HO2: Endoferric Endostagnic Petroplinthic Acrisol (Loamic, Cutanic, Ochric)</p> <p>Position: located on an upper slope within an oil-palm row, loamy Acrisol with low soil organic matter content in the topsoil, evidence of fertilizer application and burning, slightly disturbed vegetation, Ah horizon partly eroded.</p> <p>Topsoil (0 – 10 cm): Ah – A/E, yellowish brown soil horizons with weak to moderate subangular blocky soil structure, few fine and coarse roots, worm casts.</p> <p>Subsoil (10 – 100 cm): Bt1 – Bt2 – Btg1 – Btg2 – Bvm – Bg, brownish yellow soil horizons with moderate to strong subangular blocky structure, clay coatings, few fine and many coarse roots, from 43 cm downwards additionally with faint orange mottles and very few fine and coarse roots, between 62 – 78 cm with plinthite in the form of larger nodules and concretions, from 78 cm downwards additionally with abundant Fe-concretions, bleached root channels and very few very fine roots.</p>
	<p>HO3: Haplic Acrisol (Loamic, Cutanic, Ochric, Profondic)</p> <p>Position: located on a middle slope within an interrow, loamy Acrisol with low soil organic matter content in the topsoil, evidence of fertilizer application and burning, moderately disturbed vegetation, Ah horizon disturbed or partly eroded.</p> <p>Topsoil (0 – 9 cm): Ah – A/E, olive brown soil horizons with weak to moderate massive and subangular blocky structure, few fine roots, very few coarse roots and worm casts.</p> <p>E horizon (9 – 30 cm): brownish yellow soil horizon with <i>pseudosand</i> structure, few fine roots, very few coarse roots and worm casts.</p> <p>Subsoil (30 – 100 cm): 2Bt1 – 2Bt2, light olive brown and yellowish-brown soil horizons with moderate subangular and angular blocky structure, faint clay coatings, very few fine and coarse roots and termite burrows.</p>

Table A1 continued



HO4: Endoprotostagnic Acrisol (Loamic, Cutanic, Ochric, Novic)

Position: located on an upper slope within an oil-palm row, loamy Acrisol with low soil organic matter content in the topsoil, evidence of fertilizer application and burning.

Topsoil (0 – 35 cm): Ah – A/E – E/A – 2AEb, light olive brown and dark yellowish brown soil horizons (including buried Ah and transitional horizon), with a moderate granular and subangular blocky soil structure, few clay and humus coatings, few fine and very few coarse roots, termite nests and charcoal.

E horizon (35 – 47 cm): 2EB, light olive brown soil horizon with moderate subangular blocky structure, few faint clay coatings, very few fine and coarse roots, termite nests and charcoal.

Subsoil (47 – 100 cm): 2BE – 2Bt – 2Btg, light olive brown soil horizon with moderate to strong subangular blocky structure, many faint clay coatings, few fine roots and charcoal, followed by brownish yellow soil horizon with faint mottles and strong subangular and angular blocky soil structure; very few fine roots and soft concretions from 76 cm downwards.



HOR1: Acric Endogleyic Stagnosol (Loamic, Colluvic, Ochric)

Position: located in a floodplain within an interrow, clayey Stagnosol with low soil organic matter content in the topsoil, evidence of fertilizer application, former artificial drainage, levelling and burning, disturbed and partly eroded Ah horizon.

Topsoil (0 – 2 cm): Ah, dark greyish brown soil horizon with a moderate to strong granular and subangular blocky soil structure, few fine and coarse roots, and insect borrows.

E horizon (2 – 13 cm): Eg, dark greyish brown soil horizon with a moderate to strong subangular blocky soil structure, few fine roots, many coarse roots, and insect borrows.

Subsoil (13 – 100 cm): Bg – 2Btg1 – 2Btg2 – 2Btlg, stagnic properties (light orange / grey), distinct clay coatings, soil structure changing from moderate subangular blocky to strong angular blocky and prismatic with soil depth, very few fine and coarse roots, from 77 cm downwards additionally with soft reddish concretions.



HOR2: Acric Albic Gleyic Stagnosol (Loamic, Ochric)

Position: located in a floodplain within an interrow, loamy to clayey Stagnosol with low soil organic matter content in the topsoil, evidence of fertilizer application, slightly disturbed vegetation.

Topsoil (0 – 3 cm): Ah, greyish brown soil horizon with moderate to strong granular and subangular blocky structure, few fine roots and very few coarse roots.

E horizon (3 – 14 cm): Eg, pale yellow soil horizon with moderate to strong angular blocky structure and few fine and coarse roots.

Subsoil (14 – 100 cm): BEg – Btg – Btgl, stagnic properties (reddish yellow / grey), distinct clay coatings, strong prismatic structure, very few fine and coarse roots, from 38 cm downwards additionally with soft reddish concretions and reductimorphic colors around roots channels.

Table A1 continued

	<p>HOr3: Acric Gleyic Stagnosol (Loamic, Ochric, Loaminovic)</p> <p>Position: located in a floodplain within an interrow, loamy Stagnosol with low soil organic matter content in the topsoil, evidence of fertilizer application, moderately disturbed vegetation.</p> <p>Topsoil (0 – 10 cm): Ah – A/E, olive to light olive brown soil horizons with moderate to strong granular and subangular blocky structure, very few fine and coarse roots, worm casts and charcoal.</p> <p>BE horizons (10 – 32): BEg1 – BEg2, light olive and yellowish-brown soil horizons with stagnic properties (brownish yellow to reddish yellow / grey), distinct clay coatings, moderate angular blocky structure, few fine roots, few to many coarse roots, few soft concretions, charcoal.</p> <p>Subsoil (32 – 100 cm): 2Btg1 – 2Btg2 – 2Bg11 – 2Bg12, stagnic properties (reddish yellow / pale brown and reddish yellow / light grey), strong subangular and angular blocky structure, many clay coatings, reddish Fe concretions, and reddish rimmed roots.</p>
	<p>HOr4: Protostagnic Acrisol (Loamic, Cutanic, Ochric)</p> <p>Position: on a foot slope within an interrow, clayey Acrisol with low soil organic matter content in the topsoil, evidence of fertilizer application and burning, moderately disturbed vegetation.</p> <p>Topsoil (0 – 5 cm): Ah, brown to yellowish brown soil horizon with weak massive and subangular blocky structure, few fine roots, worm casts and charcoal.</p> <p>E horizon (5 – 12 cm): EA, light yellowish brown soil horizon with moderate subangular blocky structure, few fine roots, very few coarse roots, worm casts and charcoal.</p> <p>Subsoil (12 – 100 cm): BE – Bt1 – Bt2 – Btgc1 – Btgc2, brownish yellow soil horizons, BE with moderate to strong subangular blocky structure, faint clay coatings, soft red Fe-concretions, few fine roots, many coarse roots, worm casts and charcoal below horizons with structure changing with depth from moderate subangular blocky to strong subangular blocky and angular blocky, very few fine roots, few coarse roots, many faint clay coatings, soft red Fe concretions.</p>

Table A2 Soils under lowland rainforest


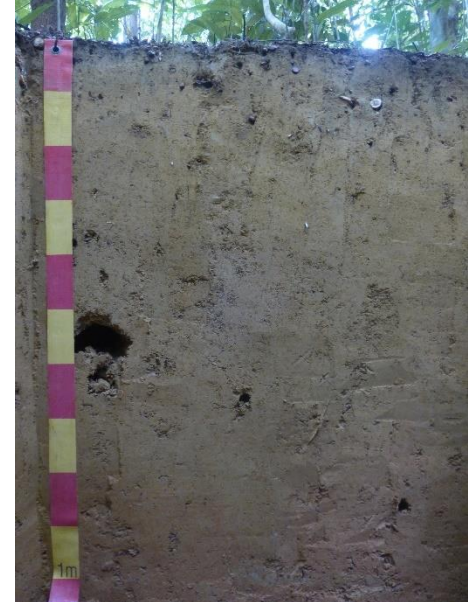

Soil profile	Position and main characteristics
	<p>HF1: Stagnic Acrisol (Loamic, Cutanic, Ochric)</p> <p>Position: located on an upper slope within a lowland restoration forest (PT REKI, Harapan rainforest), loamy Acrisol with low soil organic matter content in the topsoil, evidence of clearing, moderately disturbed vegetation.</p> <p>Topsoil (0 – 2 cm): Ah, dark yellowish brown soil horizon with a weak to moderate granular and subangular blocky soil structure, few fine and coarse roots, and insect borrows.</p> <p>E horizon (2 – 12 cm): EA, brownish yellow soil horizon with moderate granular and subangular blocky soil structure, few fine and coarse roots, worm casts and insect borrows.</p> <p>Subsoil (12 – 100 cm): B/E – Btg1 – Btg2 – Btg3, brownish yellow soil horizons with structure changing with depth from moderate subangular blocky to strong angular blocky, many faint clay coatings, very few fine and coarse roots, termite nest and insect borrows, Btg3 with soft reddish Fe-concretions.</p>
	<p>HF3: Stagnic Acrisol (Loamic, Cutanic, Densic, Ochric)</p> <p>Position: located on a middle slope within a lowland restoration forest (PT REKI, Harapan rainforest), loamy Acrisol with low soil organic matter content in the topsoil, evidence of clearing, Ah horizon slightly eroded.</p> <p>Topsoil (0 – 3 cm): Ah, brown soil horizon with weak to moderate granular and subangular blocky structure, many fine and coarse roots, earthworm casts.</p> <p>E horizon (3 – 34 cm): E/A – E, light yellowish brown soil horizons with weak to moderate subangular blocky to angular blocky structure, few fine roots, many coarse roots, insect borrows and termite nests.</p> <p>Subsoil (34 – 100 cm): Btg1 – Btg2, brownish yellow soil horizons with moderate subangular and angular blocky structure, few faint clay coatings and faint mottles (brownish yellow / pale yellow), very few fine and coarse roots, Btg2 additionally with charcoal, insect borrows and few reddish Fe nodules.</p>
	<p>HF4: Endostagnic Acrisol (Loamic, Cutanic, Ochric)</p> <p>Position: located on a summit within a lowland restoration forest (PT REKI, Harapan rainforest), loamy to clayey Acrisol with low soil organic matter content in the topsoil, evidence of clearing and burning.</p> <p>Topsoil (0 – 4 cm): Ah, yellowish brown soil horizon with weak granular and subangular blocky structure, many fine and coarse roots, termite nests.</p> <p>E horizon (4 – 35 cm): EA – E, brownish yellow soil horizons with weak to moderate granular and subangular blocky structure, very few fine and coarse roots, termite nests and insect borrows.</p> <p>Subsoil (35 – 100 cm): Bt1 – Bt2 – Btg1 – Btg2, brownish yellow soil horizons with moderate subangular and strong angular blocky structure, many distinct clay coatings and very few fine roots, Btg1 with faint mottles, Btg2 with intense mottles (yellowish red / yellow and strong brown / pale yellow), insect borrows, charcoal, very few dusky red soft Fe concretions.</p>

Table A2 continued



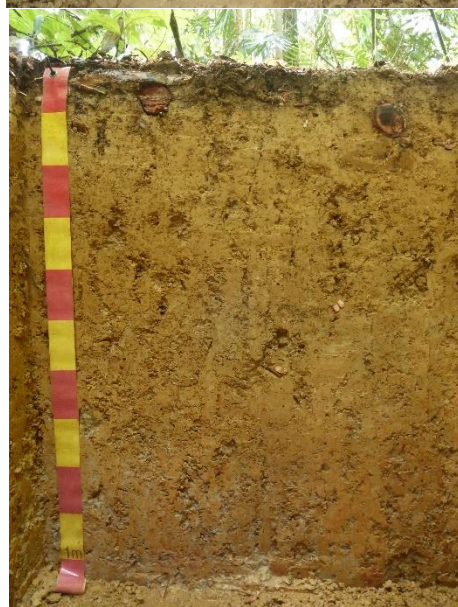
HFr1: Gleyic Stagnosol (Loamic, Ochric)

Position: located on a toe slope within a lowland restoration forest (PT REKI, Harapan rainforest), loamy Stagnosol with low soil organic matter content in the topsoil, evidence of clearing, moderately disturbed vegetation.

Topsoil (0 – 7 cm): Ah, dark yellowish brown soil horizon with weak massive and subangular blocky structure, many fine roots, few coarse roots, termite nests, and insect borrows.

EB and BE horizon (7 – 46 cm): EB – BEg, pale yellow soil horizons with weak to moderate subangular blocky structure, few fine and coarse roots, termite nests, insect borrows and earthworm casts, BEg additionally with faint mottles (yellow / light grey).

Subsoil (46 – 90 cm): Bg1 – Bg12, mottles (yellow / white), moderate subangular blocky structure, very few fine roots, Bg12 additionally with red Fe nodules.



HFr3: Stagnic Acrisol (Loamic, Cutanic, Ochric)

Position: located in a floodplain within a lowland restoration forest (PT REKI, Harapan rainforest), loamy to clayey Acrisol with low soil organic matter content in the topsoil, evidence of clearing, Ah horizon covered by litter.

Topsoil (0 – 8 cm): Ah, yellowish brown soil horizon with weak granular and subangular blocky structure, many fine and coarse roots, insect borrows and charcoal.

E horizons (8 – 24 cm): E/A – E, brownish yellow to very pale brown soil horizons with moderate subangular blocky structure, few fine and coarse roots, termite nests and insect borrows.

Subsoil (24 – 100 cm): Bt – Btg1 – Btg2 – Btg3, brownish yellow soil horizons with moderate subangular blocky to strong angular blocky structure, many distinct clay coatings, very few fine and coarse roots, Btg horizons additionally with distinct mottles (yellow / light reddish brown followed by reddish yellow / light reddish grey), Btg3 additionally with red Fe concretions.



HFr4: Acric Gleyic Stagnosol (Loamic, Ochric)

Position: located in a floodplain within a lowland restoration forest (PT REKI, Harapan rainforest), loamy Stagnosol with low soil organic matter content in the topsoil, evidence of clearing.

Topsoil (0 – 7 cm): Ah, dark yellowish brown soil horizon with moderate subangular blocky structure, few fine roots, many coarse roots, termite nests.

E horizon (7 – 16 cm): Eg, dark yellowish brown soil horizon with moderate subangular blocky structure, faint brownish yellow / yellowish brown mottles alongside a greyish bleached zone, very few fine roots and few coarse roots.

Subsoil (16 – 100 cm): Bg – Btlg – Blg, hydromorphic horizons with structure from moderate subangular blocky to strong angular blocky, very few fine roots, insect borrow, Bg with prominent mottles (brownish yellow / light brownish grey), Btlg and Blg with yellow / light brown grey to light grey mottles and very small soft red Fe concretions.

Appendix I – laboratory

Table B1 Physical and chemical soil properties of soil profiles of study areas, Harapan landscape, Jambi Province

RSG	Plot	Horizon	Depth [cm]	Bulk density [g cm ⁻¹]	C _{org} [%]	N _t [%]	CEC _{eff} [cmol kg ⁻¹]	BS [%]	CEC _{pot} [cmol kg ⁻¹]	CEC _{pot} [cmol kg _{clay}]	pH _{H2O}	pH _{CaCl2}	Sand [%]	Silt [%]	Clay [%]
Acrisol	HO1	Ah	-5	1.15	2.02	0.15	14.31	10.58	n.d.		4.63	3.96	28.3	50.8	21.0
	HO1	A/E	-11	1.19	1.50	0.12	10.67	58.02	n.d.		4.48	3.86	26.7	49.7	23.6
	HO1	E	-27	1.30	0.85	0.08	11.32	38.95	n.d.		4.48	3.71	18.2	53.1	28.8
	HO1	Bt	-39	1.35	0.62	0.06	11.64	18.48	11.45	43.31	4.48	3.78	17.9	55.7	26.4
	HO1	Btg1	-59	1.41	0.54	0.06	13.45	5.97	15.75	39.89	4.49	3.77	16.8	43.7	39.5
	HO1	Btg2	-84	1.39	0.43	0.06	6.36	3.02	6.97	14.07	4.56	3.84	11.5	39.0	49.5
	HO1	Btg3	-94	1.33	0.39	0.06	7.02	1.58	26.70	49.89	4.54	3.87	11.2	35.3	53.5
	HO1	Btgc	-100	1.39	0.41	0.06	8.23	1.21	47.52	126.70	4.72	3.91	13.9	48.6	37.5
Acrisol	HO2	Ah	-5	1.22	1.20	0.08	8.85	1.67	n.d.		4.72	3.84	43.0	34.2	22.8
	HO2	A/E	-10	1.28	1.00	0.08	5.41	33.97	n.d.		4.62	3.76	37.8	31.9	30.3
	HO2	Bt1	-18	n.d.	0.71	0.06	6.16	16.70	7.79	23.17	4.75	3.82	33.0	33.4	33.6
	HO2	Bt2	-28	1.43	0.56	0.06	6.71	7.09	10.83	30.60	4.71	3.77	33.9	30.7	35.4
	HO2	Btg1	-43	1.41	0.49	0.05	6.37	1.14	11.32	32.08	4.74	3.84	32.2	32.5	35.3
	HO2	Btg2	-62	1.43	0.41	0.04	7.00	0.00	13.06	34.83	4.63	3.80	30.9	31.6	37.5
	HO2	Bvm	-78	n.d.	n.d.	n.d.	n.d.	n.d.	n.d.	n.d.	n.d.	n.d.	plinthite		
	HO2	Bg (t.)	-89	1.40	0.27	0.03	9.22	0.73	27.33	56.03	4.60	3.79	26.2	25.0	48.8
HO2	Bg (b.)	-100	1.40	0.23	0.02	10.20	0.54	n.d.		4.67	3.84	22.4	29.9	47.8	
Acrisol	HO3	Ah	-3	1.25	2.01	0.16	1.49	3.94	n.d.		4.26	4.19	61.7	15.5	22.9
	HO3	A/E	-9	1.10	1.07	0.10	1.35	4.66	n.d.		4.29	4.14	60.5	12.8	26.7
	HO3	E	-30	1.08	0.64	0.07	1.16	1.71	n.d.		4.29	4.17	56.5	12.1	31.4
	HO3	2Bt1 (t.)	-40	1.16	0.48	0.05	1.16	1.04	6.55	19.62	4.41	4.19	54.1	12.5	33.4
	HO3	2Bt1 (b.)	-50	1.16	0.39	0.05	1.47	0.52	6.37	18.56	4.32	4.24	53.8	11.9	34.3
	HO3	2Bt2 (t.)	-75	1.27	0.32	0.05	1.39	-0.55	6.61	17.98	4.34	4.24	51.6	11.6	36.8
	HO3	2Bt2 (b.)	-100	1.27	0.29	0.05	1.38	2.37	5.76	14.47	4.32	4.22	50.9	9.2	39.8

Table B1 continued

RSG	Plot	Horizon	Depth	Bulk density	C _{org}	N _t	CEC _{eff}	BS	CEC _{pot}	CEC _{pot}	pH _{H2O}	pH _{CaCl2}	Sand	Silt	Clay
			[cm]	[g cm ⁻¹]	[%]	[%]	[cmol kg ⁻¹]	[%]	[cmol kg ⁻¹]	[cmol kg _{clay}]			[%]	[%]	[%]
Acrisol	HO4	Ah	-7	1.24	1.62	0.12	2.73	6.45	n.d.		4.17	3.94	59.8	17.7	22.4
	HO4	A/E	-13	1.18	1.18	0.09	2.37	2.95	n.d.		4.28	4.02	55.5	16.6	27.9
	HO4	E/A	-27	1.27	0.81	0.07	2.41	2.14	n.d.		4.25	4.08	54.8	18.3	26.9
	HO4	2AEb	-35	1.23	0.75	0.06	2.22	1.83	n.d.		4.32	4.15	52.8	17.6	29.6
	HO4	2EB	-47	1.36	0.52	0.05	2.09	0.86	n.d.		4.28	4.12	55.3	15.8	28.9
	HO4	2BE	-57	1.40	0.34	0.04	2.23	1.39	n.d.		4.26	4.07	51.0	17.7	31.3
	HO4	2Bt	-76	1.45	0.34	0.04	2.36	1.60	8.55	25.74	4.28	4.04	49.8	17.0	33.2
	HO4	2Btg	-100	1.49	0.25	0.04	2.53	0.33	7.68	21.73	4.23	4.03	48.9	15.8	35.3
Stagnosol	HOr1	Ah	-2	0.87	4.33	0.38	9.93	18.11	n.d.		4.45	4.07	4.2	38.4	57.4
	HOr1	Eg	-13	1.03	2.01	0.20	12.81	11.07	n.d.		4.51	3.88	2.7	35.8	61.6
	HOr1	Bg	-25	1.16	1.11	0.13	13.96	9.31	n.d.		4.47	3.67	4.1	36.1	59.9
	HOr1	2Btg1 (t.)	-37	1.27	0.69	0.10	13.03	7.46	12.00	35.40	4.52	3.66	22.4	43.7	33.9
	HOr1	2Btg1 (b.)	-48	1.27	0.60	0.09	14.47	8.19	13.90	19.66	4.57	3.67	0.7	28.6	70.7
	HOr1	2Btg2 (t.)	-63	1.16	0.62	0.10	17.01	6.71	13.40	18.95	4.55	3.71	n.d.	n.d.	n.d.
	HOr1	2Btg2 (b.)	-77	1.16	0.51	0.08	17.49	6.85	12.90	19.83	4.55	3.70	0.5	34.4	65.0
	HOr1	2Btlg (t.)	-89	1.25	0.42	0.07	17.51	7.26	12.90	20.17	4.57	3.72	1.0	35.1	64.0
	HOr1	2Btlg (b.)	-100	1.25	0.35	0.06	15.83	6.85	13.00	23.07	4.54	3.66	1.9	41.7	56.3
Stagnosol	HOr2	Ah	-3	0.91	5.43	0.44	11.44	20.35	n.d.		4.19	3.90	5.2	41.9	52.9
	HOr2	Eg	-14	1.10	1.21	0.15	10.07	12.26	n.d.		4.62	3.82	8.2	41.0	50.8
	HOr2	BEg (t.)	-26	1.39	0.68	0.07	9.08	7.87	n.d.		4.95	3.90	14.0	43.2	42.9
	HOr2	BEg (b.)	-38	1.39	0.47	0.01	9.86	9.12	n.d.		4.82	3.71	21.0	44.5	34.5
	HOr2	Btg (t.)	-54	1.45	0.29	0.06	8.03	8.44	14.30	42.06	4.84	3.67	22.2	43.8	34.0
	HOr2	Btg (b.)	-70	1.45	0.19	0.03	5.73	2.98	11.50	23.95	4.83	3.65	23.3	28.7	48.0
	HOr2	Btlg (t.)	-85	1.42	0.20	0.04	5.04	1.33	12.60	46.41	4.78	3.67	29.1	43.8	27.2
	HOr2	Btlg (b.)	-100	1.42	0.23	0.02	5.43	2.70	13.00	42.98	4.80	3.65	29.8	39.9	30.2

Table B1 continued

RSG	Plot	Horizon	Depth	Bulk density	C _{org}	N _t	CEC _{eff}	BS	CEC _{pot}	CEC _{pot}	pH _{H2O}	pH _{CaCl2}	Sand	Silt	Clay
			[cm]	[g cm ⁻¹]	[%]	[%]	[cmol kg ⁻¹]	[%]	[cmol kg ⁻¹]	[cmol kg _{clay}]			[%]	[%]	[%]
Stagnosol	HOr3	Ah	-3	1.10	2.13	0.18	4.67	53.13	n.d.		4.16	3.85	23.4	48.3	28.4
	HOr3	AE	-10	1.31	1.03	0.10	2.53	6.13	n.d.		4.42	3.94	23.3	48.1	28.6
	HOr3	BEg1	-21	1.36	0.63	0.07	3.40	5.24	n.d.		4.41	3.90	23.2	49.9	26.9
	HOr3	BEg2	-32	1.43	0.41	0.06	3.96	4.47	n.d.		4.35	3.89	20.8	47.3	31.9
	HOr3	2Btg1	-43	1.38	0.33	0.06	4.67	13.67	12.60	39.25	4.39	3.89	21.1	46.8	32.1
	HOr3	2Btg2	-60	1.47	0.30	0.06	4.16	2.80	13.00	36.21	4.39	3.88	19.9	44.3	35.9
	HOr3	2Bgl1	-80	1.50	0.28	0.06	4.70	3.40	n.d.		4.37	3.89	22.9	41.0	36.1
	HOr3	2Bgl2	-100	1.44	0.26	0.05	4.97	4.48	n.d.		4.36	3.92	19.3	44.4	36.3
Acrisol	HOr4	Ah	-5	1.23	2.28	0.20	4.19	56.39	n.d.		4.53	4.19	16.0	45.3	38.7
	HOr4	EA	-12	1.27	1.60	0.16	4.70	50.77	n.d.		4.56	4.14	14.4	44.7	41.0
	HOr4	BE	-20	1.22	1.01	0.11	4.65	36.72	n.d.		4.55	4.11	13.7	42.3	44.0
	HOr4	Bt1	-37	1.27	0.59	0.05	4.77	20.92	11.00	23.36	4.32	4.01	12.9	39.9	47.1
	HOr4	Bt2	-56	1.27	0.48	0.10	4.55	14.86	11.52	20.17	4.36	3.96	4.1	38.8	57.1
	HOr4	Btgc1 (t.)	-70	1.21	0.47	0.08	5.02	14.38	12.80	19.99	4.26	3.96	9.4	26.6	64.0
	HOr4	Btgc1 (b.)	-83	1.21	0.44	0.08	4.91	7.75	13.71	21.38	4.33	4.03	10.0	25.9	64.1
HOr4	Btgc2	-100	1.20	0.40	0.07	4.51	6.56	16.13	28.84	4.39	4.05	11.5	32.6	55.9	
Acrisol	HF1	Ah	-2	0.79	3.81	0.26	6.20	8.02	n.d.		4.16	3.67	49.9	27.8	22.3
	HF1	EA	-12	1.11	1.43	0.13	3.57	3.79	n.d.		4.44	3.83	46.8	27.2	26.0
	HF1	B/E	-31	1.29	0.80	0.09	4.72	2.29	n.d.		4.31	3.90	45.6	26.7	27.7
	HF1	Btg1	-53	1.40	0.57	0.07	4.69	1.90	21.21	72.49	4.45	3.94	42.5	28.2	29.3
	HF1	Btg2	-66	1.44	0.40	0.06	5.11	0.82	9.43	29.77	4.50	3.85	43.0	25.3	31.7
	HF1	Btg 3 (t.)	-83	1.39	0.58	0.07	3.97	2.70	8.22	23.46	4.48	3.92	39.9	25.0	35.0
	HF1	Btg3 (b.)	-100	1.09	0.70	0.09	4.96	1.38	37.08	98.08	4.41	3.93	37.0	25.2	37.8

Table B1 continued

RSG	Plot	Horizon	Depth	Bulk density	C _{org}	N _t	CEC _{eff}	BS	CEC _{pot}	CEC _{pot}	pH _{H2O}	pH _{CaCl2}	Sand	Silt	Clay
			[cm]	[g cm ⁻¹]	[%]	[%]	[cmol kg ⁻¹]	[%]	[cmol kg ⁻¹]	[cmol kg _{clay}]			[%]	[%]	[%]
Acrisol	HF3	Ah	-3	0.95	2.38	0.16	3.21	9.10	n.d.		4.15	3.53	59.3	26.6	14.1
	HF3	EA	-11	1.22	0.93	0.09	2.42	3.00	n.d.		4.46	3.75	51.3	31.7	17.1
	HF3	E (t.)	-23	1.49	0.55	0.06	2.31	2.77	n.d.		4.59	3.89	50.1	28.6	21.3
	HF3	E (b.)	-34	1.49	0.32	0.05	2.22	2.36	n.d.		4.44	3.96	49.4	28.9	21.7
	HF3	Btg1 (t.)	-51	1.56	0.30	0.04	2.50	3.55	7.34	34.24	4.54	3.93	48.6	30.0	21.4
	HF3	Btg1 (m.)	-68	1.56	0.29	0.04	2.60	0.06	6.67	24.91	4.57	3.95	45.5	27.7	26.8
	HF3	Btg1 (b.)	-84	1.56	0.28	0.04	2.66	0.30	5.61	19.70	4.53	3.98	44.0	27.5	28.5
	HF3	Btg2	-100	1.53	0.27	0.05	2.93	2.51	7.44	22.19	4.56	4.00	41.2	25.2	33.5
Acrisol	HF4	Ah	-4	0.72	4.00	0.28	5.79	6.60	n.d.		4.19	3.58	40.3	31.0	28.7
	HF4	EA	-11	1.14	0.81	0.09	3.98	1.94	n.d.		4.53	3.82	37.9	31.9	30.2
	HF4	E (t.)	-23	1.26	1.28	0.12	4.10	2.13	n.d.		4.64	3.97	34.2	31.6	34.2
	HF4	E (b.)	-35	1.26	0.53	0.07	4.61	0.63	n.d.		4.63	4.02	31.3	31.7	37.0
	HF4	Bt1	-53	1.40	0.45	0.06	5.59	4.98	15.91	41.26	4.63	3.92	30.5	31.0	38.6
	HF4	Bt2 (t.)	-65	1.40	0.40	0.06	6.10	6.35	6.26	14.29	4.56	3.90	27.6	28.5	43.8
	HF4	Bt2 (b.)	-78	1.40	0.36	0.05	6.43	0.96	7.06	15.37	4.56	3.97	26.4	27.7	45.9
	HF4	Btg1	-92	1.42	0.32	0.05	6.78	0.02	6.91	15.04	4.52	3.88	25.8	28.3	45.9
Stagnosol	HF4	Btg2	-100	1.40	0.35	0.05	7.29	0.89	7.35	14.64	4.66	3.90	23.3	26.5	50.2
	HFr1	Ah	-7	0.88	3.29	0.22	7.48	7.79	n.d.		4.02	3.45	26.9	39.5	33.6
	HFr1	E (t.)	-20	1.09	0.86	0.08	4.57	2.38	n.d.		4.24	3.84	48.2	27.6	24.2
	HFr1	E (b.)	-33	1.09	0.53	0.05	3.43	0.57	n.d.		4.68	4.05	46.4	31.3	22.4
	HFr1	Eg	-46	1.47	0.27	0.04	3.39	0.28	n.d.		4.69	4.09	68.3	18.2	13.4
	HFr1	Bg1 (t.)	-58	1.52	0.21	0.03	3.84	4.98	7.40	45.40	4.69	4.09	63.9	19.7	16.3
	HFr1	Bg1 (b.)	-69	1.52	0.15	0.03	3.69	-1.12	7.30	32.15	4.67	4.09	62.0	15.3	22.7
	HFr1	Bgl2	-90	1.53	0.12	0.03	3.68	-0.68	7.30	30.68	4.66	4.02	59.9	16.3	23.8

Table B1 continued

RSG	Plot	Horizon	Depth	Bulk density	C _{org}	N _t	CEC _{eff}	BS	CEC _{pot}	CEC _{pot}	pH _{H2O}	pH _{CaCl2}	Sand	Silt	Clay
			[cm]	[g cm ⁻¹]	[%]	[%]	[cmol kg ⁻¹]	[%]	[cmol kg ⁻¹]	[cmol kg _{clay}]			[%]	[%]	[%]
Acrisol	HFr3	Ah	-8	0.67	3.93	0.29	16.85	7.80	n.d.		4.19	3.51	11.6	54.4	33.9
	HFr3	E/A	-14	1.16	1.31	0.13	11.70	4.78	n.d.		4.58	3.75	14.2	52.3	33.4
	HFr3	E	-24	1.27	0.89	0.10	11.91	4.69	n.d.		4.71	3.86	12.5	52.3	33.6
	HFr3	Bt	-42	1.27	0.65	0.08	4.92	2.98	6.77	17.83	4.69	3.89	11.3	50.7	38.0
	HFr3	Btg1 (t.)	-53	1.33	0.54	0.08	5.89	2.34	6.17	14.72	4.60	3.88	10.4	47.7	41.9
	HFr3	Btg1 (b.)	-64	1.33	0.52	0.08	7.02	1.08	6.92	13.37	4.60	3.88	8.2	40.1	51.7
	HFr3	Btg2 (t.)	-75	1.24	0.46	0.07	8.28	1.05	6.72	11.66	4.62	3.85	6.5	35.9	57.6
	HFr3	Btg2 (b.)	-86	1.24	0.44	0.08	9.19	1.26	7.25	13.00	4.56	3.80	5.0	39.2	55.8
	HFr3	Btg3	-100	1.22	0.39	0.07	9.66	1.71	7.17	12.14	4.57	3.79	7.4	33.6	59.0
Stagnosol	HFr4	Ah	-7	0.90	3.92	0.26	6.23	4.64	n.d.		3.80	3.53	25.5	50.4	24.1
	HFr4	Eg	-16	1.33	0.71	0.08	3.84	3.54	n.d.		4.38	3.79	26.9	52.0	21.0
	HFr4	Bg	-34	1.42	0.43	0.07	4.76	1.76	n.d.		4.38	3.82	27.3	47.9	24.9
	HFr4	Btlg (t.)	-53	1.43	0.39	0.06	4.99	0.99	14.90	45.43	4.42	3.83	24.0	43.1	32.8
	HFr4	Btlg (b.)	-73	1.43	0.32	0.05	5.03	2.69	15.10	44.10	4.35	3.82	29.2	36.5	34.2
	HFr4	Blg (t.)	-86	1.48	0.22	0.05	4.95	1.11	n.d.		4.39	3.86	39.9	31.4	28.7
	HFr4	Blg (b.)	-100	1.48	0.20	0.04	3.94	1.13	n.d.		4.41	3.82	50.6	25.2	24.3

Table B2 Si concentrations of various Si fractions in soils under oil-palm plantations and lowland rainforest

RSG	Plot	Horizon	Si _M [$\mu\text{g g}^{-1}$]		Si _{Ad} [$\mu\text{g g}^{-1}$]		Si _{Org} [mg g^{-1}]		Si _{Occ} [mg g^{-1}]		Si _{Ba} [mg g^{-1}]		Si _{Pa} [mg g^{-1}]		Si _{total} [mg g^{-1}]
			\bar{X}	σ	\bar{X}	σ	\bar{X}	σ	\bar{X}	σ	\bar{X}	σ	\bar{X}	σ	\bar{X}
Acrisol	HO1	Ah	13.35±	0.00	9.13±	0.53	0.12±	0.00	0.26±	0.02	1.62		0.08		6034
		A/E	13.28±	0.19	9.46±	0.06	0.09±	0.00	0.30±	0.01	2.83		0.52		5911
		E	12.05±	0.18	10.12±	0.05	0.07±	0.00	0.34±	0.02	n.d.		1.76±	0.53	6022
		Bt	4.64±	0.31	10.65±	0.40	0.07±	0.00	0.21±	0.00	n.d.		1.19±	0.41	5693
		Btg1	7.08±	0.03	14.80±	0.49	0.09±	0.00	0.28±	0.00	n.d.		1.65		5141
		Btg2	8.50±	0.05	19.00±	0.14	0.12±	0.00	0.36±	0.01	n.d.		2.86±	0.11	4976
		Btg3	9.04±	0.11	21.75±	0.33	0.13±	0.00	0.40±	0.00	n.d.		2.10±	0.79	4557
		Btgc	9.14±	0.23	22.05±	0.41	0.13±	0.00	0.68±	0.07	n.d.		8.17±	4.23	4507
Acrisol	HO2	Ah	9.74±	0.03	7.48±	0.02	0.59±	0.03	0.11±	0.00	2.68		n.d.		5796
		A/E	10.81±	0.29	8.37±	0.21	0.21±	0.04	0.13±	0.01	3.76		n.d.		5452
		Bt1	9.72±	0.20	9.51±	0.31	0.13±	0.00	0.12±	0.00	n.d.		2.25±	0.38	5327
		Bt2	10.73±	0.18	10.92±	0.20	0.09±	0.01	0.13±	0.00	n.d.		1.87		5321
		Btg1	9.90±	0.50	11.42±	0.30	0.10±	0.00	0.15±	0.01	n.d.		1.09		5231
		Btg2	11.70±	0.69	13.70±	0.13	0.10±	0.00	0.16±	0.00	n.d.		2.47±	0.24	5209
		Bg (t.)	15.11±	0.33	19.17±	0.27	0.12±	0.00	0.18±	0.01	n.d.		4.91±	2.81	4817
		Bg (b.)	13.60±	0.00	18.28±	0.44	0.14±	0.01	0.21±	0.00	n.d.		5.99		4430
Acrisol	HO3	Ah	7.07±	0.11	10.56±	0.82	0.10±	0.00	0.22±	0.01	n.d.		3.21		6304
		A/E	4.00±	0.06	4.54±	0.16	0.05±	0.00	0.19±	0.01	n.d.		5.85±	0.80	6408
		E	4.61±	0.21	7.21±	0.18	0.05±	0.00	0.23±	0.00	n.d.		5.19±	0.64	6172
		2Bt1 (t.)	4.39±	0.30	8.07±	0.09	0.06±	0.00	0.25±	0.01	n.d.		6.31±	4.11	6052
		2Bt1 (b.)	4.06±	0.10	12.84±	0.46	0.07±	0.00	0.26±	0.01	n.d.		9.10±	1.51	5935
		2Bt2 (t.)	3.82±	0.11	4.84±	0.14	0.07±	0.00	0.26±	0.01	n.d.		7.67±	0.52	5862
		2Bt2 (b.)	3.76±	0.16	7.79±	0.28	0.07±	0.00	0.27±	0.00	n.d.		3.68		5848

Table B2 continued

RSG	Plot	Horizon	Si _M [$\mu\text{g g}^{-1}$]		Si _{Ad} [$\mu\text{g g}^{-1}$]		Si _{Org} [mg g^{-1}]		Si _{Occ} [mg g^{-1}]		Si _{Ba} [mg g^{-1}]		Si _{Pa} [mg g^{-1}]		Si _{total} [mg g^{-1}]
			\bar{X}	σ	\bar{X}	σ	\bar{X}	σ	\bar{X}	σ	\bar{X}	σ	\bar{X}	σ	\bar{X}
Acrisol	HO4	Ah	4.85±	0.16	6.14±	0.08	0.05±	0.00	0.12±	0.00	n.d.		4.02±	0.83	6494
		A/E	4.90±	0.25	6.84±	0.41	0.04±	0.00	0.18±	0.02	n.d.		4.56±	1.37	6806
		E/A	4.70±	0.00	5.28±	0.15	0.04±	0.00	0.12±	0.00	n.d.		2.95		6398
		2AEb	5.51±	0.12	9.02±	0.20	0.05±	0.00	0.16±	0.01	n.d.		3.39±	1.45	6824
		2EB	5.00±	0.30	7.68±	0.92	0.05±	0.00	0.22±	0.01	n.d.		4.01		6122
		2BE	6.38±	0.24	7.28±	0.15	0.06±	0.00	0.25±	0.00	n.d.		8.26±	1.47	6432
		2Bt	7.36±	0.04	6.67±	0.22	0.07±	0.00	0.25±	0.00	n.d.		6.02		6183
		2Btg	8.08±	0.18	12.49±	0.37	0.08±	0.00	0.57±	0.01	n.d.		6.60		6070
Stagnosol	HOr1	Ah	23.90±	0.58	20.53±	0.49	0.27±	0.01	0.41±	0.04	10.08		3.83		5404
		Eg	17.87±	0.01	14.40±	0.30	0.13±	0.00	0.41±	0.00	n.d.		10.31±	0.73	4797
		Bg	21.03±	0.49	19.42±	0.53	0.35±	0.03	0.18±	0.00	n.d.		7.51±	0.07	4630
		2Btg1 (t.)	16.76±	0.22	20.57±	0.13	0.15±	0.00	0.20±	0.00	n.d.		4.43±	1.81	4861
		2Btg1 (b.)	18.90±	0.11	24.64±	0.58	0.17±	0.00	0.23±	0.01	n.d.		11.05±	4.71	4482
		2Btg2 (t.)	21.40±	0.07	28.89±	0.09	0.21±	0.03	0.24±	0.01	n.d.		11.66±	5.84	4225
		2Btg2 (b.)	27.88±	0.09	31.19±	0.13	0.20±	0.00	0.24±	0.01	n.d.		7.58±	1.76	4627
		2Btlg (t.)	26.41±	0.11	30.40±	0.11	0.20±	0.00	0.25±	0.00	n.d.		5.17±	0.67	4452
2Btlg (b.)	23.37±	0.11	23.99±	0.12	0.19±	0.00	0.25±	0.01	n.d.		3.35		4921		
Stagnosol	HOr2	Ah	20.88±	0.03	23.29±	0.13	0.38±	0.00	0.24±	0.01	13.74		n.d.		3962
		Eg	12.53±	0.46	16.12±	0.29	0.13±	0.00	0.18±	0.00	n.d.		5.72±	1.56	4243
		BEg (t.)	9.94±	0.57	13.01±	0.13	0.12±	0.00	0.17±	0.00	n.d.		5.68±	0.99	4693
		BEg (b.)	13.18±	0.35	13.69±	0.24	0.13±	0.00	0.17±	0.00	n.d.		3.79±	0.44	4556
		Btg1 (t.)	12.51±	0.59	12.58±	0.48	0.16±	0.00	0.12±	0.00	n.d.		2.79		4774
		Btg1 (b.)	10.38±	0.54	10.09±	0.04	0.15±	0.00	0.11±	0.00	n.d.		1.74		5507
		Btg2 (t.)	12.14±	0.05	11.55±	0.08	0.15±	0.00	0.21±	0.01	n.d.		0.00		5044
		Btg2 (b.)	14.85±	0.27	16.54±	0.19	0.19±	0.01	0.51±	0.02	n.d.		0.91		4959

Table B2 continued

RSG	Plot	Horizon	Si _M [$\mu\text{g g}^{-1}$]		Si _{Ad} [$\mu\text{g g}^{-1}$]		Si _{Org} [mg g^{-1}]		Si _{Occ} [mg g^{-1}]		Si _{Ba} [mg g^{-1}]		Si _{Pa} [mg g^{-1}]		Si _{total} [mg g^{-1}]
			\bar{X}	σ	\bar{X}	σ	\bar{X}	σ	\bar{X}	σ	\bar{X}	σ	\bar{X}	σ	\bar{X}
Stagnosol	HOr3	Ah	8.19±	0.18	4.98±	0.72	0.14±	0.03	0.11±	0.01	2.25		3.04		6704
		AE	8.00±	0.20	6.22±	0.64	0.09±	0.00	0.15±	0.00	n.d.		2.28		6682
		BEg1	8.27±	0.03	8.57±	0.26	0.08±	0.00	0.15±	0.01	n.d.		1.67±	0.18	6701
		BEg2	9.41±	0.09	9.28±	0.43	0.08±	0.00	0.13±	0.00	n.d.		2.39		6617
		2Btg1	11.11±	0.03	12.64±	0.07	0.10±	0.00	0.20±	0.01	n.d.		2.54±	0.12	6231
		2Btg2	12.17±	0.17	17.43±	0.13	0.13±	0.01	0.20±	0.02	n.d.		2.72		6232
		2Bgl1	13.46±	0.00	20.71±	0.35	0.15±	0.00	0.26±	0.00	n.d.		2.97±	0.31	6366
		2Bgl2	13.98±	0.03	16.54±	0.45	0.16±	0.00	0.24±	0.01	n.d.		3.32±	1.05	6074
Acrisol	HOr4	Ah	5.37±	0.08	12.00±	0.06	0.09±	0.00	0.19±	0.02	n.d.		3.85		5566
		EA	4.41±	0.11	13.30±	0.02	0.07±	0.00	0.22±	0.01	n.d.		4.50		5971
		BE	6.04±	0.54	17.15±	0.34	0.07±	0.00	0.26±	0.03	n.d.		5.83		5763
		Bt1	15.02±	0.07	9.99±	1.47	0.12±	0.00	0.32±	0.00	n.d.		6.74		5644
		Bt2	9.31±	0.03	19.24±	0.16	0.15±	0.00	0.35±	0.01	n.d.		6.05		5446
		Btgc1 (t.)	11.04±	0.11	19.65±	0.20	0.16±	0.00	0.42±	0.02	n.d.		14.16		5097
		Btgc1 (b.)	11.66±	0.01	23.97±	0.39	0.17±	0.00	0.47±	0.00	n.d.		10.04		5310
		Btgc2	10.89±	0.01	22.63±	0.75	0.16±	0.00	0.56±	0.01	n.d.		11.60		4771
Acrisol	HF1	Ah	12.04±	0.06	11.44±	0.18	0.68±	0.11	0.13±	0.01	4.62±	0.35	n.d.		7241
		EA	11.00±	0.14	10.98±	0.19	0.76±	0.06	0.14±	0.00	n.d.		2.12±	0.55	7132
		B/E	10.99±	0.07	12.56±	0.18	0.44±	0.05	0.15±	0.00	n.d.		3.16		7518
		Btg1	11.51±	0.17	14.65±	0.57	0.26±	0.03	0.18±	0.00	n.d.		1.77		7821
		Btg2	13.30±	0.51	15.57±	0.83	0.16±	0.00	0.18±	0.01	n.d.		1.93±	0.60	7568
		Btg 3 (t.)	10.91±	0.00	15.65±	0.02	0.30±	0.03	0.18±	0.00	n.d.		2.53±	0.86	7462
		Btg3 (b.)	13.86±	0.03	20.15±	0.33	0.51±	0.02	0.23±	0.00	n.d.		2.77±	0.46	7401

Table B2 continued

RSG	Plot	Horizon	Si _M [$\mu\text{g g}^{-1}$]		Si _{Ad} [$\mu\text{g g}^{-1}$]		Si _{Org} [mg g^{-1}]		Si _{Occ} [mg g^{-1}]		Si _{Ba} [mg g^{-1}]		Si _{Pa} [mg g^{-1}]		Si _{total} [mg g^{-1}]
			\bar{X}	σ	\bar{X}	σ	\bar{X}	σ	\bar{X}	σ	\bar{X}	σ	\bar{X}	σ	\bar{X}
Acrisol	HF3	Ah	6.56±	0.11	6.76±	0.22	0.72±	0.10	0.08±	0.00	3.84±	0.48	n.d.		8230
		EA	6.36±	0.16	6.05±	0.12	0.17±	0.01	0.09±	0.00	n.d.		5.59		8673
		E (t.)	8.10±	0.08	8.59±	0.17	0.09±	0.01	0.11±	0.00	n.d.		3.31±	0.63	8243
		E (b.)	8.61±	0.12	9.99±	0.28	0.10±	0.00	0.12±	0.00	n.d.		3.76		8195
		Btg1 (t.)	7.73±	0.07	9.63±	0.03	0.09±	0.00	0.12±	0.00	n.d.		3.32±	0.80	8275
		Btg1 (m.)	8.36±	0.08	11.23±	0.12	0.10±	0.01	0.14±	0.00	n.d.		3.83±	0.36	8161
		Btg1 (b.)	8.85±	0.03	12.89±	0.08	0.12±	0.00	0.16±	0.00	n.d.		4.13±	1.13	7921
		Btg2	10.69±	0.16	16.46±	0.15	0.13±	0.00	0.18±	0.00	n.d.		4.32		8187
		Acrisol	HF4	Ah	9.02±	0.19	8.50±	0.78	0.62±	0.04	0.12±	0.02	4.52		n.d.
EA	10.14±			0.41	9.28±	1.01	0.25±	0.01	0.14±	0.02	n.d.		3.95±	0.14	7868
E (t.)	10.09±			0.47	10.85±	0.86	0.09±	0.00	0.17±	0.02	n.d.		5.31±	0.28	8534
E (b.)	10.98±			0.30	13.00±	1.09	0.08±	0.00	0.18±	0.02	n.d.		5.75±	0.85	8021
Bt1	11.64±			0.30	14.00±	1.10	0.10±	0.00	0.20±	0.02	n.d.		7.52±	0.46	7856
Bt2 (t.)	13.15±			0.34	16.22±	1.07	0.11±	0.00	0.21±	0.02	n.d.		6.75±	0.13	7401
Bt2 (b.)	13.72±			0.51	17.36±	0.97	0.12±	0.00	0.21±	0.02	n.d.		5.94±	1.33	7281
Btg1	15.44±			0.26	20.08±	1.00	0.13±	0.00	0.22±	0.02	n.d.		5.77±	0.21	7424
Btg2	16.44±			0.20	22.11±	0.98	0.14±	0.00	0.22±	0.02	n.d.		11.59±	0.89	7266
Stagnosol	HFr1	Ah	5.73±	0.22	5.93±	0.03	0.59±	0.06	0.06±	0.00	3.25±	0.46	0.76±	0.22	9386
		E (t.)	4.36±	0.16	3.80±	0.11	0.18±	0.03	0.06±	0.00	n.d.		2.29±	0.24	9561
		E (b.)	4.81±	0.18	4.73±	0.26	0.07±	0.00	0.06±	0.01	n.d.		3.81±	0.89	9894
		Eg	5.50±	0.04	7.44±	1.08	0.07±	0.00	0.07±	0.01	n.d.		2.46±	0.35	9434
		Bg1 (t.)	5.74±	0.09	8.53±	1.04	0.09±	0.00	0.08±	0.01	n.d.		2.49±	0.65	9335
		Bg1 (b.)	6.10±	0.12	9.12±	0.78	0.10±	0.00	0.08±	0.01	n.d.		3.30±	1.02	9427
		Bg2	7.38±	0.16	9.70±	1.03	0.11±	0.00	0.09±	0.01	n.d.		3.73		9150

Table B2 continued

RSG	Plot	Horizon	Si _M [$\mu\text{g g}^{-1}$]		Si _{Ad} [$\mu\text{g g}^{-1}$]		Si _{Org} [mg g^{-1}]		Si _{Occ} [mg g^{-1}]		Si _{Ba} [mg g^{-1}]		Si _{Pa} [mg g^{-1}]		Si _{total} [mg g^{-1}]
			\bar{X}	σ	\bar{X}	σ	\bar{X}	σ	\bar{X}	σ	\bar{X}	σ	\bar{X}	σ	\bar{X}
Acrisol	HFr3	Ah	10.07±	0.41	10.53±	0.89	0.38±	0.24	0.14±	0.00	4.17±	1.45	n.d.		7939
		E/A	10.20±	0.23	10.14±	0.52	0.28±	0.01	0.17±	0.01	n.d.		6.57		8291
		E	10.76±	0.19	11.71±	0.01	0.27±	0.01	0.20±	0.01	n.d.		3.00±	0.37	4624
		Bt	13.27±	0.18	15.93±	0.27	0.17±	0.00	0.23±	0.01	n.d.		3.67±	1.38	8372
		Btg1 (t.)	15.25±	0.01	19.64±	0.36	0.16±	0.01	0.26±	0.02	n.d.		3.58		7859
		Btg1 (b.)	18.12±	0.18	24.49±	0.48	0.17±	0.01	0.30±	0.00	n.d.		7.34		3996
		Btg2 (t.)	19.71±	0.52	27.50±	0.29	0.19±	0.02	0.34±	0.00	n.d.		9.69±	3.79	7092
		Btg2 (b.)	21.24±	0.66	29.16±	0.58	0.21±	0.03	0.37±	0.00	1.17		8.68		6877
		Btlg	20.86±	0.65	28.80±	0.16	0.22±	0.03	0.33±	0.00	n.d.		13.20		6994
Stagnosol	HFr4	Ah	7.62±	0.01	6.32±	0.13	0.92±	0.17	0.07±	0.00	3.85		0.25		8442
		Eg	6.23±	0.12	7.10±	0.17	0.33±	0.00	0.09±	0.00	n.d.		1.22		8627
		Bg	9.13±	0.23	11.52±	0.24	0.18±	0.01	0.14±	0.00	n.d.		2.62		8097
		Btlg (t.)	11.33±	0.01	14.65±	0.05	0.20±	0.01	0.19±	0.00	n.d.		2.22		8432
		Btlg (b.)	12.81±	0.22	16.25±	0.31	0.18±	0.00	0.24±	0.02	1.17		2.54		7800
		Blg (t.)	10.92±	0.13	14.90±	0.01	0.20±	0.03	0.19±	0.02	1.78		4.34		9069
		Blg (b.)	10.04±	0.30	15.15±	0.84	0.20±	0.00	0.15±	0.01	2.38		1.81		7292

Appendices

Table B3 Contents of Si fractions in soils under oil-palm plantations and rainforest (per dm⁻³ of soil)

RSG	Plot	Soil horizon	Si _M (mg dm ⁻³)	Si _{Ad} (mg dm ⁻³)	Si _{Org} (mg dm ⁻³)	Si _{Occ} (mg dm ⁻³)	Si _{Ba} (mg dm ⁻³)	Si _{Pa} (mg dm ⁻³)
Acrisol	HO1	Ah	0.0015	0.0011	13.96	29.57	186.14	8.93
	HO1	A/E	0.0016	0.0011	10.70	35.67	337.11	61.44
	HO1	E	0.0016	0.0013	8.92	44.61	0.00	228.89
	HO1	Bt	0.0006	0.0014	9.73	28.51	0.00	160.11
	HO1	Btg1	0.0010	0.0021	13.20	39.85	0.00	232.80
	HO1	Btg2	0.0012	0.0026	16.42	50.19	0.00	397.20
	HO1	Btg3	0.0012	0.0029	17.60	53.08	0.00	278.94
	HO1	Btgc	0.0013	0.0031	18.55	94.40	0.00	1135.05
Acrisol	HO2	Ah	0.0012	0.0009	72.55	13.04	327.28	0.00
	HO2	A/E	0.0014	0.0011	27.44	16.17	481.32	0.00
	HO2	Bt1	0.0013	0.0013	17.28	16.54	0.00	305.13
	HO2	Bt2	0.0015	0.0016	12.87	18.98	0.00	267.20
	HO2	Btg1	0.0014	0.0016	13.57	20.46	0.00	154.05
	HO2	Btg2	0.0017	0.0020	14.43	23.19	0.00	353.55
	HO2	Bg (t.)	0.0021	0.0027	16.51	25.10	0.00	687.24
	HO2	Bg (b.)	0.0019	0.0026	20.19	28.76	0.00	837.91
Acrisol	HO3	Ah	0.0009	0.0013	12.94	26.97	0.00	400.74
	HO3	A/E	0.0004	0.0005	5.27	20.51	0.00	643.19
	HO3	E	0.0005	0.0008	5.18	24.36	0.00	560.75
	HO3	2Bt1 (t.)	0.0005	0.0009	6.43	28.45	0.00	731.66
	HO3	2Bt1 (b.)	0.0005	0.0015	7.91	30.21	0.00	1055.74
	HO3	2Bt2 (t.)	0.0005	0.0006	9.01	32.47	0.00	973.80
	HO3	2Bt2 (b.)	0.0005	0.0010	9.28	33.95	0.00	467.10
Acrisol	HO4	Ah	0.0006	0.0008	6.49	15.47	0.00	498.89
	HO4	A/E	0.0006	0.0008	4.51	21.80	0.00	538.17
	HO4	E/A	0.0006	0.0007	4.51	15.84	0.00	374.20
	HO4	2AEb	0.0007	0.0011	6.25	20.14	0.00	417.17
	HO4	2EB	0.0007	0.0010	7.08	29.25	0.00	545.17
	HO4	2BE	0.0009	0.0010	8.94	34.43	0.00	1156.34
	HO4	2Bt	0.0011	0.0010	10.13	35.58	0.00	873.19
	HO4	2Btg	0.0012	0.0019	12.07	84.42	0.00	983.80
Stagnosol	HOr1	Ah	0.0021	0.0018	23.28	35.57	877.07	333.41
	HOr1	Eg	0.0018	0.0015	13.54	42.53	0.00	1062.41
	HOr1	Bg	0.0024	0.0023	40.55	21.43	0.00	871.26
	HOr1	2Btg1 (t.)	0.0021	0.0026	18.72	25.33	0.00	562.00
	HOr1	2Btg1 (b.)	0.0024	0.0031	21.26	29.39	0.00	1403.78
	HOr1	2Btg2 (t.)	0.0025	0.0034	24.23	27.75	0.00	1352.60
	HOr1	2Btg2 (b.)	0.0032	0.0036	23.71	27.39	0.00	879.54
	HOr1	2Btlg (t.)	0.0033	0.0038	24.71	31.78	0.00	645.83
	HOr1	2Btlg (b.)	0.0029	0.0030	23.50	31.02	0.00	418.68

Appendices

Table B3 continued

RSG	Plot	Soil horizon	Si _M (mg dm ⁻³)	Si _{Ad} (mg dm ⁻³)	Si _{Org} (mg dm ⁻³)	Si _{Occ} (mg dm ⁻³)	Si _{Ba} (mg dm ⁻³)	Si _{Pa} (mg dm ⁻³)
Stagnosol	HOr2	Ah	0.0019	0.0021	34.40	22.17	1250.61	0.00
		Eg	0.0014	0.0018	14.60	20.04	0.00	629.23
		BEg (t.)	0.0014	0.0018	16.65	23.63	0.00	789.97
		BEg (b.)	0.0018	0.0019	17.81	23.62	0.00	527.43
		Btg (t.)	0.0018	0.0018	22.75	17.13	0.00	404.02
		Btg (b.)	0.0015	0.0015	21.74	16.08	0.00	251.86
		Btg1 (t.)	0.0017	0.0016	21.45	29.62	0.00	0.00
		Btg1 (b.)	0.0021	0.0023	27.42	71.90	0.00	128.73
Stagnosol	HOr3	Ah	0.0009	0.0005	14.96	11.76	247.26	334.14
		AE	0.0010	0.0008	11.54	19.12	0.00	298.74
		BEg1	0.0011	0.0012	11.31	20.86	0.00	227.47
		BEg2	0.0013	0.0013	11.95	18.39	0.00	342.16
		2Btg1	0.0015	0.0017	14.41	28.01	0.00	351.12
		2Btg2	0.0018	0.0026	19.04	29.06	0.00	399.62
		2Bgl1	0.0020	0.0031	23.24	38.46	0.00	444.82
		2Bgl2	0.0020	0.0024	22.92	34.36	0.00	477.40
Acrisol	HOr4	Ah	0.0007	0.0015	10.52	23.86	0.00	473.47
		EA	0.0006	0.0017	8.59	28.46	0.00	571.07
		BE	0.0007	0.0021	9.10	31.95	0.00	711.15
		Bt1	0.0019	0.0013	15.15	40.25	0.00	855.91
		Bt2	0.0012	0.0024	19.17	44.82	0.00	767.88
		Btgc1 (t.)	0.0013	0.0024	19.31	51.23	0.00	1713.69
		Btgc1 (b.)	0.0014	0.0029	19.99	56.80	0.00	1214.72
		Btgc2	0.0013	0.0027	19.30	67.05	0.00	1391.59
Acrisol	HF1	Ah	0.0010	0.0009	53.83	9.93	364.89	0.00
		EA	0.0012	0.0012	84.63	15.63	0.00	234.88
		B/E	0.0014	0.0016	57.28	19.80	0.00	408.03
		Btg1	0.0016	0.0021	36.22	25.41	0.00	248.22
		Btg2	0.0019	0.0022	23.31	25.38	0.00	277.99
		Btg3 (t.)	0.0015	0.0022	41.09	24.68	0.00	351.41
		Btg3 (b.)	0.0015	0.0022	55.70	24.88	0.00	301.55
Acrisol	HF3	Ah	0.0006	0.0006	68.38	7.82	364.93	0.00
		EA	0.0008	0.0007	20.73	11.10	0.00	682.30
		E (t.)	0.0012	0.0013	13.70	16.56	0.00	493.08
		E (b.)	0.0013	0.0015	14.27	17.30	0.00	560.01
		Btg1 (t.)	0.0012	0.0015	14.79	18.61	0.00	517.72
		Btg1 (m.)	0.0013	0.0018	16.16	22.32	0.00	596.98
		Btg1 (b.)	0.0014	0.0020	18.67	24.86	0.00	643.97
		Btg2	0.0016	0.0025	19.64	27.78	0.00	661.20

Appendices

Table B3 continued

RSG	Plot	Soil horizon	Si _M (mg dm ⁻³)	Si _{Ad} (mg dm ⁻³)	Si _{Org} (mg dm ⁻³)	Si _{Occ} (mg dm ⁻³)	Si _{Ba} (mg dm ⁻³)	Si _{Pa} (mg dm ⁻³)
Acrisol	HF4	Ah	0.0006	0.0006	44.68	8.64	325.44	0.00
	HF4	EA	0.0012	0.0011	28.00	16.45	0.00	450.35
	HF4	E (t.)	0.0013	0.0014	11.52	21.78	0.00	669.20
	HF4	E (b.)	0.0014	0.0016	10.23	22.68	0.00	724.43
	HF4	Bt1	0.0016	0.0020	13.72	27.35	0.00	1053.26
	HF4	Bt2 (t.)	0.0018	0.0023	15.99	29.54	0.00	944.92
	HF4	Bt2 (b.)	0.0019	0.0024	16.47	29.40	0.00	831.13
	HF4	Btg1	0.0022	0.0029	18.55	30.74	0.00	819.35
	HF4	Btg2	0.0023	0.0031	19.33	30.30	0.00	1622.40
Stagnosol	HFr1	Ah	0.0005	0.0005	51.90	5.42	286.32	66.98
	HFr1	E (t.)	0.0005	0.0004	19.56	6.14	0.00	249.57
	HFr1	E (b.)	0.0005	0.0005	7.64	6.74	0.00	415.81
	HFr1	Eg	0.0008	0.0011	10.61	10.79	0.00	362.06
	HFr1	Bgl1 (t.)	0.0009	0.0013	13.82	12.77	0.00	378.89
	HFr1	Bgl1 (b.)	0.0009	0.0014	15.57	12.01	0.00	501.20
	HFr1	Bgl2	0.0011	0.0015	17.27	13.16	0.00	570.38
Acrisol	HFr3	Ah	0.0007	0.0007	25.19	9.22	279.27	0.00
	HFr3	E/A	0.0012	0.0012	32.36	19.88	0.00	762.58
	HFr3	E	0.0014	0.0015	33.68	24.77	0.00	380.82
	HFr3	Bt	0.0017	0.0020	21.70	28.80	0.00	466.23
	HFr3	Btg1 (t.)	0.0020	0.0026	21.88	34.74	0.00	475.95
	HFr3	Btg1 (b.)	0.0024	0.0033	23.16	39.59	0.00	975.99
	HFr3	Btg2 (t.)	0.0024	0.0034	23.31	41.59	0.00	1201.15
	HFr3	Btg2 (b.)	0.0026	0.0036	26.16	45.47	145.08	1076.32
	HFr3	Btg3	0.0025	0.0035	27.28	40.05	0.00	1610.40
Stagnosol	HFr4	Ah	0.0007	0.0006	82.88	6.67	346.16	22.82
	HFr4	Eg	0.0008	0.0009	43.63	12.41	0.00	162.10
	HFr4	Bg	0.0013	0.0016	25.66	20.48	0.00	372.20
	HFr4	Btlg (t.)	0.0016	0.0021	29.24	26.48	0.00	316.86
	HFr4	Btlg (b.)	0.0018	0.0023	25.60	33.91	167.31	363.22
	HFr4	Blg (t.)	0.0016	0.0022	29.32	27.87	263.44	642.32
	HFr4	Blg (b.)	0.0015	0.0022	30.30	22.44	352.24	267.88



Figure A1: Si fractions in mg dm⁻³ per soil horizon in Acrisols (HO1-4) and Stagnosols (HOr1-4) under oil-palm cultivation.



Figure A2: Si fractions in mg dm^{-3} per soil horizon in Acrisols (HO1-4) and Stagnosols (HOr1-4) under natural rainforest.

Appendix II – fieldwork 2018

Table A1 Representative elevation transects of topsoil sampling under oil-palm plantations

Plot	GPS position 1		GPS position 2		Elevation [m]
HO1	01°54.583' S	103°15.996' E	01°54.587' S	103°16.015' E	85
HO2	01°53.012' S	103°16.017' E	01°52.987' S	103°16.018' E	76
HO3	01°51.442' S	103°18.490' E	01°51.445' S	103°18.522' E	25
HO4	01°47.188' S	103°16.246' E	01°47.195' S	103°16.229' E	60
HOr1	01°54.107' S	103°22.887' E	01°54.124' S	103°22.993' E	28
HOr3	01°51.662' S	103°18.357' E	01°51.656' S	103°18.383' E	48
HOr4	01°42.687' S	103°17.544' E	01°42.666' S	103°17.536' E	33

Table A2 Topsoil sampling. fieldwork 2018



HO1 – oil-palm row

HO1 – oil-palm row (detailed view)

Table A3 Sediment traps in interrows of well-drained oil-palm plantations.



HO1 – September 2018



HO1 – February 2019



HO1 – May 2019



HO3 – September 2018



HO3 – January 2019



HO3 – April 2019

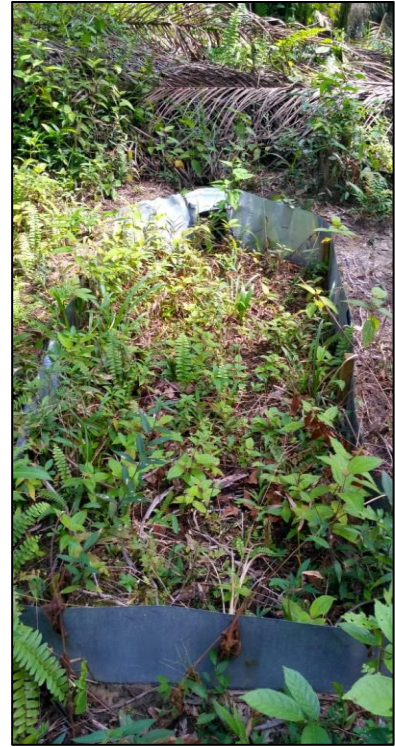
Appendices



HO4 – September 2018



HO4 – January 2019



HO4 – May 2019



Well-drained – Interrow



Riparian – Interrow

Appendix II - laboratory

Table B1 Mean topsoil Si concentrations in different management zones of oil-palm plantations

Management zone	Plot	Water regime	Si _{Am} [mg g ⁻¹ soil]		Si _M [μg g ⁻¹ soil]	
			\bar{X}	σ	\bar{X}	σ
Palm circle	HO1	Well-drained	1.93 ± 0.25		12.23 ± 4.83	
Palm circle	HO2	Well-drained	1.92 ± 0.70		7.61 ± 4.13	
Palm circle	HO3	Well-drained	1.78 ± 1.08		18.38 ± 5.47	
Palm circle	HO4	Well-drained	1.20 ± 0.43		6.45 ± 3.10	
Oil-palm row	HO1	Well-drained	2.27 ± 0.93		10.65 ± 1.96	
Oil-palm row	HO2	Well-drained	2.28 ± 0.31		5.17 ± 1.15	
Oil-palm row	HO3	Well-drained	1.23 ± 0.54		4.77 ± 0.49	
Oil-palm row	HO4	Well-drained	1.68 ± 0.35		4.94 ± 0.83	
Interrow	HO1	Well-drained	n.d.		n.d.	
Interrow	HO2	Well-drained	2.34 ± 0.81		5.52 ± 1.16	
Interrow	HO3	Well-drained	1.63 ± 0.21		5.72 ± 1.56	
Interrow	HO4	Well-drained	1.69 ± 0.30		5.64 ± 2.39	
FronD pile	HO1	Well-drained	4.42 ± 1.47		22.47 ± 10.7	
FronD pile	HO2	Well-drained	5.86 ± 2.25		10.81 ± 2.37	
FronD pile	HO3	Well-drained	3.35 ± 0.92		14.26 ± 4.03	
FronD pile	HO4	Well-drained	2.24 ± 0.50		7.18 ± 1.50	
Palm circle	HO _r 1	Riparian	0.94 ± 1.02		8.46 ± 2.54	
Palm circle	HO _r 2	Riparian	2.21 ± 0.62		12.44 ± 1.55	
Palm circle	HO _r 3	Riparian	1.46 ± 0.46		7.49 ± 2.34	
Palm circle	HO _r 4	Riparian	1.16 ± 0.33		13.82 ± 1.56	
Oil-palm row	HO _r 1	Riparian	2.27 ± 1.62		8.23 ± 4.78	
Oil-palm row	HO _r 2	Riparian	2.02 ± 0.54		20.74 ± 3.48	
Oil-palm row	HO _r 3	Riparian	1.88 ± 0.20		7.50 ± 0.97	
Oil-palm row	HO _r 4	Riparian	2.17 ± 0.42		11.30 ± 0.42	
Interrow	HO _r 1	Riparian	2.29 ± 0.64		9.07 ± 2.67	
Interrow	HO _r 2	Riparian	2.86 ± 0.69		16.26 ± 2.50	
Interrow	HO _r 3	Riparian	2.76 ± 0.46		7.92 ± 1.03	
Interrow	HO _r 4	Riparian	2.93 ± 0.76		12.26 ± 2.49	
FronD pile	HO _r 1	Riparian	2.51 ± 0.81		13.53 ± 4.70	
FronD pile	HO _r 2	Riparian	2.46 ± 1.51		26.83 ± 2.71	
FronD pile	HO _r 3	Riparian	3.95 ± 1.24		15.57 ± 4.63	
FronD pile	HO _r 4	Riparian	2.93 ± 0.77		22.30 ± 11.1	

Appendices

Table B2 (a) Topsoil Si concentrations in different management zones of well-drained oil-palm plantations.

Management zone	Plot	Si _{Am} [mg g ⁻¹ soil]			Si _M [μg g ⁻¹ soil]		
		x	\bar{X} (plot)	σ (plot)	x	\bar{X} (plot)	σ (plot)
Palm circle 1	HO1	1.77	1.93 ± 0.25		12.04	12.23 ± 4.83	
Palm circle 2	HO1	2.33					
Palm circle 3	HO1	1.98					
Palm circle 4	HO1	1.68					
Palm circle 5	HO1	1.89					
Palm circle 1	HO2	2.53	1.92 ± 0.70		5.36	7.61 ± 4.13	
Palm circle 2	HO2	2.70					
Palm circle 3	HO2	1.87					
Palm circle 4	HO2	1.43					
Palm circle 5	HO2	1.06					
Palm circle 1	HO3	0.85	1.78 ± 1.08		14.52	18.38 ± 5.47	
Palm circle 2	HO3	0.86					
Palm circle 3	HO3	1.66					
Palm circle 4	HO3	3.46					
Palm circle 5	HO3	2.09					
Palm circle 1	HO4	0.68	1.20 ± 0.43		5.24	6.45 ± 3.10	
Palm circle 2	HO4	1.77					
Palm circle 3	HO4	1.27					
Palm circle 4	HO4	0.88					
Palm circle 5	HO4	1.40					
Oil-palm row 1	HO1	2.85	2.27 ± 0.93		8.01	10.65 ± 1.96	
Oil-palm row 2	HO1	0.99					
Oil-palm row 3	HO1	2.86					
Oil-palm row 4	HO1	1.59					
Oil-palm row 5	HO1	3.09					
Oil-palm row 1	HO2	2.14	2.28 ± 0.31		6.27	5.17 ± 1.15	
Oil-palm row 2	HO2	2.78					
Oil-palm row 3	HO2	2.26					
Oil-palm row 4	HO2	1.95					
Oil-palm row 5	HO2	2.29					
Oil-palm row 1	HO3	0.35	1.23 ± 0.54		4.75	4.77 ± 0.49	
Oil-palm row 2	HO3	1.43					
Oil-palm row 3	HO3	1.57					
Oil-palm row 4	HO3	1.11					
Oil-palm row 5	HO3	1.71					
Oil-palm row 1	HO4	1.57	1.68 ± 0.35		6.15	4.94 ± 0.83	
Oil-palm row 2	HO4	1.29					
Oil-palm row 3	HO4	2.19					
Oil-palm row 4	HO4	1.88					
Oil-palm row 5	HO4	1.50					
Interrow 1	HO2	3.72	2.34 ± 0.81		7.42	5.52 ± 1.16	
Interrow 2	HO2	1.63					
Interrow 3	HO2	1.99					
Interrow 4	HO2	2.30					
Interrow 5	HO2	2.04					
Interrow 1	HO3	1.78	1.63 ± 0.21		4.50	5.72 ± 1.56	
Interrow 2	HO3	1.40					
Interrow 3	HO3	1.91					
Interrow 4	HO3	1.53					
Interrow 5	HO3	1.52					
Interrow 1	HO4	1.57	1.69 ± 0.30		9.63	5.64 ± 2.39	
Interrow 2	HO4	2.21					
Interrow 3	HO4	1.64					
Interrow 4	HO4	1.57					
Interrow 5	HO4	1.45					
Fronde pile 1	HO1	6.57	4.42 ± 1.47		17.35	22.47 ± 10.66	
Fronde pile 2	HO1	3.50					
Fronde pile 3	HO1	4.62					
Fronde pile 4	HO1	4.70					
Fronde pile 5	HO1	2.69					
Fronde pile 1	HO2	7.06	5.86 ± 2.25		10.06	10.81 ± 2.37	
Fronde pile 2	HO2	9.05					
Fronde pile 3	HO2	3.51					
Fronde pile 4	HO2	5.53					
Fronde pile 5	HO2	4.14					
Fronde pile 1	HO3	3.26	3.35 ± 0.92		10.39	14.26 ± 4.03	
Fronde pile 2	HO3	4.05					
Fronde pile 3	HO3	1.84					
Fronde pile 4	HO3	3.47					
Fronde pile 5	HO3	4.10					
Fronde pile 1	HO4	1.89	2.24 ± 0.50		7.05	7.18 ± 1.50	
Fronde pile 2	HO4	2.19					
Fronde pile 3	HO4	3.04					
Fronde pile 4	HO4	1.77					
Fronde pile 5	HO4	2.33					

Appendices

Table B2 (b) Topsoil Si concentrations in different management zones of riparian oil-palm plantations

Management zone	Plot	Si _{Am} [mg g ⁻¹ soil]			Si _M [μg g ⁻¹ soil]		
		x	\bar{X} (plot)	σ (plot)	x	\bar{X} (plot)	σ (plot)
Palm circle 1	HOr1	0.22	0.94 ± 1.02		5.73	8.46 ± 2.54	
Palm circle 2	HOr1	0.09			9.66		
Palm circle 3	HOr1	2.61			12.16		
Palm circle 4	HOr1	0.66			8.05		
Palm circle 5	HOr1	1.11			6.72		
Palm circle 1	HOr2	1.76	2.21 ± 0.62		13.62	12.44 ± 1.55	
Palm circle 2	HOr2	2.70			9.76		
Palm circle 3	HOr2	1.47			12.63		
Palm circle 4	HOr2	2.95			12.75		
Palm circle 5	HOr2	2.17			13.42		
Palm circle 1	HOr3	0.68	1.46 ± 0.46		6.48	7.49 ± 2.34	
Palm circle 2	HOr3	1.65			10.78		
Palm circle 3	HOr3	1.48			8.70		
Palm circle 4	HOr3	1.58			6.83		
Palm circle 5	HOr3	1.91			4.64		
Palm circle 1	HOr4	1.28	1.16 ± 0.33		16.24	13.82 ± 1.56	
Palm circle 2	HOr4	0.66			13.95		
Palm circle 3	HOr4	1.10			13.33		
Palm circle 4	HOr4	1.56			11.92		
Palm circle 5	HOr4	1.20			13.67		
Oil-palm row 1	HOr1	0.60	2.27 ± 1.62		2.13	8.23 ± 4.78	
Oil-palm row 2	HOr1	1.87			6.57		
Oil-palm row 3	HOr1	2.40			12.14		
Oil-palm row 4	HOr1	4.91			13.94		
Oil-palm row 5	HOr1	1.59			6.39		
Oil-palm row 1	HOr2	2.03	2.02 ± 0.54		19.30	20.74 ± 3.48	
Oil-palm row 2	HOr2	1.22			18.74		
Oil-palm row 3	HOr2	1.84			26.89		
Oil-palm row 4	HOr2	2.38			18.73		
Oil-palm row 5	HOr2	2.62			20.03		
Oil-palm row 1	HOr3	2.07	1.88 ± 0.20		8.72	7.50 ± 0.97	
Oil-palm row 2	HOr3	1.95			7.21		
Oil-palm row 3	HOr3	1.86			8.28		
Oil-palm row 4	HOr3	1.97			6.49		
Oil-palm row 5	HOr3	1.54			6.77		
Oil-palm row 1	HOr4	1.47	2.17 ± 0.42		10.90	11.30 ± 0.42	
Oil-palm row 2	HOr4	2.21			11.02		
Oil-palm row 3	HOr4	2.26			11.30		
Oil-palm row 4	HOr4	2.27			11.31		
Oil-palm row 5	HOr4	2.62			11.98		
Interrow 1	HOr1	1.58	2.29 ± 0.64		13.47	9.07 ± 2.67	
Interrow 2	HOr1	2.05			6.98		
Interrow 3	HOr1	3.07			6.99		
Interrow 4	HOr1	2.84			9.43		
Interrow 5	HOr1	1.91			8.46		
Interrow 1	HOr2	3.36	2.86 ± 0.69		19.01	16.26 ± 2.50	
Interrow 2	HOr2	3.72			16.00		
Interrow 3	HOr2	2.77			17.91		
Interrow 4	HOr2	2.39			15.96		
Interrow 5	HOr2	2.05			12.44		
Interrow 1	HOr3	2.20	2.76 ± 0.46		8.08	7.92 ± 1.03	
Interrow 2	HOr3	2.52			6.54		
Interrow 3	HOr3	2.66			9.41		
Interrow 4	HOr3	3.43			8.02		
Interrow 5	HOr3	2.96			7.59		
Interrow 1	HOr4	3.19	2.93 ± 0.76		10.46	12.26 ± 2.49	
Interrow 2	HOr4	1.78			10.67		
Interrow 3	HOr4	3.83			12.26		
Interrow 4	HOr4	2.68			16.53		
Interrow 5	HOr4	3.13			11.37		
Fronde pile 1	HOr1	1.46	2.51 ± 0.81		21.41	13.53 ± 4.70	
Fronde pile 2	HOr1	2.14			13.01		
Fronde pile 3	HOr1	2.35			8.80		
Fronde pile 4	HOr1	3.49			12.27		
Fronde pile 5	HOr1	3.12			12.16		
Fronde pile 1	HOr2	4.51	2.46 ± 1.51		25.28	26.83 ± 2.71	
Fronde pile 2	HOr2	1.54			30.01		
Fronde pile 3	HOr2	1.43			26.97		
Fronde pile 4	HOr2	1.18			28.73		
Fronde pile 5	HOr2	3.63			23.19		
Fronde pile 1	HOr3	3.40	3.95 ± 1.24		13.24	15.57 ± 4.63	
Fronde pile 2	HOr3	3.65			14.54		
Fronde pile 3	HOr3	5.43			19.07		
Fronde pile 4	HOr3	4.94			21.28		
Fronde pile 5	HOr3	2.34			9.69		
Fronde pile 1	HOr4	2.50	2.93 ± 0.77		16.99	22.30 ± 11.06	
Fronde pile 2	HOr4	2.57			20.67		
Fronde pile 3	HOr4	2.42			14.57		
Fronde pile 4	HOr4	2.88			17.56		
Fronde pile 5	HOr4	4.28			41.70		

Table B3 Weekly loss of eroded soil material and Si_{Am} in eroded soil material from sediments traps under oil-palm plantations (sloping terrain)

Date	Month	Trap	Plot	Si _{Am} [mg g ⁻¹ soil]		Eroded soil material	Si _{Am} in eroded soil material	Eroded soil material	Si _{Am} in eroded soil material
				\bar{x}	σ	[g per 2m ² trap]	[mg per 2m ² trap]	[g m ²]	[mg m ²]
2018-10-02	October	HO1_2	HO1	0.21 ± 0.03	5.59	1.18	2.80	0.6	
2018-12-19	December	HO1_2	HO1	0.79 ± 0.07	11.67	9.23	5.84	4.6	
2019-02-04	February	HO1_1	HO1	1.48 ± 0.18	30.83	45.56	15.42	22.8	
2019-02-04	February	HO1_2	HO1	1.59 ± 0.07	41.10	65.29	20.55	32.6	
2019-02-12	February	HO1_1	HO1	1.61 ± 0.26	42.08	67.90	21.04	34.0	
2019-02-12	February	HO1_2	HO1	2.66 ± 0.29	39.92	106.11	19.96	53.1	
2019-02-21	February	HO1_1	HO1	1.28 ± 0.05	25.26	32.42	12.63	16.2	
2019-03-29	March	HO1_1	HO1	1.99 ± 0.04	37.83	75.23	18.92	37.6	
2019-03-29	March	HO1_2	HO1	3.26 ± 0.04	31.40	102.33	15.70	51.2	
2019-04-02	April	HO1_1	HO1	1.92 ± 0.11	200.29	383.69	100.15	191.8	
2019-04-02	April	HO1_2	HO1	1.53 ± 0.28	67.23	103.14	33.62	51.6	
2019-04-09	April	HO1_1	HO1	1.35 ± 0.02	161.75	218.07	80.88	109.0	
2019-04-09	April	HO1_2	HO1	2.10 ± 0.49	121.74	255.20	60.87	127.6	
2019-04-19	April	HO1_1	HO1	1.80 ± 0.23	186.72	336.06	93.36	168.0	
2019-04-19	April	HO1_2	HO1	1.01 ± 0.04	134.16	135.93	67.08	68.0	
2019-04-30	April	HO1_1	HO1	1.87 ± 0.24	133.01	248.75	66.51	124.4	
2019-04-30	April	HO1_2	HO1	1.53 ± 0.19	172.16	263.54	86.08	131.8	
2019-05-08	May	HO1_1	HO1	0.90 ± 0.12	171.75	155.15	85.88	77.6	
2019-05-08	May	HO1_2	HO1	1.59 ± 0.28	93.65	148.78	46.83	74.4	
2019-05-30	May	HO1_1	HO1	2.15 ± 0.08	80.67	173.83	40.34	86.9	
2019-05-30	May	HO1_2	HO1	2.09 ± 0.18	122.74	256.72	61.37	128.4	
2018-09-22	September	HO3_1	HO3	1.45 ± 0.24	124.31	179.64	62.16	89.8	
2018-09-22	September	HO3_2	HO3	1.44 ± 0.25	42.84	61.76	21.42	30.9	

Table B3 continued

2018-10-18	October	HO3_1	HO3	1.69 ± 0.22	19.95	33.80	9.98	16.9
2018-10-18	October	HO3_2	HO3	1.97 ± 0.19	6.72	13.25	3.36	6.6
2018-11-05	November	HO3_1	HO3	1.30 ± 0.11	93.32	121.30	46.66	60.6
2018-11-05	November	HO3_2	HO3	1.17 ± 0.25	97.70	113.91	48.85	57.0
2018-11-12	November	HO3_1	HO3	0.24 ± 0.04	8.36	1.99	4.18	1.0
2018-11-12	November	HO3_2	HO3	0.44	20.11	8.78	10.06	4.4
2018-11-20	November	HO3_1	HO3	1.12 ± 0.68	87.21	97.31	43.61	48.7
2018-11-20	November	HO3_2	HO3	0.91 ± 0.19	97.14	88.53	48.57	44.3
2018-11-28	November	HO3_1	HO3	0.92 ± 0.06	59.13	54.43	29.57	27.2
2018-11-28	November	HO3_2	HO3	0.34	27.89	9.47	13.94	4.7
2018-12-11	December	HO3_1	HO3	0.47 ± 0.11	339.32	159.91	169.66	80.0
2018-12-11	December	HO3_2	HO3	0.16	66.67	10.58	33.34	5.3
2018-12-17	December	HO3_1	HO3	1.18 ± 0.12	88.58	104.96	44.29	52.5
2018-12-17	December	HO3_2	HO3	0.97 ± 0.10	111.93	108.53	55.97	54.3
2019-01-03	January	HO3_1	HO3	0.36 ± 0.01	66.16	23.80	33.08	11.9
2019-01-03	January	HO3_2	HO3	0.25	36.69	9.17	18.35	4.6
2019-01-07	January	HO3_1	HO3	0.26 ± 0.07	57.58	15.16	28.79	7.6
2019-01-07	January	HO3_2	HO3	0.25	55.62	13.95	27.81	7.0
2019-01-14	January	HO3_1	HO3	0.89 ± 0.39	66.12	58.54	33.06	29.3
2019-01-14	January	HO3_2	HO3	0.88 ± 0.18	49.11	43.28	24.56	21.6
2019-01-28	January	HO3_1	HO3	1.11 ± 0.49	44.74	49.54	22.37	24.8
2019-02-04	February	HO3_1	HO3	0.88 ± 0.14	487.59	428.93	243.80	214.5
2019-02-04	February	HO3_2	HO3	1.35 ± 0.20	431.29	580.42	215.65	290.2
2019-02-13	February	HO3_1	HO3	0.66 ± 0.06	387.81	256.66	193.91	128.3
2019-02-13	February	HO3_2	HO3	0.34 ± 0.19	40.13	13.58	20.07	6.8
2019-02-21	February	HO3_1	HO3	0.37	65.28	24.24	32.64	12.1
2019-03-14	March	HO3_1	HO3	0.61	18.06	10.96	9.03	5.5
2019-03-28	March	HO3_1	HO3	0.11	75.35	8.12	37.68	4.1
n.d.	March	n.d.	HO3	0.96 ± 0.10	n.d.	n.d.	n.d.	n.d.

Table B3 continued

2019-04-01	April	HO3_1	HO3	1.60 ± 0.11	36.99	59.07	18.50	29.5
2019-04-01	April	HO3_2	HO3	0.89 ± 0.14	53.63	47.92	26.82	24.0
2019-04-08	April	HO3_1	HO3	0.52 ± 0.09	69.87	36.32	34.94	18.2
2019-04-08	April	HO3_2	HO3	0.72 ± 0.14	59.92	42.87	29.96	21.4
2019-04-29	April	HO3_1	HO3	0.59 ± 0.25	43.59	25.66	21.80	12.8
2019-04-29	April	HO3_2	HO3	1.30 ± 0.07	31.80	41.23	15.90	20.6
2019-05-07	May	HO3_1	HO3	0.34 ± 0.13	91.91	31.28	45.96	15.6
2018-09-22	September	HO4_1	HO4	0.93 ± 0.07	47.19	43.91	23.60	22.0
2018-09-22	September	HO4_2	HO4	0.58 ± 0.02	66.24	38.67	33.12	19.3
2018-10-12	October	HO4_1	HO4	0.66 ± 0.07	29.13	19.31	14.57	9.7
2018-10-12	October	HO4_2	HO4	1.25 ± 0.17	29.62	37.12	14.81	18.6
2018-11-05	November	HO4_1	HO4	1.49 ± 0.05	37.52	56.02	18.76	28.0
2018-11-05	November	HO4_2	HO4	1.61 ± 0.57	54.48	87.61	27.24	43.8
2018-11-12	November	HO4_1	HO4	0.54 ± 0.00	97.00	52.53	48.50	26.3
2018-11-12	November	HO4_2	HO4	0.87 ± 0.02	24.67	21.36	12.33	10.7
2018-11-28	November	HO4_1	HO4	2.05 ± 0.10	98.97	203.27	49.48	101.6
2018-11-28	November	HO4_2	HO4	0.89 ± 0.15	9.50	8.41	4.75	4.2
2018-12-11	December	HO4_1	HO4	1.27 ± 0.09	97.17	122.99	48.58	61.5
2018-12-11	December	HO4_2	HO4	0.13 ± 0.07	10.44	1.41	5.22	0.7
2018-12-18	December	HO4_1	HO4	0.03	22.42	0.68	11.21	0.3
2018-12-27	December	HO4_2	n.d.	n.d.	n.d.	n.d.	n.d.	n.d.
2019-01-02	January	HO4_1	HO4	1.29 ± 0.09	58.14	74.73	29.07	37.4
2019-01-02	January	HO4_2	HO4	0.63 ± 0.17	64.15	40.64	32.08	20.3
2019-01-07	January	HO4_1	HO4	2.15 ± 0.03	45.88	98.52	22.94	49.3
2019-01-07	January	HO4_2	HO4	0.56 ± 0.13	19.82	11.10	9.91	5.6
2019-01-28	January	HO4_1	HO4	2.03 ± 0.06	75.12	152.32	37.56	76.2
2019-01-28	January	HO4_2	HO4	0.96 ± 0.21	86.62	83.29	43.31	41.6
2019-02-06	February	HO4_1	HO4	0.16 ± 0.00	89.64	13.98	44.82	7.0
2019-02-06	February	HO4_2	HO4	0.55 ± 0.05	49.72	27.41	24.86	13.7

Table B3 continued

2019-02-13	February	HO4_1	HO4	0.40 ± 0.12	27.49	11.10	13.75	5.6
2019-02-13	February	HO4_2	HO4	0.17 ± 0.07	21.40	3.72	10.70	1.9
2019-02-27	February	HO4_1	HO4	1.95 ± 0.36	62.60	121.84	31.30	60.9
2019-03-14	March	HO4_1	HO4	3.01 ± 0.02	72.83	219.01	36.42	109.5
2019-03-14	March	HO4_2	HO4	0.56 ± 0.11	47.16	26.62	23.58	13.3
2019-03-25	March	HO4_2	HO4	0.86 ± 0.03	43.41	37.48	21.71	18.7
2019-03-25	March	HO4_1	HO4	0.63 ± 0.14	23.71	14.83	11.86	7.4
2019-04-01	April	HO4_1	HO4	0.99 ± 0.02	34.91	34.47	17.46	17.2
2019-04-01	April	HO4_2	HO4	0.47 ± 0.25	31.48	14.95	15.74	7.5
2019-04-08	April	HO4_1	HO4	0.81 ± 0.29	27.29	22.22	13.65	11.1
2019-04-08	April	HO4_2	HO4	0.27 ± 0.02	38.32	10.29	19.16	5.1
2019-04-20	April	HO4_1	HO4	0.66	65.94	43.38	32.97	21.7
2019-04-20	April	HO4_2	HO4	6.84 ± 0.00	46.69	319.18	23.35	159.6
2019-04-29	April	HO4_1	HO4	0.66 ± 0.00	26.37	17.38	13.19	8.7
2019-04-29	April	HO4_2	HO4	0.52 ± 0.10	22.49	11.62	11.25	5.8
2019-05-07	May	HO4_1	HO4	0.48 ± 0.18	20.99	10.17	10.50	5.1
2019-05-07	May	HO4_2	HO4	0.51 ± 0.04	16.60	8.50	8.30	4.3
2019-05-29	May	HO4_1	HO4	0.23 ± 0.01	20.55	4.63	10.28	2.3
2019-05-29	May	HO4_2	HO4	4.36 ± 0.11	28.62	124.87	14.31	62.4

Table B4 Mean Si concentrations and statistical analysis on log transformed data.

Management zone	Water regime		N	Si _M		Shapiro-Wilk	Levene	N	Si _{Am}		Shapiro-Wilk	Levene
				μg g ⁻¹ _{soil}		p-value	p-value		mg g ⁻¹ _{soil}	p-value	p-value	
Palm circle	Well-drained	HO	4	11.17 ± 5.42		0.68		4	1.71 ± 0.35		<i>0.04</i>	
Oil-palm row	Well-drained	HO	4	6.38 ± 2.85		<i>0.01</i>	0.26	4	1.87 ± 0.51		0.28	0.50
Interrow	Well-drained	HO	3	5.62 ± 0.10		0.80		3	1.88 ± 0.39		0.18	
FronD pile	Well-drained	HO	4	13.68 ± 6.54		1.00		4	3.97 ± 1.54		0.96	
Palm circle	Riparian	HOr	4	10.55 ± 3.06		0.43		4	1.44 ± 0.55		0.87	
Oil-palm row	Riparian	HOr	4	11.94 ± 6.09		0.39	0.89	4	2.08 ± 0.17		0.89	0.15
Interrow	Riparian	HOr	4	11.38 ± 3.74		0.76		4	2.71 ± 0.29		0.14	
FronD pile	Riparian	HOr	4	19.56 ± 6.13		0.65		4	2.96 ± 0.69		0.26	

Mean ± standard deviation. Statistics were conducted by one-way ANOVA and Tukey–Kramer post hoc test. Normally distributed data, whereby the homogeneity of variances was asserted. * Italics suggest that the homogeneity of variances was not asserted.

Table B5 Corresponding ANOVA analysis showing significant differences

ANOVA	Si _M		Si _{Am}	
	p-value HO	p-value HOr	p-value HO	p-value HOr
frond - oil-palm row	0.102	0.189	0.026	0.204
interrow - oil-palm row	0.997	1.000	0.999	0.397
stem - oil-palm row	0.295	0.992	0.983	0.089
interrow - frond	0.099	0.187	0.048	0.962
palm circle - frond	0.891	0.121	0.014	0.002
palm circle - interrow	0.268	0.992	0.969	0.005

Appendix III - fieldwork

Table A1 Sampling of oil-palm parts. fieldwork 2019



Palm fronds:

Oil palms and a detailed view of an oil-palm crown showing palm fronds of different age: mature palm fronds and senescing fronds.



Fruit bunches:

Oil-palm crown with ripe fruit bunches.



Fruit bunch:

A harvesting tool *Egreg* is used to cut off senescing fronds and ripe fruit bunches.

Table A1 continued



Frond bases:
Frond bases were cut off oil-palm stems at ~ 1.5 m height.



Oil-palm parts:
Ripe fruit bunch showing single fruit in fibrous casts. The fruit bunch is attached to the oil-palm stem by its fibrous stalk. Single leaflets of frond no. 9, 17 and a senescing frond (left to right) next to a piece of the rachis.



Oil-palm parts:
Sampled oil-palm components were already cut and chopped in the field. Fruit was cut off the fruitbunch and left as such.

Appendix III - laboratory

Table B1 Si and Ca concentrations in oil-palm parts and statistical analyses

Oil-palm part	Water regime	N	Total Si [%]		Ca [%]		Si/Ca ratio	Shapiro-Wilk test p-value (ND)	Levene test p-value (VAR)
			\bar{X}	σ	\bar{X}	σ			
Frono no. 9	Well-drained	HO	4	1.06 ± 0.38	0.50 ± 0.12	2.1	0.95		
Frono no. 17	Well-drained	HO	4	1.74 ± 0.47	0.63 ± 0.11	2.8	0.72		
Senescing frond	Well-drained	HO	4	3.58 ± 0.59	0.95 ± 0.10	3.8	0.65		
Rachis	Well-drained	HO	4	0.29 ± 0.03	0.54 ± 0.12	0.5	0.69	0.06 '!	
Frono base	Well-drained	HO	4	0.32 ± 0.09	0.24 ± 0.05	1.3	0.02^b		
Fruit-bunch stalk	Well-drained	HO	4	0.44 ± 0.06	0.40 ± 0.12	1.1	0.01		
Fruit pulp	Well-drained	HO	4	0.37 ± 0.07	0.15 ± 0.05	2.4	0.91		
Kernel	Well-drained	HO	4	0.26 ± 0.07	0.07 ± 0.02	3.9	0.84		
Frono no. 9	Riparian	HOr	4	1.08 ± 0.44	0.39 ± 0.11	2.7	0.35		
Frono no. 17	Riparian	HOr	4	1.34 ± 0.29	0.49 ± 0.10	2.7	0.38		
Senescing frond ^a	Riparian	HOr	3	3.74 ± 1.13	0.88 ± 0.06	4.3	0.56		
Rachis ^a	Riparian	HOr	3	0.29 ± 0.03	0.44 ± 0.10	0.7	0.78	0.02 '**	
Frono base	Riparian	HOr	4	0.31 ± 0.14	0.21 ± 0.04	1.5	0.03		
Fruit-bunch stalk	Riparian	HOr	4	0.48 ± 0.12	0.35 ± 0.13	1.4	0.34		
Fruit pulp	Riparian	HOr	4	0.43 ± 0.03	0.15 ± 0.08	2.9	0.69		
Kernel	Riparian	HOr	4	0.28 ± 0.06	0.10 ± 0.03	2.9	0.73		

^a n=3 as no senescing fronds were left hanging on palm trees (differing management practice on HOr2)

Statistics was done with the non-parametric Kruskal-Wallice test and Whitney-Mann-U test.

^bItalic-bold = not asserted

Table B2 Morphological characteristics of oil palms taken for sampling and Si accumulation in fruit bunches.

Water regime	Plot	Oil palm	Stem [m]	Hanging fronds [#]	Fruit colour	FB [#]	FFB [kg]	dry FB [kg]	Si in dry FB [g]
Well-drained	HO1	1	7	2	dark-red	≥1	17.6	9.3	33
Well-drained	HO1	2	7	1	dark-red	2	15.6	8.2	30
Well-drained	HO1	3	6	4	dark-red	≥1	18.7	9.9	36
Well-drained	HO2	1	7 – 8	5	orange-red	1	8.9	4.7	17
Well-drained	HO2	2	7 – 8	5	orange	1	16.7	8.8	32
Well-drained	HO2	3	8	7	orange-red	≥1	13.2	6.9	25
Well-drained	HO3	1	7	1	dark-red	≥1	19.0	10.0	36
Well-drained	HO3	2	7	4	dark-red	≥1	13.0	6.8	25
Well-drained	HO3	3	8	4	dark-red	6	36.8	19.4	70
Well-drained	HO4	1	5	8	dark-red	4	13.0	6.9	25
Well-drained	HO4	2	5	8	red	2	16.7	8.8	32
Well-drained	HO4	3	6	9	dark-red	3	16.0	8.4	30
Riparian	HOr1	1	5	1	dark-red	4	12.6	6.6	27
Riparian	HOr1	2	6	4	dark-red	3	17.6	9.3	37
Riparian	HOr1	3	5	6	dark-red	5	16.7	8.8	35
Riparian	HOr2	1	4	0	dark-red	3	13.2	7.0	28
Riparian	HOr2	2	4	0	dark-red	3	16.7	8.8	35
Riparian	HOr2	3	4	0	dark-red	1	19.0	10.0	40
Riparian	HOr3	1	6	1	dark-red	≥1	24.0	12.6	51
Riparian	HOr3	2	6	1	dark-red	≥1	36.2	19.1	76
riparian	HOr3	3	5	1 (green)	dark-red	≥1	19.2	10.1	40
riparian	HOr4	1	5	from frond pile	dark-red	1	16.4	8.6	35
riparian	HOr4	2	4	from frond pile	dark-red	1	18.9	10.0	40
riparian	HOr4	3	5	2	dark-red	≥1	12.0	6.3	25

Dry FB weight calculated after Corley et al. (1971). Si concentration in dry FB calculated by multiplying dry FB weight by mean Si concentration of fruit bunch components (stalk, fruit, and kernel).